CHARACTERIZATION OF CHOLINERGIC, NEUROPATHOLOGICAL, AND NEUROINFLAMMATORY CHANGES IN HUMAN BRAIN NUCLEI INVOLVED IN THE SLEEP-WAKE CYCLE IN NEURODEGENERATIVE DISORDERS

by

Gabrielle Marie Hanson

Submitted in partial fulfillment of the requirements for
the degree of Master of Science

at

Dalhousie University
Halifax, Nova Scotia
August 2024

Dedication

This thesis is dedicated to my parents, whose unwavering support have profoundly shaped my academic journey. Your ongoing encouragement and belief in my abilities have been invaluable, and I am profoundly thankful for the strong work ethic you instilled in me.

I also dedicate this thesis to the memory of my late great-grandparents, whose journey through dementia inspired my commitment to finding explanations and solutions for neurodegenerative disorders.

Table of Contents

List of Tables

List of Figures

Abstract

Neurodegenerative disorders (NDDs) embody the progressive loss of structure or function of neurons, typically culminating in neuronal cell death and include conditions such as Alzheimer's disease (AD), dementia with Lewy bodies (DLB), and multiple sclerosis (MS). AD is characterized neuropathologically by aggregation and accumulation of amyloid-β (Aβ) plaques and tau neurofibrillary tangles (NFTs), DLB by the presence of α-synuclein Lewy bodies and neurites, and MS by the presence of demyelinating lesions. Despite differences in their underlying neuropathology, they share symptoms of sleep disturbances such as insomnia, sleep apnea, rapid eye movement sleep behaviour disorder, and other sleep-wake cycle disturbances. Moreover, disrupted sleep patterns in NDDs have been shown to worsen existing neurological symptoms, thereby further diminishing patients' quality of life and potentially accelerating the disease process. Functions such as sleep, wakefulness, memory, and cognition are all in part modulated by the cholinergic system. Acetylcholine (ACh), a key neurotransmitter in the cholinergic system, is synthesized by choline acetyltransferase (ChAT) and interacts with nicotinic and muscarinic acetylcholine receptors before being hydrolyzed by the enzymes acetylcholinesterase (AChE) and butyrylcholinesterase (BChE). The basal forebrain (BF) and brainstem (BS), brain regions crucial for the sleep-wake cycle, exhibit significant expression of ChAT, AChE, and BChE. Cholinergic system changes are prevalent in NDD brains, and appears to exert notable effects on neuroinflammation, neuropathology, neurodegeneration, and cognitive functions. The contribution of neuropathology and neuroinflammation to sleep-wake cycle dysfunction in AD, DLB, and MS is not well known. This study investigated cholinergic, neuropathological, and neuroinflammatory changes in nuclei related to sleep in the basal forebrain (BF) and brainstem (BS) in AD, DLB, MS and cognitively normal (CN) brains. Formalin-fixed human tissue blocks from AD, DLB, MS, and CN brains containing the medial septum, vertical limb of the diagonal band of Broca, and nucleus basalis of Meynert of the BF and the pedunculopontine nucleus, laterodorsal tegmental nucleus, dorsal raphe nucleus, and locus coeruleus (LC) of the BS were utilized in this study. BF and BS sections were examined with histochemical and immunohistochemical techniques to evaluate for cholinergic, neuroinflammatory, and neuropathological markers. Results showed significant reductions in ChAT-, AChE-, and NADPH-diaphorase- positive neurons, and LC pigmented neurons in AD and DLB brains, but not MS. Aβ- and cholinesterase-positive plaques as well as tau NFTs were observed frequently in AD but sparsely in DLB, which also exhibited moderate α-synuclein pathology. pTDP-43 pathology was identified in just one case among all the brains examined, specifically within the AD group, with no significant difference observed when compared to CN brains. MS cases showed several demyelinated lesions throughout varying regions of the BF and BS. Elevated neuroinflammation was noted in all NDD brains. Results demonstrated that cholinergic, neuropathological, and neuroinflammatory changes are observed in BF and BS nuclei involved in sleep in many NDD brains and may underlie sleep-wake disturbances. Investigating the intricate mechanisms and contributors of sleep dysfunction in NDDs could help facilitate better understanding of these conditions and provide new avenues for development of novel curative and diagnostic approaches.

List of Abbreviations Used

α7nAChR	alpha-7 nicotinic acetylcholine receptor
Å	angstrom
°C	degree Celsius
µL	microlitre
µm	micrometer
Aβ	amyloid-β
ac	anterior commissure
ACh	acetylcholine
AChE	acetylcholinesterase
AD	Alzheimer's disease
ATP	adenosine triphosphate
BChE	butyrylcholinesterase
BW 284 C 51	1,5-bis (4-allyl dimethylammonium phenyl) pentan-3-one dibromide
cc	corpus callosum
Cd	caudate nucleus
CERAD	Consortium to Establish a Registry for Alzheimer's Disease
Ch1	medial septal nucleus
Ch2	nucleus of the vertical limb of the diagonal band of Broca
Ch3	nucleus of the horizontal limb of the diagonal band of Broca
Ch4	nucleus basalis of Meynert
Ch4ai	anterointermediate sector of the nucleus basalis of Meynert
Ch4am/al	anteromedial/anterolateral sector of the nucleus basalis of Meynert
Ch4p	posterior sector of the nucleus basalis of Meynert
Ch5	pedunculopontine nucleus
Ch6	laterodorsal tegmental nucleus
ChAT	choline acetyltransferase
ChE	cholinesterase
ChEI	cholinesterase inhibitor
cl	Claustrum

CN	Cognitively Normal
CNS	Central Nervous System
CSF	cerebrospinal fluid
DAB	3,3'-diaminobenzidine
dH_2O	distilled water
DMT	disease-modifying therapy
DN	dystrophic neurite
DR	dorsal raphe nucleus
g	gram
GABA	gamma-aminobutyric acid
GP	globus pallidus
GPe	globus pallidus externus
GPi	globus pallidus internus
H&E	hematoxylin and eosin
H_2O_2	hydrogen peroxide
hr	hour
IFN	interferon
IgG	immunoglobulin G
IL-1β	interleukin-1β
IL-6	interleukin-6
Ins	insula
KDa	kilodalton
LC	locus coeruleus
M	molar
mAChR	muscarinic acetylcholine receptor
MB	maleate buffer, pH 7.4
mL	milliliter
mM	millimolar
mm	millimeter
MMB	mammillary body
MRI	magnetic resonance imaging

nAChR	nicotinic acetylcholine receptor
NADPH-d	nicotinamide adenine dinucleotide phosphate-diaphorase
NIA-AA	National Institute of Aging and Alzheimer's Association
NCI	neuronal cytoplasmic inclusion
NFT	neurofibrillary tangle
NMDA	*N*-methyl-D-aspartate
NO	nitric oxide
NOS	nitric oxide synthase
NT	neuropil thread
opt	optic tract
OSA	obstructive sleep apnea
PB	phosphate buffer, pH 7.4
PD	Parkinson's disease
pH	potential hydrogen
PNS	Peripheral Nervous System
PSG	polysomnography
pTau	phosphorylated tau
pTDP-43	phosphorylated Tar DNA-binding protein-43
Put	putamen
REM	rapid eye movement
REMBD	rapid eye movement sleep behaviour disorder
RLS	restless legs syndrome
SCN	suprachiasmatic nucleus
SLE	Systemic Lupus Erythematosus
son	supra optic nucleus
SWS	slow wave sleep
TBS	0.05 M tris buffered saline, pH 7.6
Thal	Thalamus
TMN	tuberomammillary nucleus
TNF-α	tumor necrosis factor-alpha
vAChT	vesicular acetylcholine transporter

y	years

Acknowledgements

I would like to express my deepest gratitude to my supervisor, Dr. Sultan Darvesh, for taking me on as a student and believing in me despite my lack of prior experience. Your mentorship and unwavering support has been instrumental in shaping my journey. You have taught me how to think critically, embrace the mindset of a scientist, and challenged me to strive for excellence. Your passion for research and endless curiosity continues to inspire me.

Meghan Cash, thank you for teaching me the essential techniques I needed to succeed. Your advice, support, enthusiastic energy, and dedication have been crucial to my development and success.

I would also like to thank the rest of the Darvesh Lab for their support and camaraderie throughout this journey.

I would also like to extend my heartfelt appreciation to my thesis supervisory committee, Dr. Kazue Semba, Dr. Alon Friedman, and Dr. Bill Baldridge, and my external examiner, Dr. Sean Christie. Their guidance and feedback have been essential in refining my work.

Lastly, I am deeply thankful to my family and friends for their unwavering support and encouragement throughout this journey. Their belief in me has been a constant source of strength.

CHAPTER 1. Introduction

1.1. Neurodegenerative Disorders

Neurodegenerative disorders (NDDs) encompass a diverse array of conditions that gradually impair function and structure of the nervous system, leading to a progressive decline in cognitive function, motor skills, and in many cases, autonomy . Some of the most prevalent NDDs in Canada include Alzheimer's disease (AD), dementia with Lewy bodies (DLB), Parkinson's disease (PD), amyotrophic lateral sclerosis (ALS), and multiple sclerosis (MS; Government of Canada, 2014). Dementia is a broad term describing a decline in cognitive function, memory, reasoning, and behaviour significant enough to interfere with daily living (Gale et al., 2018). Dementia has a hetereogenous presentation that can be caused by various neurological and medical conditions such as neurodegeneration, vascular conditions, and metabolic disorders (Gale et al., 2018). Dementia affects roughly 750,000 Canadians as of 2024 with numbers expected to rise to nearly 1 million by 2030, and will continue to increase as the population ages (Alzheimer Society of Canada, 2024b). Out of this proportion of dementia patients, about 60%-80% of these are caused by AD and 5% by DLB (Alzheimer Society of Canada, 2024b). MS, another prevalent neurodegenerative condition in Canada, affects roughly 90,000 Canadians as of 2023 (MS Canada, 2023a). Advancements in medical technology, research, and increased awareness have led to earlier and more accurate diagnoses of these conditions, resulting in more diagnoses, contributing to a perceived rise in prevalence and incidence (Alzheimer's Association, 2024a). Increases in the number of individuals diagnosed with NDDs can amplify existing social, economic, and health care system burden (Alzheimer Society of Canada,

2024b). Despite advancements in diagnostic testing and clinico-pathological correlations, there are deficiencies in effective disease-modifying therapies for AD and DLB. Until such therapies are discovered, intervention of NDDs focuses on multimodal treatment approaches employing health care providers from varied disciplines and medications to alleviate symptoms, aimed at improving quality of life and slowing disease progression (Alzheimer's Association, 2024a; Gale et al., 2018; Giacobini et al., 2022).

1.1.1. Alzheimer's Disease

AD stands as one of the most pressing and pervasive health challenges of the modern era, profoundly affecting millions of individuals worldwide (Ferrari & Sorbi, 2021; World Health Organization, 2023). The discovery of AD traces back to the early 20th century when Czech psychiatrist and neuropathologist Oskar Fisher first described abnormal protein deposits in the brains of dementia cases (Goedert, 2008). Following this groundbreaking clinicopathological study, German psychiatrist and neuropathologist Alois Alzheimer made further descriptions of neuropathological hallmarks of AD that would reshape our understanding of NDDs (Stelzmann et al., 1995). In 1901, Alzheimer encountered a 51-year-old female patient named Auguste Deter who presented with disturbances of memory, cognition, sleep, behaviour, and orientation (Hippius & Neundörfer, 2003; Stelzmann et al., 1995). Over time, her condition deteriorated rapidly leading to severe cognitive impairments and ultimately death. Intrigued by her case and its difficulty to be classified as a recognized illness, Alzheimer examined Auguste's brain post-mortem and made a startling discovery. Examination of her brain revealed atrophy of the cerebral cortex, abnormal protein deposits, and atherosclerosis (Alzheimer, 2006; Stelzmann et al., 1995). These observations by Fischer and Alzheimer marks the first

documentation of what we now recognize as amyloid-β (Aβ) plaques and tau neurofibrillary tangles (NFTs), the neuropathological hallmarks of AD. Fischer and Alzheimer's seminal work not only identified the characteristic neuropathological changes associated with the disease, but also highlighted the clinical symptoms and progressive nature of the disorder. Following his discovery, research into AD expanded rapidly, fueled by advancements in neuroscience and medicine (Alzheimer's Association, 2024b). Over the decades, scientists have made significant strides in unraveling the complex mechanisms underlying the disease, identifying genetic risk factors, and developing diagnostic tools and therapeutic interventions (Alzheimer's Association, 2024b). Despite these advancements, methods to definitively diagnose and effectively cure AD is not currently available (Alzheimer's Association, 2024a; Gunes et al., 2022).

1.1.1.1. Clinical Presentation and Diagnosis

AD typically manifests through a gradual and progressive decline in cognitive abilities and functional independence. Its clinical presentation encompasses various domains, illustrating the widespread impact on the brain. Symptom presentation can be highly heterogenous among patients, reflecting individual differences in the underlying severity, composition, and distribution of neuropathology (Duara & Barker, 2022). The current consensus on the clinical criteria for a diagnosis of AD is based on the criteria described by the National Institute on Aging and Alzheimer's Association (NIA-AA) (McKhann et al., 2011). A diagnosis of AD requires an initial diagnosis of dementia. Dementia encompasses a wide spectrum of conditions characterized by a notable deterioration in cognitive abilities and behavior, which impedes daily functioning, and is not better explained by other medical, neurological, or psychiatric conditions (Gale et al.,

2018). The dementia diagnostic process involves a comprehensive assessment of cognitive functions, including memory, language, executive function, and visuospatial skills through objective cognitive testing, alongside a thorough medical history provided by the patients and a knowledgeable informant, such as a family member. Cognitive testing is performed by a physician or other qualified healthcare professionals and can examine components including memory, language, attention, visuospatial function, and executive function (Tsoi et al., 2015). The Mini-Mental State Examination (Folstein et al., 1975) is a widely used proprietary cognitive testing instrument. Other tests with high diagnostic performance include the Behavioural Neurology Assessment (Darvesh et al., 2005) for dementia and the Montreal Cognitive Assessment (Nasreddine et al., 2005) for MCI, among many others (Tsoi et al., 2015).

Cognitive testing and medical history must demonstrate the presence of impairment in a minimum of two of the following domains: memory, reasoning, visuospatial abilities, language, and behaviour (McKhann et al., 2011).

The diagnosis of dementia encompasses a spectrum of severity, which can range from mild to severe. Outside of the dementia spectrum is the diagnosis of mild cognitive impairment (MCI; (Albert et al., 2011; Petersen, 2003). Individuals with MCI experience subtle but noticeable changes in cognitive function, such as memory loss or difficulties with language or executive function, that are greater than expected for their age and educational and socio-cultural background but do not significantly impair their ability to carry out daily activities. While some individuals with MCI may progress to dementia, others remain stable or even experience improvement in cognitive function over time

(Albert et al., 2011; Petersen, 2003). Differentiating between a diagnosis of MCI or AD is crucial for early intervention and prognosis.

A diagnosis of AD may be specified when characteristic symptoms are present and the criteria for dementia have been met (McKhann et al., 2011). AD may be classified as probable, possible, or definite, describing different levels of certainty (McKhann et al., 2011; J. C. Morris et al., 1989). During life, AD may only be classified as probable or possible (American Psychiatric Association, 2013; McKhann et al., 2011). Probable AD indicates a higher level of confidence in the diagnosis, whereas possible suggests a lower level of certainty in the diagnosis. A diagnosis of probable AD may be provided when the dementia symptoms have an insidious onset and there is a history indicating progressive cognitive decline. Cognitive deficits must be prominently associated with either an amnestic or nonamnestic presentation. Amnestic AD is the most common presentation, where deficits involve impairment in learning and recall. Nonamnestic AD may present with prominent deficits in the domains of either language, visuospatial, or executive function. A diagnosis of probable AD should not be assigned when other conditions, such as cerebrovascular events, medications side effects, or another NDD, could provide an alternative explanation of clinical presentation. In contrast, possible AD may be designated when there is evidence of cognitive impairment, reflective of core clinical criteria for AD, but course or symptoms are atypical. Atypical course can include a sudden onset of cognitive impairment or a lack of historical detail of progressive decline. Atypical symptoms reflect mixed etiology and may include the evidence of a concomitant condition such as cerebrovascular disease or features of DLB. Lastly, definite AD is diagnosed post-mortem following neuropathological examination

indicating the presence of AD pathology including Aβ plaques and tau NFTs with clinical dementia presentation (Montine et al., 2012a; J. C. Morris et al., 1989).

1.1.1.2. Biological Diagnostic Techniques

The challenges of early and accurate diagnosis have created a need for imaging and testing for biomarkers associated with the disease process (Jack et al., 2018). With advances in the field of diagnostic imaging and biomarker testing assays, there is increased confidence in the ability to diagnose patients while they are alive (Blennow et al., 2010; Valotassiou et al., 2018). These methods are used to increase confidence that the clinical presentation can be attributed to AD neuropathophysiology (McKhann et al., 2011). In AD diagnosis, a biomarker refers to a measurable indicator found in biological samples, such as blood or imaging scans, providing insight into the underlying pathological processes associated with the condition (Jack et al., 2018). These biomarkers can provide information about the underlying pathological processes associated with AD, such as the presence of abnormal protein deposits like Aβ and tau, and markers such as neurofilament light protein for neurodegeneration, and proteins related to neuroinflammation (Hok-A-Hin et al., 2023; Jack et al., 2018). Recent research and consensus recommendations have encouraged the inclusion of AD biomarker testing into clinical use (Dubois et al., 2021; Jack et al., 2018; Patel et al., 2024). However, the use of testing relating to AD biomarkers for diagnosis remain controversial (Frisoni & Visser, 2015).

Neuroimaging techniques serve as tools in the diagnosis of AD, offering insights into the structural, functional, and pathophysiological changes occurring in the brain (Y.-T. T. Wang et al., 2023). Magnetic Resonance Imaging (MRI) is a non-invasive imaging

technology that produces three dimensional detailed anatomical images using powerful magnets that cause protons in the body's tissues to emit signals (National Institute of Biomedical Imaging and Bioengineering, 2022). MRI is particularly useful for examining soft tissues such as the brain, spinal cord, muscles, and organs (Johns Hopkins Medicine, 2024a). It can detect a wide range of abnormalities, including tumors, injuries, inflammation, and structural abnormalities (Johns Hopkins Medicine, 2024a). In the context of AD, MRI can be used to observe brain atrophy as the result of neuronal loss, as well as rule out other potential causes of cognitive impairment such as stroke or tumors (Chouliaras & O'Brien, 2023; Johnson et al., 2012). Other imaging techniques used for examination of tissues include positron emission tomography (PET) and single-photon emission computed tomography (SPECT) which detect positron emission and gamma rays, respectively (Maschio & Ni, 2022). PET scans are utilized in AD to detect abnormal levels of Aβ and tau protein, indicative of the presence of Aβ plaques and tau NFTs, while SPECT can be used to assess glucose metabolism in the brain (Maschio & Ni, 2022). Examining intensities of glucose metabolism in the brain can be correlated to synaptic activity and blood perfusion, hence reflecting brain activity, allowing visualization of areas of reduced brain activity that can be associated with AD (Mergenthaler et al., 2013). Radiotracers such as [^{18}F]fluorodeoxyglucose PET or [^{99m}Tc]-hexamethyl propylene amine oxime SPECT can be used to examine glucose metabolism. Brains of AD patients typically show hypoperfusion or hypometabolism in temporoparietal regions, reflecting hallmark AD pathophysiology distribution (Valotassiou et al., 2018). AD neuropathological aggregates can be visualized through PET by using radioligands with specific targets such as [^{18}F]florbetapir or [^{11}C]Pittsburgh

compound B for Aβ and [^{18}F]flortaucipir for tau (J. Wang et al., 2023). PET scans can reveal the distribution and severity of Aβ and tau deposits while SPECT can assess functional information across different brain regions, aiding in the staging of AD and guiding treatment decisions (J. Wang et al., 2023). Novel PET and SPECT tracers are currently being developed to target biomarkers such as butyrylcholinesterase (BChE; (Darvesh, 2016; DeBay et al., 2017; Macdonald et al., 2010). Overall, the integration of various imaging modalities like MRI, PET, and SPECT in AD diagnosis offers health care providers a comprehensive understanding of the structural, functional, and neuropathological changes occurring in the brain, facilitating early detection, more accurate diagnosis, and the possibility of monitoring disease progression (Chouliaras & O'Brien, 2023; Maschio & Ni, 2022).

In addition to neuroimaging techniques, testing assays are currently being developed to meet the demand for diagnosing and identifying AD-related brain changes during life (Mankhong et al., 2022). These testing assays include examining biomarkers such as Aβ and tau protein in bodily fluids like cerebrospinal fluid (CSF) and blood. CSF is a clear, colorless fluid that surrounds the brain and spinal cord, providing structural and nutrient support while removing waste products from the central nervous system (CNS; Blennow & Zetterberg, 2018). In CSF, the abundance and composition of biomarkers can be quantified through various analytical techniques, including enzyme-linked immunosorbent assays (ELISA), mass spectrometry, and immune-PCR (Blennow & Zetterberg, 2018; Grigoli et al., 2024). Blood testing is another method of fluid analysis used as a non-invasive and cost-effective tool for examining AD-related biomarkers. However, proteins originating from the brain encounter interference as they enter the

bloodstream due to the selective nature of the blood-brain barrier, which primarily permits the passage of vital nutrients, ions, and metabolic waste products, leading to significantly reduced biomarker concentrations in the blood (Grigoli et al., 2024). Although blood may be preferred over CSF for measuring AD-related biomarkers due to its accessibility, its reliability for biomarkers for AD has been challenging and controversial (Blennow & Zetterberg, 2018; Grigoli et al., 2024). Despite these challenges, advancements in ultrasensitive immunoassays and mass spectrometry offer renewed optimism for progress in this area (Grigoli et al., 2024). Analogous to neuroimaging techniques, these fluid biomarker assays offer insights into the underlying pathological changes in the brain by examine key proteins associated with AD pathology, including Aβ, tau, and neurofilament light, reflective processes of amyloid deposition, tau phosphorylation, and neuronal injury, respectively (Blennow et al., 2010; Grigoli et al., 2024). Plasma biomarker assays offer a less invasive alternative to CSF for assessing AD pathology, however, they lack specificity, sensitivity, and reliability, although its use is still being investigated (Blennow et al., 2010; Blennow & Zetterberg, 2018).

Integrating neuroimaging findings and biomarker analyses with clinical assessments can enable clinicians to make more accurate diagnoses, stage disease progression, and monitor treatment responses in individuals with AD (Chouliaras & O'Brien, 2023; Mankhong et al., 2022; Maschio & Ni, 2022; Patel et al., 2024). Although AD's neuroimaging and biomarker testing technologies require ongoing research, they hold great potential for advancing early diagnosis and treatment strategies.

1.1.1.3. Treatment

AD is a complex NDD for which there is presently no cure. The lack of effective treatments can be primarily attributed to our deficiency in understanding of the pathophysiological process, and limitations surrounding diagnosis accuracy (Abdallah, 2024). Current treatment approaches aim to manage symptoms, slow disease progression, and improve quality of life for patients living with the condition (Alzheimer's Association, 2024a). However, there is ongoing research into disease-modifying treatments that aim to target the underlying pathology of AD with the goal of slowing or halting disease progression (Abdallah, 2024). Additionally, non-pharmacological interventions, including cognitive stimulation, physical exercise, and social engagement, play an essential role in managing symptoms and improving overall well-being for individuals living with AD (Alzheimer Society of Canada, 2024a).

The current standard for AD treatment is rooted in the cholinergic theory of AD (Hampel et al., 2018). The cholinergic theory of AD proposes that dysfunction in the cholinergic system, specifically a deficiency in the neurotransmitter acetylcholine (ACh), plays a central role in the development and progression of the disease. According to this theory, the degeneration of cholinergic neurons, particularly those in the basal forebrain (BF), leads to a reduction in cholinergic neurotransmission, contributing to cognitive decline and memory impairment characteristic of AD (Hampel et al., 2018). This theory has led to the development of cholinesterase inhibitors (ChEIs), medications that aim to enhance cholinergic activity in the brain. ChEIs such as donepezil, rivastigmine, and galantamine continue to be the primary approved pharmacological treatments for cognitive impairments in AD (Conti Filho et al., 2023; Scheltens et al., 2021).

Additional treatments currently used for AD target the glutamatergic system, such as memantine, a *N*-methyl-D-aspartate (NMDA) receptor antagonist (Kuns et al., 2024; National Institute on Aging, 2023). Glutamate is a neurotransmitter involved in learning and memory processes. In AD, excessive activation of NMDA receptors by glutamate can lead to excitotoxicity, causing damage to neurons. By antagonizing NMDA receptors, memantine helps regulate glutamate activity, preventing excessive stimulation and protecting neurons from damage. This mechanism of action is thought to improve cognitive function and improve behavioural disturbances in those living with AD. Due to their distinct mechanisms of action compared to ChEIs, NMDA antagonists can be prescribed alongside these drugs in combination therapy (Kuns et al., 2024; National Institute on Aging, 2023).

Immunotherapy for AD represents an innovative treatment approach aimed at targeting the underlying pathology of the disease, specifically the accumulation of Aβ in the brain. This therapeutic strategy involves harnessing the immune system to identify and remove Aβ aggregates, thereby potentially slowing or halting disease progression (Valiukas et al., 2022). This strategy uses monoclonal antibodies designed to selectively bind and mark them for destruction by microglia or other immune cells to facilitate clearance of Aβ plaques from the brain (Cummings, 2023). Several monoclonal antibody drugs targeting Aβ have been developed and evaluated in clinical trials for AD. Examples include lecanemab, donanemab, and aducanumab, among others (Ebell et al., 2024; Wu et al., 2023). These drugs have demonstrated moderate slowing of cognitive and functional decline in individuals with MCI or mild AD, however there were significant variances in outcomes and effectiveness, and can cause serious side effects (Alzheimer's

Association, 2024a; Rabinovici, 2021; Van Dyck et al., 2023). These immunotherapies have posed great controversy, relating to the considerable variability in their efficacy and safety, speed of approval by the United States Food and Drug Administration (FDA), financial incentives, and more (Rabinovici, 2021; Ross et al., 2023). The controversies surrounding AD drugs underscores the ongoing necessity for research and development of novel, safe, ethical, and efficacious treatments.

In addition to pharmacotherapy, non-pharmacological interventions play a crucial role in AD management, focusing on enhancing overall well-being, maintaining independence, and optimizing cognitive function (Alzheimer's Association, 2024a; Scales et al., 2018; World Health Organization, 2023). These include sensory practices, lifestyle modifications, and structured routines, among others (Scales et al., 2018; World Health Organization, 2023). Sensory practices may include aromatherapy and multi-sensory stimulation aimed at producing calming effects and light therapy to promote synchronization of sleep-wake cycles (Scales et al., 2018). Lifestyle modifications such as exercise, nutrition/diet, and social engagement can aid with stress, energy, and general well-being (Alzheimer Society of Canada, 2024a). Structured routines can provide familiarity and predictability, reducing anxiety and confusion in dementia patients. Consistent schedules and activities within routines can promote independence, cognitive stimulation, and physical and emotional well-being (Poon et al., 2018).

Ultimately, a multifaceted approach that combines pharmacological interventions, non-pharmacological therapies, and supportive care is essential in effectively managing AD and optimizing outcomes for individuals living with the condition and their caregivers.

1.1.1.4. Neuropathological Evaluation

Neuropathological evaluation of the brain involves examining brain tissue under a microscope to identify and analyze abnormalities associated with various neurological conditions (National Institute on Aging, 2022). This process typically includes staining brain tissue sections to visualize specific structures, such as neurons, glial cells, and protein deposits like Aβ or tau. Neuropathologists assess the distribution, density, and characteristics of these abnormalities to make a diagnosis and understand the underlying pathology of the disease. Neuropathological evaluation is essential for confirming diagnoses, advancing research, and guiding treatment strategies for neurological disorders (National Institute on Aging, 2022).

CERAD has developed a consensus protocol outlining the neuropathological evaluation of AD in post-mortem brain tissue (Mirra et al., 1991). The neuropathological diagnosis of AD involves the examination of brain tissue post-mortem to identify characteristic hallmarks of the disease. This protocol includes assessment of gross and microscopic neuropathological changes. Gross neuropathological changes should be assessed in regions including the brain, spinal cord, meninges, and vasculature, and any abnormalities should be noted which may include neocortical atrophy, ventricular enlargement, vascular deformities, evidence of stroke, or loss of pigmentation of the substantia nigra or locus coeruleus (LC; Mirra et al., 1991).

Microscopic examination should assess a minimum of five brain regions including the middle frontal gyrus, superior and middle temporal gyri, inferior parietal lobule, hippocampus, entorhinal cortex, and midbrain including the substantia nigra (Mirra et al., 1991). Histological staining methods for identification of plaques and NFTs include

immunohistochemistry with specific antibodies against Aβ and tau, as well as histochemistry using Thioflavin-S or Bielschowsky silver staining. Abundance of plaques and tau NFTs in a medium-powered field are semi-quantitatively scored as none, sparse, moderate, or frequent (Fig. 1.1). An age-related plaque score is additionally assigned which consider a patient's age alongside plaque abundance, reflecting aging-related pathology in the frontal, temporal, and parietal cortices, and is then integrated with clinical information to indicate the probability of a diagnosis of AD.

Consideration should be given to assessing additional pathological findings that may be linked to other NDDs or neurological conditions. Additional pathological findings may include infarcts which are associated with vascular dementia, pigmented neuron loss of the substantia nigra or LC and the presence of Lewy bodies, which are both associated with Parkinson's disease (PD) and DLB, where the presence of these reduce the likelihood of the diagnosis being AD. After thorough examination and consideration of the findings, the pathologist must then rank all neuropathologic diagnoses.

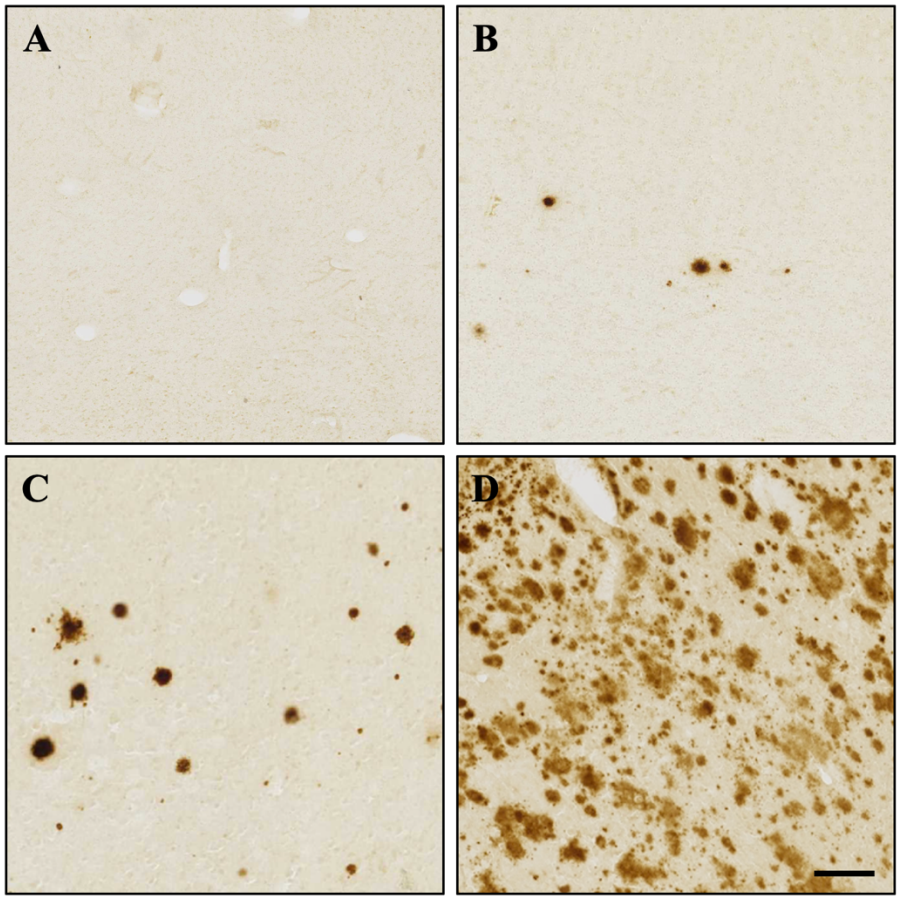

Figure 1.1 Photomicrographs depicted representative fields of view of tissue stained for Aβ based on CERAD plaque score of 0 (A), sparse (B), moderate (C), and frequent (D) (Mirra et al., 1991). Scale bar = 200µm.

The ABC score, proposed by the NIA-AA, is a comprehensive system used to evaluate neuropathological changes associated with Alzheimer's disease (AD) (Montine et al., 2012a). It incorporates three key aspects: A for Aβ plaque deposition (Thal et al., 2002), B for tau NFT staging (Braak et al., 2006), and C for neuritic plaque density (Table 1.1; Mirra et al., 1991).

The 'A' aspect of the ABC score is based on the Thal phases, which categorize and reflect the progressive distribution of Aβ plaques across different brain regions (Fig. 1.2; Montine et al., 2012a; Thal et al., 2002). Phase 0 is indicated by the absence of deposition, while phase 1 is marked by deposition in the frontal, parietal, temporal, and occipital cortices. Phase 2 is characterized by deposition in entorhinal regions, cornu Ammonis 1 of the hippocampus, and the insular cortex. Phase 3 shows deposition in specific regions of the basal forebrain, followed by phase 4 with deposition in specific midbrain and medulla structures. Phase 5 is identified by deposition in specific regions of the pons, and often the cerebellum, with each phase sequentially building on the Aβ plaque pathology identified in the preceding phase. Each phase corresponds to a specific 'A' score: 0 (Thal phase 0), 1 (Thal phase 1 or 2), 2 (Thal phase 3), to 3 (Thal phase 4 or 5; (Montine et al., 2012a; Thal et al., 2002).

The 'B' aspect assesses tau NFT deposition using Braak staging, which identifies the progressive spread of tau NFT pathology throughout the brain (Fig. 1.3; Braak et al., 2006; Montine et al., 2012a). NFTs are observed in specific brain structures across each Braak stage: Stage 0 signifies the absence of NFTs, Stage I indicates deposition in the transentorhinal region with occasional involvement of subcortical nuclei including the locus coeruleus and magnocellular nuclei of the basal forebrain, Stage II denotes

Table 1.1 ABC score for AD neuropathologic change

"A"	Thal phase for Aβ plaques	"B"	Braak NFT stage	"C"	CERAD neuritic plaque score
0	0	0	None	0	None
1	1 or 2	1	I or II	1	Sparse
2	3	2	III or IV	2	Moderate
3	4 or 5	3	V or VI	3	Frequent

Adapted from Montine *et al.* (2012).

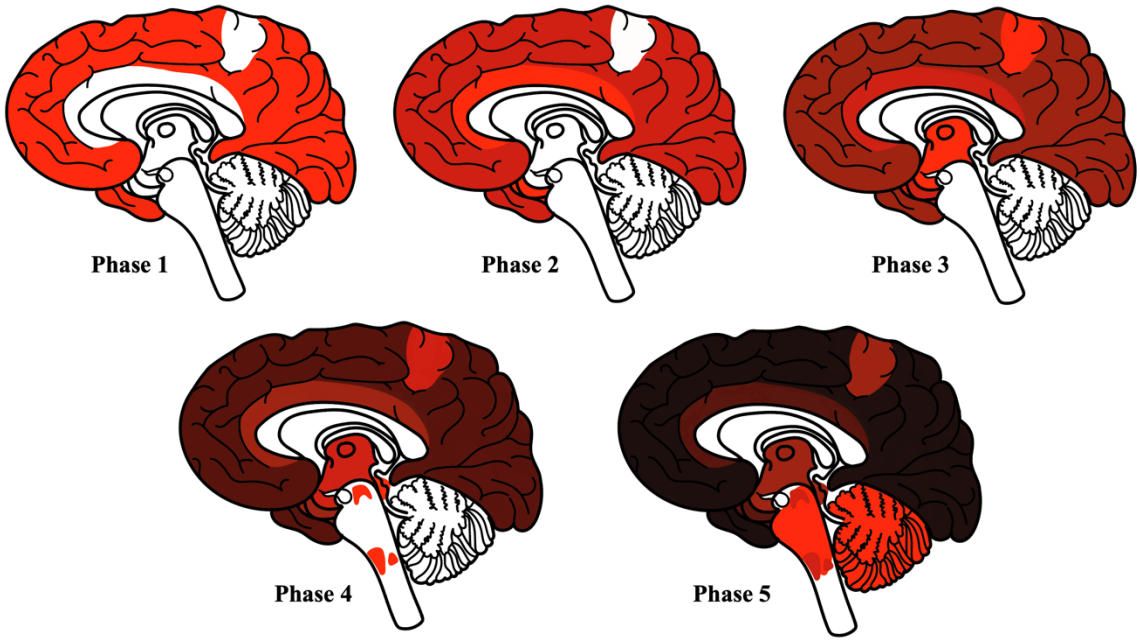

Figure 1.2 Representation of Thal phases of amyloid-β (Aβ) plaque deposition in Alzheimer's disease (Thal et al., 2002). Aβ plaques are identified in specific brain structures at each Thal Phase as follows: Phase 0 is characterized by the absence of deposition; Phase 1 is marked by deposition in the frontal, parietal, temporal, and occipital cortices; Phase 2 is defined by deposition in the entorhinal regions, cornu Ammonis 1 of the hippocampus, and the insular cortex; Phase 3 involves deposition in specific regions of the basal forebrain; Phase 4 sees deposition in certain structures of the midbrain and medulla; Phase 5 is identified by deposition in specific regions of the pons and often the cerebellum. Each phase builds sequentially on the Aβ plaque pathology observed in the preceding phase. Adapted from Thal *et al.* (2002).

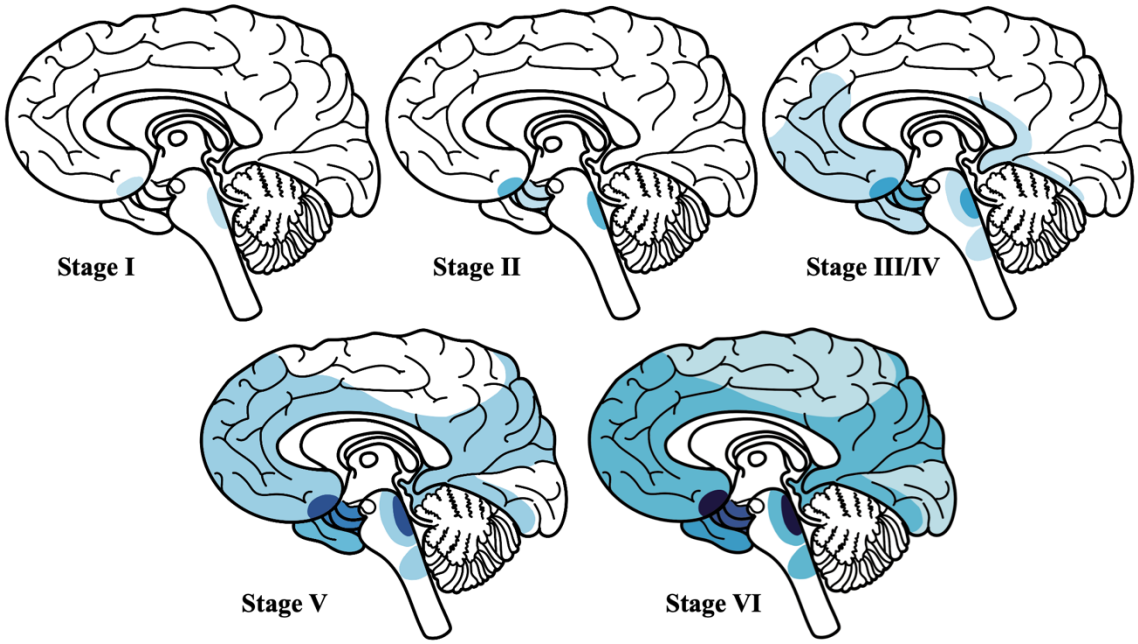

Figure 1.3 Representation of Braak staging of tau pathology deposition in Alzheimer's disease. Neurofibrillary tangles (NFTs) are identified in specific brain structures at each Braak stage as follows: Stage 0 indicates no NFTs detected, Stage I involves deposition in the transentorhinal region and subcortical nuclei such as the locus coeruleus and magnocellular nuclei of the basal forebrain, Stage II sees deposition in the entorhinal region, Stage III shows deposition in the fusiform and lingual gyri, Stage IV involves deposition in the medial temporal gyrus and neocortical association areas, Stage V includes deposition in the peristriate region of the occipital lobe and extends into frontal and superolateral regions, Stage VI features deposition in the parastriate and striate areas of the occipital cortex and further extension into many neocortical areas (Braak et al., 2006). Adapted from Jouanne et al. (2017).

deposition in the entorhinal region, Stage III signifies deposition in the fusiform and lingual gyri, Stage IV indicates deposition in the medial temporal gyrus and neocortical association areas, Stage V denotes deposition in the peristriate region of the occipital lobe and extends into frontal and superolateral regions, and Stage VI signifies deposition in the parastriate and striate areas of the occipital cortex and further extension into many neocortical areas. Each Braak stage corresponds to a specific ‘B’ score: 0 (Braak stage 0), 1 (Braak stage I or II), 2 (Braak stage III or IV), or 3 (Braak stage V or VI; (Montine et al., 2012a).

Finally, the 'C' aspect evaluates semi-quantitative neuritic plaque density (Fig. 1.1) using CERAD scoring, which categorizes the relative density of neuritic plaques in specific brain regions (Figure 1.4; Mirra et al., 1991; Montine et al., 2012a). Each CERAD semi-quantitative score corresponds to a specific ‘C’ score: 0 (none), 1 (sparse), 2 (moderate), or 3 (frequent; (Mirra et al., 1991; Montine et al., 2012a).

By integrating scores from these three aspects, a designation of “Not”, “Low”, “Intermediate” or High” is given to describe the level of AD neuropathologic change (Table 1.2; Montine et al., 2012a). A designation of “Intermediate” or “High” AD neuropathologic change is considered sufficient explanation for dementia. This ABC scoring system provides a comprehensive assessment of AD neuropathological changes, facilitating diagnosis and staging of the disease.

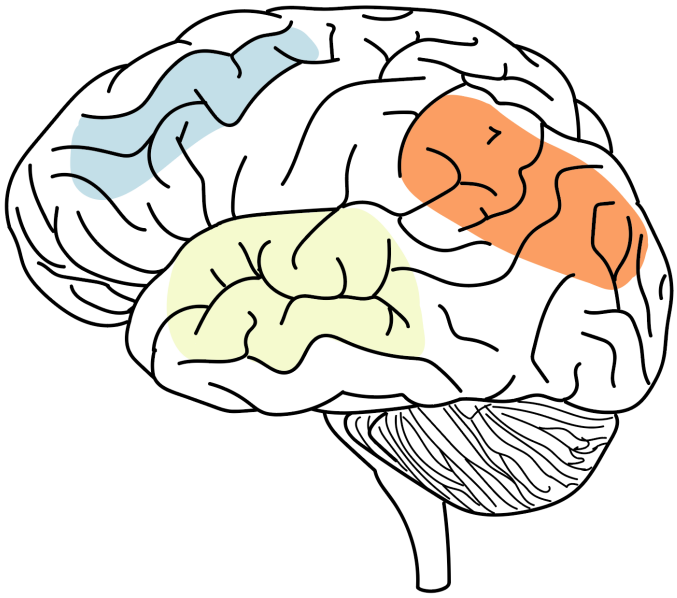

Figure 1.4 Representation of the CERAD recommended brain sampling areas of the neocortex, including the superior and middle temporal gyri (yellow), middle frontal gyrus (blue), and inferior parietal lobule (orange; Adapted from (Mirra et al., 1991).

Table 1.2 ABC score for level of AD neuropathologic change

AD neuropathologic change		**"B" score**		
"A" score	**"C" score**	0 or 1	2	3
0	0	Not	Not	Not
1	0 or 2	Low	Low	Low
	2 or 3	Low	Intermediate	Intermediate
2	Any "C" score	Low	Intermediate	Intermediate
3	0 or 1	Low	Intermediate	Intermediate
	2 or 3	Low	Intermediate	High

Adapted from Montine *et al.* (2012).

1.1.2. Dementia with Lewy Bodies

DLB is a complex neurodegenerative disorder that accounts for 5%-10% of all dementia cases (Alzheimer Society of Canada, 2023a). DLB is characterized by the presence of abnormal α-synuclein protein deposits within the brain (McKeith et al., 2005). Under normal conditions, α-synuclein is a small (14 KDa) acidic soluble protein encoded by the *SNCA* gene, primarily localized in presynaptic terminals of neurons (Calabresi et al., 2023). α-synuclein is named after its α-helical structure and for its initial identification as a protein associated with synaptic terminals ("syn-" for synaptic) and its localization within the nucleus ("-uclein"), reflecting its structural and functional characteristics (Burré et al., 2018). It functions in regulating synaptic vesicle trafficking and neurotransmitter release, thereby contributing to normal synaptic function and neuronal communication. In pathological conditions, α-synuclein undergoes abnormal aggregation due to protein misfolding and forms insoluble deposits (Burré et al., 2018; Calabresi et al., 2023; McKeith et al., 2005). These α-synuclein deposits are known as Lewy bodies (LBs) and Lewy neurites (LNs) after the neurologist and neuropathologist who first described them in the early 20th century, Dr. Frederic Heinrich Lewy (Holdorff, 2002). α-synuclein aggregate deposits appear as spherical eosinophilic cytoplasmic inclusions within neurons (LBs) or as thread-like structures (LNs) located in neuronal processes (Burré et al., 2018). This pathological process disrupts normal cellular functions leading to neuronal dysfunction, synaptic impairment, and ultimately neurodegeneration, and contributes to the progressive loss of motor and cognitive functions (Calabresi et al., 2023). LBs and LNs are characteristic features of NDDs such as DLB, PD, and multiple system atrophy (Calabresi et al., 2023).

DLB manifests with a spectrum of symptoms, including: cognitive decline symptoms such as executive dysfunction, slow processing speed, and some memory deficits; visual hallucinations; fluctuating attention and alertness; parkinsonism; rapid eye movement sleep behaviour disorder (REMBD); and psychiatric symptoms such as depression and anxiety (Alzheimer Society of Canada, 2023a; McKeith et al., 2005, 2017). Parkinson's disease (PD) is another neurodegenerative disorder (NDD) classified as a synucleinopathy, characterized by the same underlying neuropathology as DLB, involving abnormal deposits of α-synuclein in the form of LBs and LNs (Alzheimer Society of Canada, 2023a, 2023b; McKeith et al., 2005). While both DLB and PD share some common underlying brain changes, their symptomatology, temporal sequence of symptom presentation, and clinical trajectories vary, necessitating distinct diagnostic and management strategies (Alzheimer Society of Canada, 2023b; McKeith et al., 2005). DLB manifests with cognitive and psychiatric symptoms before or concurrently with motor symptoms and has a more rapid cognitive decline and greater impairment in visual processing compared to PD-related dementia, known as PD dementia (PDD; McKeith et al., 2005). A 1-year rule is typically applied for differentiating between DLB and PD, which states that if cognitive symptoms appear within one year of motor symptoms, the diagnosis is DLB, whereas if cognitive symptoms develop more than a year after motor symptoms, the diagnosis is PD with dementia (McKeith et al., 2017). Meanwhile, PD initially presents with motor symptoms such as tremor, bradykinesia (slowness of movement), rigidity, and postural instability, with cognitive impairment, including dementia, often developing in later stages of the disease (McKeith & Burn, 2000). Dementia that occurs in the context of well-established PD is then diagnosed as PDD

(McKeith et al., 2005). Despite these differences, it should be noted that variations in the sequence of symptom onset may occur among individuals. Moreover, significant overlap in the clinical presentation of DLB and PD can complicate accurate diagnosis, especially in the initial phases of the illness (Alzheimer Society of Canada, 2023a, 2023b; McKeith & Burn, 2000). Understanding the distinctions between DLB and PD is crucial for accurate diagnosis and individualized treatment interventions.

1.1.2.1. Clinical Presentation and Diagnosis

DLB typically manifests through a gradual and progressive decline in cognitive abilities of sufficient magnitude to interfere with normal social or occupational functioning (McKeith et al., 2017). DLB presents with a diverse array of symptoms that can fluctuate in severity and may overlap with other neurodegenerative disorders (McKeith & Burn, 2000). The array in symptoms observed in DLB correspond to the diverse regions of the brain affected, encompassing both subcortical and cortical areas associated with cognitive impairments such as attention, executive function, and visuospatial deficits, alongside extrapyramidal regions implicated in motor symptoms (McKeith et al., 2005). The current consensus on the clinical criteria for a diagnosis of DLB is based on the criteria described by the Dementia with Lewy Bodies Consortium (McKeith et al., 2017). A diagnosis of DLB requires an initial diagnosis of dementia. Dementia encompasses a progressive decline in cognitive abilities and behavior, of sufficient magnitude to interfere with daily living, and not attributed to other medical, neurological, or psychiatric conditions (Gale et al., 2018). The dementia diagnostic process involves a comprehensive assessment of cognitive functions, including memory, language, executive function, and visuospatial skills, through objective cognitive testing

and a thorough medical history provided by the patient and a knowledgeable informant, such as a family member. Cognitive testing is conducted by physicians or other qualified healthcare professionals and evaluates components such as memory, language, attention, visuospatial function, and executive function (Tsoi et al., 2015). While dementia screening tools that assess for general impairment like the Mini-Mental State Examination (Folstein et al., 1975) and Montreal Cognitive Assessment (Nasreddine et al., 2005) are helpful in screening for dementia, comprehensive neuropsychological evaluations should include tests that address various cognitive domains that are more specific to those seen in DLB (McKeith et al., 2017). It is common to observe disproportionate deficits in attention, executive function, and visuospatial processing compared to memory and naming abilities in individuals with DLB (McKeith et al., 2017). Tools that evaluate attention and executive function that can help to differentiate DLB from Alzheimer's disease (AD) and normal aging include tests of processing speed and divided attention, such as Stroop tasks, computerized tasks of reaction time, and trail-making tasks (McKeith et al., 2017; Stebbins, 2007). In addition, tests for visuospatial function can be used such as complex figure copying, puzzle tasks, spatial matching, and others to detect spatial and perceptual deficits that often occur in the early stages of DLB (McKeith et al., 2017; Stebbins, 2007). Contrary to AD dementia, memory and object naming tend to be less affected in DLB, especially in the earlier stages. No DLB-specific assessment batteries have been developed (Walker et al., 2015). However, an example of an appropriate cognitive testing tool that includes assessments for the above listed deficits related to DLB in addition to general impairment is the Behavioural Neurology Assessment (Darvesh et al., 2005). Finally, for a diagnosis of dementia, cognitive testing

and medical history must demonstrate impairment in at least two of the following domains: memory, reasoning, visuospatial abilities, language, and behavior (McKhann et al., 2011).

A diagnosis of DLB may be given when the criteria for dementia have been met, an essential requirement, and core clinical features are present (McKeith et al., 2017). Core clinical features include: spontaneous fluctuation in cognition, attention, and arousal; visual hallucinations; parkinsonism; and rapid eye movement sleep behaviour disorder (REMBD). DLB fluctuations are typically delirium-like and present as spontaneous alterations in cognitive, attention, and arousal, and may also include episodes of staring or zoning out. Visual hallucinations occur in about 80% of individuals with DLB. These hallucinations are typically well-formed and involve people or animals, and sometimes evoke emotional responses in those living with DLB. Parkinsonism refers to motor features typically seen in PD and include tremor, rigidity, bradykinesia, and postural instability. Parkinsonism occurs eventually in about 85% of individuals with DLB. REMBD is a parasomnia characterized by a loss of normal atonia during the REM phase of sleep, resulting in dream enactment behaviour that can be particularly violent and may cause injuries to the patient themselves or bed partner (Boeve et al., 2004).

Supportive clinical features frequently appear early. While not specific to diagnosis, these symptoms might suggest DLB in someone with dementia, especially if they persist over time or if multiple symptoms appear together. Supportive clinical features in DLB include: severe sensitivity to antipsychotic agents; postural instability; repeated falls; syncope or other transient episodes of unresponsiveness; severe autonomic dysfunction such as sexual dysfunction and incontinence; hypersomnia; hyposmia; visual

hallucinations; systematized delusions; apathy, anxiety, and depression (McKeith et al., 2017).

A DLB diagnosis may be classified as probable or possible during life, describing different levels of certainty that the clinical presentation is associated with underlying Lewy-related pathology (McKeith et al., 2017). Probable DLB indicated a higher level of certainty in the diagnosis, whereas possible suggests a lower level of certainty in the diagnosis. A diagnosis of probable DLB may be given when two or more core clinical features of DLB are present, including fluctuation, visual hallucinations, parkinsonism, and REMBD, with or without the presence of indicative biomarkers (described below). Probable DLB can also be diagnosed when one core clinical feature is present with one or more indicative biomarkers. Alternatively, possible DLB may be designated when there is only one core clinical feature present with no biomarker evidence, or one or more biomarkers are present but there are no core clinical features. However, probable DLB should not be diagnosed on the basis of biomarkers alone (McKeith et al., 2017).

A diagnosis of DLB becomes less likely if there's another physical illness or brain disorder, like cerebrovascular disease, which can explain the symptoms either fully or partially, which might suggest mixed pathology. Additionally, if parkinsonism symptoms emerge as the sole core feature during advanced dementia stages (McKeith et al., 2017).

After death, the most confident diagnosis of DLB can be made by considering neuropathological findings on top of clinical presentation (McKeith et al., 2005, 2017). The presence of Lewy bodies alone is not sufficient for a diagnosis of DLB. For instance, numerous cases of AD may fulfill the neuropathological criteria for DLB, yet clinically they did not exhibit symptoms of DLB. Therefore, it's crucial to consider both

neuropathological results and clinical presentation. Neuropathological criteria for the diagnosis of DLB are described in detail below.

1.1.2.2. Biological Diagnostic Techniques

While direct biomarker evidence of Lewy-related pathology remains unavailable for clinical diagnosis, several indirect methods, including the assessment of indicative biomarkers, have been proven useful (Bousiges & Blanc, 2022; McKeith et al., 2017). An indicative biomarker in the context of DLB refers to a biological marker or characteristic that suggests the presence or progression of the disease (Bousiges & Blanc, 2022). These tools can help clinicians distinguish DLB from other conditions.

Structural imaging such as magnetic resonance imaging (MRI) and computerized tomography (CT), PET and SPECT imaging examining glucose metabolism, and examination of EEG activity are tools used to assess for indicative biomarkers. MRI or CT structural imaging may detect atrophy patterns characteristic of certain NDDs. Imaging techniques can be performed in combination with radiotracers such as metabolism PET or perfusion SPECT to examine glucose metabolism, providing insight into regional differences in brain activity (Bousiges & Blanc, 2022; K. Ishii et al., 2015). In DLB, hypometabolism is often seen in brain regions such as the occipital cortex, temporal and parietal lobes (K. Ishii et al., 2015). A notable finding frequently observed in metabolic imaging examinations for DLB is the "cingulate island sign," denoting the relatively preserved metabolism of the posterior cingulate cortex. This sign serves as a valuable tool in distinguishing DLB from AD (McKeith et al., 2017; Patterson et al., 2019).

Indicative biomarkers for DLB may include abnormalities in imaging studies examining the dopaminergic system using single-photon emission computed tomography (SPECT) or positron emission tomography (PET) scans, which typically show reduced uptake in the basal ganglia, characteristic of DLB (Bousiges & Blanc, 2022). The dopaminergic system is a neurotransmitter system involved in various brain functions, including motor control, reward processing, mood regulation, and cognitive function (Eisenhofer & Reichmann, 2012). Dopamine is synthesized within dopaminergic neurons by the conversion of tyrosine to L-dopa by tyrosine hydroxylase. L-dopa is then converted to dopamine by an enzyme called L-aromatic amino acid decarboxylase. The dopamine is then loaded into vesicles for storage and is available for release into the synaptic cleft. After dopamine release, reuptake is performed by the dopamine transporter (DAT) protein from the synaptic cleft back into the presynaptic neuron. This process is crucial for regulating the concentration of dopamine in the synaptic cleft, thereby controlling the duration and intensity of dopaminergic signaling (Eisenhofer & Reichmann, 2012). In the context of DLB, abnormalities in DAT levels, as detected through imaging techniques like SPECT or PET can provide valuable diagnostic information by detecting the loss of dopaminergic neurons characteristic of DLB pathology (Bousiges & Blanc, 2022). Imaging techniques to assess for the integrity of the dopaminergic system involves administering a radiotracer, such as [^{123}I] N-ω-fluoropropyl-2β-carbomethoxy-3β-(4-iodophenyl) nortropane SPECT and [^{18}F] (E)-N-(3-iodoprop-2-enyl)-2β-carbofluoroethoxy-3β-(49-methyl-phenyl) nortropane PET, that binds to DAT in the brain (Jakobson Mo et al., 2018). Other available indicative biomarker imaging techniques include [^{123}I] metaiodobenzylguanidine myocardial

scintigraphy, a radiotracer which evaluates the function of the sympathetic nervous system, for which values are reduced in DLB and other conditions with Lewy pathology (Bousiges & Blanc, 2022; McKeith et al., 2017).

Besides imaging techniques, sleep studies are frequently conducted to assess sleep disturbances linked with DLB (Boeve, 2019; Pao et al., 2013). Assessing for REMBD is crucial since it is present in 70-80% of cases (McKeith et al., 2017). Polysomnography (PSG) a comprehensive sleep study, serves as a valuable diagnostic tool in evaluating sleep (Gerstenslager & Slowik, 2024; Mayo Clinic, 2023; Pao et al., 2013). PSG provides detailed information about sleep architecture, including sleep stages (such as REM and non-REM sleep), sleep onset latency, total sleep time, and sleep efficiency. This comprehensive assessment encompasses various aspects of sleep architecture and physiological parameters to aid in the diagnosis and management of DLB-related sleep disorders such as REMBD. By monitoring brain activity, muscle tone, and eye movements during REM sleep, polysomnography accurately identifies the absence of muscle atonia characteristic of REMBD, enabling clinicians to diagnose this common sleep disturbance in DLB patients. The key components of PSG include electroencephalography (EEG) to assess brain activity, electromyography (EMG) for measuring muscle tone, electrooculography (EOG) to monitor eye movements, as well as respiratory and heart rate monitoring (Gerstenslager & Slowik, 2024; Mayo Clinic, 2023; Pao et al., 2013). EEG electrodes are placed on the scalp to measure electrical activity in the brain. This allows for the classification of sleep stages and the detection of potential abnormalities in brain activity during sleep, such as abnormal brain wave patterns or arousals (Pao et al., 2013). EMG electrodes are positioned on the chin and on leg muscles

to monitor muscle tone and activity, particularly during REM sleep. While REM sleep typically involves normal muscle atonia regulated by the brainstem, heightened muscle tone during this phase can suggest conditions like REMBD, marked by abnormal and possibly injurious behaviors such as dream enactment (Boeve, 2019; McKeith et al., 2017). EOG electrodes are placed near the eyes to monitor eye movements. This helps identify the different stages of sleep, as well as detect rapid eye movements characteristic of REM sleep (Gerstenslager & Slowik, 2024). Respiratory monitoring involves the measurement of airflow, respiratory effort, and oxygen saturation levels during sleep. This allows for the detection of sleep-disordered breathing events such as apneas (complete cessation of airflow) and hypopneas (partial reduction in airflow), which are common in disorders such as obstructive sleep apnea. Heart rate monitoring involves the continuous recording of heart rate and rhythm during sleep. Changes in heart rate variability and nocturnal arrhythmias can provide important information about cardiovascular health and autonomic function during sleep (Dos Santos et al., 2022). By combining these various components, PSG provides a comprehensive assessment of sleep architecture, sleep-related breathing disorders, and other physiological parameters during sleep, aiding in the diagnosis and management of sleep disorders that may accompany DLB (Mayo Clinic, 2023).

Other tools used as a supportive biomarker in the diagnosis of DLB include examination of quantitative EEG activity (L. Bonanni et al., 2008; McKeith et al., 2017). Quantitative EEG can detect particular abnormalities associated with DLB, primarily localized in the posterior regions of the brain. These abnormalities include a dominant frequency before the alpha wave, which may stay steady or mix with other brain wave

activities in patterns that seem to repeat (L. Bonanni et al., 2008). These EEG findings have been hypothesized to be associated with the frequency and severity of fluctuations and REMBD (L. Bonanni et al., 2008; McKeith et al., 2017).

In summary, diagnosing DLB involves evaluating the patient's history, conducting physical and cognitive tests, and utilizing advanced tools such as imaging techniques with radiotracers like PET and SPECT, along with specialized sleep studies to assess REM sleep behavior disorder (REMBD). These methodologies collectively provide clinicians with crucial insights into the neurobiological underpinnings of DLB, aiding in early and accurate diagnosis. Moving forward, understanding these diagnostic findings serves as a pivotal step towards implementing targeted treatments and interventions aimed at managing the complex array of symptoms associated with DLB.

1.1.2.3. Treatment

Treatment and management approaches for DLB is complex, necessitating a multifaceted strategy (McKeith et al., 2017). The main components of treatment approaches comprise a thorough initial assessment for a precise diagnosis, early detection of symptoms requiring intervention, and providing guidance, education, and support to caregivers through a collaborative team approach (Alzheimer Society of Canada, 2023a; McKeith et al., 2017). DLB patients are prone to cognitive deterioration, including delirium, particularly when dealing with concurrent health issues. Moreover, certain medications such as neuroleptics have the potential to be highly dangerous in DLB patients, while dopaminergic and anticholinergic therapies may negatively affect cognition and behavior, potentially inducing confusion and psychosis. Treatment for DLB prioritizes addressing cognitive, psychiatric, motor, and other prevalent symptoms

through a selective blend of pharmacological and non-pharmacological methods (Alzheimer Society of Canada, 2023a; McKeith et al., 2017).

Pharmacological interventions play a crucial role in managing the multifaceted symptoms of DLB such as cognitive decline, motor symptoms, and fluctuations. Medications used in DLB management to help manage cognitive symptoms are cholinesterase inhibitors (ChEIs) such as donepezil and rivastigmine (Alzheimer Society of Canada, 2023a; McKeith et al., 2017). These drugs aim to enhance cholinergic transmission in the brain by increasing levels of acetylcholine (ACh), potentially ameliorating cognitive deficits, confusion, and difficulties with reasoning (Hampel et al., 2018). By modulating ACh levels, ChEIs may help alleviate some of the cognitive symptoms that significantly impact daily functioning in DLB patients (Hampel et al., 2018; McKeith et al., 2017).

Another important aspect of pharmacological management in DLB is addressing the neuropsychiatric symptoms that often accompany the disease (McKeith et al., 2017). DLB patients frequently experience hallucinations, delusions, and behavioral disturbances, which can be challenging to manage. It should be noted that patients with DLB are often hypersensitive to antipsychotic medications (McKeith et al., 2017). One key factor contributing to the hypersensitivity of DLB patients to antipsychotics is their potential to block dopamine receptors in the brain. Antipsychotic medications, particularly typical antipsychotics, including phenothiazines and butyrophenones, predominantly target dopamine D2 receptors (Chokhawala & Stevens, 2024). In DLB patients, who already have a compromised dopaminergic system due to underlying neurodegenerative processes, blocking dopamine receptors can exacerbate motor

symptoms and lead to adverse outcomes in DLB patients, sometimes indirectly contributing to an increased risk of mortality (Abadir et al., 2022; McKeith et al., 2017). However, some atypical antipsychotic medications, like quetiapine, can be used to target these symptoms while minimizing the risk of exacerbating motor impairment or inducing adverse reactions (McKeith et al., 2017). Careful consideration is given to the choice of antipsychotic medication to balance efficacy with safety, as traditional antipsychotics are generally avoided due to their potential to worsen symptoms or cause harm (McKeith et al., 2017). Additionally, medications such as selective serotonin reuptake inhibitors are options to treat depressive symptoms often experienced by DLB patients (McKeith et al., 2017).

Furthermore, DLB patients commonly present with motor symptoms such as tremor, rigidity, postural instability, and gait impairment (Alzheimer Society of Canada, 2023a; McKeith et al., 2017). Pharmacological interventions for these motor symptoms typically involve dopaminergic therapies, including levodopa preparations and dopamine agonists (McKeith et al., 2017). These medications aim to replenish dopamine levels in the brain, potentially improving motor function and mobility in affected individuals. However, parkinsonism in DLB typically shows lower responsiveness to dopaminergic therapies as compared to Parkinson's disease (PD), and their administration may heighten the likelihood of psychosis. It is crucial to carefully adjust dosages to alleviate motor symptoms but to also maintain vigilant monitoring to minimize the potential for worsening psychiatric manifestations (McKeith et al., 2017).

In addition to managing cognitive and motor symptoms, pharmacological interventions in DLB may address other clinical manifestations, such as sleep

disturbances (Allan, 2019; McKeith et al., 2017; National Institute of Neurological Disorders and Stroke, 2024). Sleep disturbances in DLB such as REMBD can significantly exacerbate pre-existing symptoms such as cognitive fluctuations and neuropsychiatric symptoms, including hallucinations and delusions (Boeve, 2019). Autonomic dysfunction and sleep disturbances can contribute to overall disease burden, impairing quality of life for both patients and caregivers (National Institute of Neurological Disorders and Stroke, 2024). Both pharmacological and non-pharmacological interventions aimed at alleviating autonomic symptoms can be prescribed to enhance patient comfort and overall quality of life (Allan, 2019). Similarly, REMBD may be managed with a combination of pharmacological and non-pharmacological strategies (Howell et al., 2023). Non-pharmacological interventions may include optimizing sleep hygiene practices, establishing regular sleep-wake routines, ensuring a comfortable sleep environment, and implementing behavioral therapies. Pharmacological treatments employ medications like clonazepam, which targets REMBD and improve overall sleep quality. Careful monitoring of these medications is essential to detect and manage potential side effects and interactions with other medications used to treat symptoms of DLB (Howell et al., 2023; McKeith et al., 2017).

Overall, pharmacological interventions in DLB necessitate a tailored approach that considers the diverse array of symptoms experienced by affected individuals. Close collaboration between healthcare providers, patients, and caregivers is essential to optimize treatment outcomes while minimizing adverse effects and drug interactions. Additionally, non-pharmacological interventions, including behavioural therapeutic strategies, physical exercise, sleep hygiene practices, and psychosocial support,

complement pharmacotherapy to enhance overall symptom management and improve the well-being of DLB patients and their caregivers (Alzheimer Society of Canada, 2023a).

1.1.2.4. Neuropathological Evaluation

The DLB Consortium has developed a consensus protocol outlining the neuropathological evaluation of DLB in post-mortem brain tissue (McKeith et al., 2005, 2017). The neuropathological diagnosis of DLB involves the microscopic examination of brain tissue post-mortem to identify characteristic hallmarks of the disease, α-synuclein LBs and LNs. Lewy pathology in brain tissue can be identified using various staining techniques such as hematoxylin and eosin (H&E) and immunohistochemical techniques specific for α-synuclein (McKeith et al., 2005). While H&E staining may effectively identify LBs in the brainstem, its efficacy diminishes for those found in cortical regions due to differences in composition (McKeith et al., 2005). Additionally, this staining method does not stain LNs. Immunohistochemistry staining for α-synuclein is considered the most accurate method as it detects all types of LBs and LNs (McKeith et al., 2005). It is crucial to assess both the extent of Lewy pathology and Alzheimer's disease-related pathology (including amyloid-β (Aβ) plaques and tau neurofibrillary tangles (NFTs)) to accurately determine how closely neuropathological findings align with the clinical presentation of DLB. This consideration is particularly important as many cases exhibit concurrent AD-related pathology, indicating a propensity for mixed pathology in DLB (McKeith et al., 2005).

The neuropathological evaluation of DLB involves a semi-quantitative characterization of the density and regional involvement of Lewy pathology in the brain. Sampling of brain tissue for neuropathological examination is obtained from key regions,

including the brainstem (BS; particularly the 9th and 10th cranial nerve nuclei, locus coeruleus (LC), and the substantia nigra), basal forebrain/limbic regions (including the nucleus basalis of Meynert (Ch4), the amygdala, transentorhinal, and cingulate), and neocortical regions (temporal, frontal, and parietal). Lewy pathology density should be semi-quantitatively characterized from the above regions using the staging system described by the DLB Consortium (McKeith et al., 2005). The semi-quantitative staging system is as follows: Stage 0 = no pathology; Stage 1 = mild pathology; Stage 2 = moderate pathology; Stage 3 = severe pathology; Stage 4 = very severe pathology (McKeith et al., 2005). Cases should be assigned a likelihood that the pathological findings will be associated with a typical DLB clinical syndrome (Table 1.3).

Table 1.3 DLB Clinical Syndrome Likelihood Based on NIA-AA AD Neuropathological Criteria

	AD neuropathologic change		
Lewy-related pathology	***NIA-AA none/low (Braak stage 0-II)***	***NIA-AA intermediate (Braak stage III-IV)***	***NIA-AA high (Braak stage V-VI)***
Diffuse neocortical *Involvement of the entire neocortex*	High	High	Intermediate
Limbic (transitional) *Affects the limbic system, particularly the hippocampus and surrounding regions*	High	Intermediate	Low
Brainstem-predominant *Primarily affects the brainstem*	Low	Low	Low
Amygdala-predominant *Primarily affects the amygdala*	Low	Low	Low
Olfactory bulb only *Restricted to the olfactory bulb*	Low	Low	Low
Substantia nigra neuronal loss to be assessed to subclassify cases into those likely or not to have parkinsonism[3]			

Adapted from McKeith *et al.* (2017).
[1]McKhann et al. (2011)
[2]Braak et al. (2006)
[3]Outeiro et al. (2019)

1.1.3. Multiple Sclerosis

MS is a chronic and immune-mediated condition of the central nervous system (CNS) that is characterized by inflammation, demyelination, and neurodegeneration (Bø et al., 1994; MS Canada, 2023a). It is one of the most common neurological conditions affecting young adults, typically diagnosed between the ages of 20 and 49 years old (MS Canada, 2023a). MS is believed to result from a combination of lifestyle, environmental, biological, and genetic factors that trigger an abnormal immune response against myelin, a protective sheath that insulates nerve fibers, facilitating efficient transmission of nerve impulses (García-García et al., 2024; MS Canada, 2023a). The hallmark neuropathological feature of MS is myelin degeneration, characterized by the formation of multiple demyelinating lesions primarily within the CNS. These lesions are characterized by inflammation, where immune cells, including T and B cells, infiltrate the CNS and attack myelin (Haki et al., 2024). This inflammatory process leads to demyelination, causing disruptions in nerve signal transmission along affected pathways. Over time, ongoing inflammation and demyelination can result in irreversible axonal and neuronal damage and loss, contributing to the progressive neurological disability seen in MS (Haki et al., 2024; MS Canada, 2023b). Clinical manifestations of MS vary widely among individuals and depend on the location and extent of CNS lesions (MS Canada, 2023b). Common symptoms include sensory disturbances such as numbness or tingling, motor deficits such as weakness or spasticity, visual impairments, fatigue, and cognitive changes, and sleep disturbances such as insomnia, sleep-related movement and breathing disorders, and circadian rhythm disturbances (MS Canada, 2023b; Sakkas et al., 2019).

Sleep disturbances in those living with MS can significantly impact quality of life, exacerbate other MS symptoms, such as fatigue, depression, or medication side effects.

MS can present as a relapsing-remitting course, where episodes of neurological symptoms (relapses or exacerbations) alternate with periods of partial or complete recovery (remissions). In some cases, MS may follow a progressive course from the onset (primary progressive MS), or it may transition from relapsing-remitting to a progressive phase over time (secondary progressive MS).

Despite advances in understanding and treatment, MS remains a challenging condition with unpredictable clinical course and variable response to therapies (The Multiple Sclerosis International Federation, 2021, p. 2). Ongoing research efforts are focused on elucidating the underlying mechanisms of MS, identifying biomarkers for early diagnosis and disease monitoring, and developing more effective therapies to better treat this condition (MS Canada, 2024).

1.1.3.1. Clinical Presentation and Diagnosis

The clinical presentation of MS is highly variable, reflecting the diverse regions of the CNS that can be affected. Symptoms are unpredictable and vary in their severity and duration (Johns Hopkins Medicine, 2024b). Initial symptoms frequently include sensory disturbances such as numbness, tingling, or a "pins and needles" sensation in the limbs, face, or trunk. Motor symptoms, such as muscle weakness, spasticity, and difficulty with coordination and balance, are also common. Visual symptoms, including optic neuritis, which manifests as painful eye movements and temporary vision loss in one eye, red-green color distortion, and diplopia (double vision), are often early indicators of the disease. As MS progresses, additional neurological deficits may develop.

Fatigue is a prevalent and often debilitating symptom that can significantly impact daily functioning. Cognitive impairment, including difficulties with memory, attention, and executive function, can occur and may progressively worsen over time. Autonomic dysfunction, presenting as bladder and bowel incontinence, urinary urgency, and constipation, is also common. Emotional disturbances, such as depression and anxiety, are frequently observed and may be a direct consequence of the disease process or a reaction to the chronic nature of the illness (Johns Hopkins Medicine, 2024b; National Institute of Neurological Disorders and Stroke, 2023). Additionally, sleep disturbances are also common among MS patients, with prevalence estimated to be between 42% and 65% (Sakkas et al., 2019). Example of sleep disturbances commonly seen in MS patients include insomnia, sleep-related movement disorders including restless legs syndrome (RLS), sleep-related breathing disorders like obstructive sleep apnea (OSA), and circadian rhythm disturbances (Sakkas et al., 2019). The nature of sleep disturbances in MS is significantly influenced by the neuroanatomical location of demyelinated lesions, as different regions of the brain each play distinct roles in the sleep-wake cycle (G. Morris et al., 2018). Medication-related side-effects may also include disruption of the sleep-wake cycle. Poor sleep may further exacerbate pre-existing symptoms and may also intensify immune activation, thereby potentially reducing quality of life and accelerating the disease process (G. Morris et al., 2018).

An MS attack, also known as a relapse, exacerbation, or flare-up, is defined as a period of neurological disturbance, which is attributable to inflammatory demyelinating lesions in the CNS. These episodes are characterized by the sudden onset or worsening of

symptoms such as sensory disturbances, motor weakness, visual problems, or coordination issues, as described above (McDonald et al., 2001).

The current classification system for MS is based on the clinical progression of the disease (Confavreux et al., 2000; National Institute of Neurological Disorders and Stroke, 2023). The most common type of MS is relapsing-remitting MS (RRMS), accounting for roughly 80% of cases, and is characterized by episodes of symptom attacks followed by periods of partial or complete remission. Periods of remission may last for weeks, months, or years. Another type of MS is primary-progressive MS (PPMS). PPMS is characterized by a continuous and gradual progression of neurological symptoms from the onset of the disease, without distinct relapses or remissions. PPMS accounts for approximately 10-15% of MS cases. One another type of MS is secondary-progressive MS (SPMS), which accounts for roughly 10% of cases. SPMS typically develops in individuals who initially have RRMS. SPMS is characterized by progressive symptom worsening, with minor remission periods. Patients may continue to experience occasional relapses, but the disease course becomes predominantly progressive. Lastly, progressive-relapsing MS (PRMS), the least common form of MS, accounting for roughly 5% of cases, is characterized by a steady progression of neurological decline from disease onset, combined with acute relapses (Confavreux et al., 2000; National Institute of Neurological Disorders and Stroke, 2023).

The current consensus on the clinical criteria for diagnosing MS is based on the 2017 McDonald criteria, which have been revised from their original publication in 2001 and a second revision in 2010 (McDonald et al., 2001; Polman et al., 2011; Thompson et al., 2018). The McDonald criteria, which integrate clinical, neuroimaging, and laboratory

data, are widely used to diagnose MS. A diagnosis of MS requires the objective evidence of dissemination in time and space of MS lesions (Table 1.4). Imaging methods, such as magnetic resonance imaging (MRI), can be used to detect lesions in the brain and can provide evidence of dissemination of lesions in both time and space. MRI abnormality criteria for dissemination in space may be fulfilled if one or more T2-hyperintense lesions are in two or more of four areas of the CNS including periventricular, cortical or juxtacortical, and infratentorial brain regions, and the spinal cord. Dissemination in time can be demonstrated by evidence of new lesions by comparing follow-up MRI scans to baseline scans or clinical relapses occurring at different points, indicating ongoing disease activity. MRI abnormality findings are integrated with clinical and other paraclinical diagnostic methods. Clinical evidence includes a detailed medical history to document symptom onset, duration, and progression, as well as a comprehensive neurological examination to identify signs of CNS involvement. Laboratory investigations include cerebrospinal fluid (CSF) analysis to examine for elevated levels of immunoglobulin G (IgG) and the presence of oligoclonal bands, indicative of the inflammatory and immunological nature of MS lesions (Thompson et al., 2018). IgG refers to a type of antibody that is often elevated in the CSF due to an elevated immune response within the CNS in MS patients. Oligoclonal bands are specific patterns of IgG seen in the CSF but not in the blood, indicating localized antibody production and serving as a key diagnostic marker for multiple sclerosis. MRI and CSF investigations can supplement a clinical diagnosis and may be essential when the clinical presentation alone is insufficient for a definitive diagnosis. Following a diagnostic evaluation, an individual is usually classified either as having MS or as not having MS. A patient with appropriate

Table 1.4 2017 McDonald Criteria for a diagnosis of multiple sclerosis (MS)

Number of clinical attacks	Number of lesions with objective clinical evidence	Additional data needed for a diagnosis of MS
≥2	≥2	None
≥2	1 (as well as clear-cut evidence of a previous attack involving a lesion in a distinct anatomical location)	None
≥2	1	Dissemination in space (DIS) demonstrated by an additional clinical attack implicating a different central nervous system (CNS) site or by magnetic resonance imaging (MRI)
1	≥2	Dissemination in time (DIT) demonstrated by an additional clinical attack or by MRI *or* demonstration of cerebrospinal fluid (CSF) -specific oligoclonal bands
1	1	DIS demonstrated by an additional clinical attack implicating a different CNS site or by MRI *and* DIT demonstrated by an additional clinical attack or by MRI *or* demonstration of CSF-specific oligoclonal bands

Adapted from Thompson *et al.* (2018).

clinical presentation who has not yet been fully evaluated or who meets only some of the criteria is considered to have 'possible MS' (Thompson et al., 2018). In summary, the clinical presentation and diagnosis of MS involve a comprehensive and multidisciplinary approach, considering the heterogeneous nature of the disease and its wide range of symptoms. Early and accurate diagnosis is essential for the timely initiation of disease-modifying therapies, which can improve long-term outcomes and quality of life for individuals with MS.

1.1.3.2. Treatment

Although there is no cure for MS, the primary objective of treatment revolves around disease modification, symptom management, and preserving neurological function, often achieved through disease-modifying therapies (DMTs) aimed at reducing the frequency of relapses and slowing disease progression (Yamout et al., 2024). DMTs for MS include injectable medications, oral medications, and monoclonal antibodies, each targeting different aspects of the immune system to reduce inflammation and disease activity. Injectable therapies, including interferon (IFN) β formulations (e.g., IFN β-1a, IFN β-1b) and glatiramer acetate, are commonly employed as first-line treatments. IFN β can modify T and B cell activity, cytokine secretion, and T regulatory cells, while glatiramer acetate specifically modulates T regulatory cells, thereby reducing the inflammatory cascade implicated in MS pathology (Babaesfahani, Patel, et al., 2024; Khanna & Gerriets, 2024; Yamout et al., 2024). Oral DMTs such as fingolimod, dimethyl fumarate, and teriflunomide offer convenience and efficacy in modulating lymphocyte trafficking or reducing immune cell proliferation centrally and peripherally (Kim et al., 2015; Yamout et al., 2024). Monoclonal antibody treatments for MS are biologic drugs,

such as natalizumab and ocrelizumab, that specifically target key immune mediators involved in the autoimmune response against myelin (Babaesfahani, Khanna, et al., 2024; Freeman & Zéphir, 2024). These therapies aim to reduce inflammation in the central nervous system (CNS), thereby slowing disease progression and potentially reducing relapse rates in individuals with multiple sclerosis (Yamout et al., 2024).

In addition to DMTs, symptomatic management of MS is equally essential in enhancing quality of life (MS Canada, 2023c). Pharmacological interventions like muscle relaxants to alleviate spasticity, while anticonvulsants and analgesics address neuropathic pain (Bernatoniene et al., 2023; MS Canada, 2023c). Anticonvulsants and analgesics address neuropathic pain in MS by modulating abnormal neuronal activity and stabilizing hyperexcitable nerve membranes, thereby reducing pain signals. They act on various targets such as voltage-gated sodium channels, calcium channels, and neurotransmitter systems to alleviate pain associated with nerve damage (Bernatoniene et al., 2023). Other medications are available to treat symptoms related to autonomic dysfunction, depression, fatigue, speech/swallowing difficulties, and other MS-related symptoms. Rehabilitation therapies, including physical therapy and occupational therapy, are also essential in maintaining mobility, strength, and independence. Furthermore, supportive care strategies such as lifestyle modifications like regular exercise tailored to individual abilities, a balanced diet, and stress management techniques can help manage symptoms and improve overall well-being. Psychological support, including counseling and participation in support groups, is crucial for addressing the emotional and social aspects of living with a chronic disease like MS. Educating patients and their caregivers about the condition, treatment options, and coping strategies is also integral to empowering

individuals to actively manage their condition and make informed decisions about their care (MS Canada, 2023c).

1.1.3.3. Neuropathological Evaluation

The hallmark neuropathological feature of MS involves multifocal areas of demyelinated lesions within the white (WM) and grey matter (GM) in the CNS, characterized by varying levels of neuroinflammation, gliosis, and neurodegeneration (Bø, 2009; Bø et al., 1994, 2003). MS demyelinated lesions can be identified using staining techniques such as Luxol fast blue or myelin basic protein (MBP) immunohistochemistry (Bø et al., 1994; Darvesh, LeBlanc, et al., 2010). Lesions can be classified by their location in GM (juxtacortical, intracortical, subpial, and deep GM) or WM (Bø, 2009; Bø et al., 1994, 2003; Haider et al., 2014). Type I lesions, also referred to as leukocortical lesions, affect both subcortical white matter (WM) and the cortex. Type II lesions, known as intracortical lesions, are confined entirely within the cortex and often feature a blood vessel at their center. Type III lesions, also called subpial lesions, extend from the pial surface into the cortex, reaching cortical layer 3 or 4 (Peterson et al., 2001). Lesions can be further histologically classified into active, chronic active, and chronic inactive categories, based on the density and distribution of microglia (Bø et al., 1994). Active WM MS lesions are characterized by hypercellularity throughout, reflecting ongoing inflammation and active demyelination, with prominent infiltration of immune cells such as lymphocytes and activated microglia. Chronic active WM MS lesions are characterized by a hypercellular rim and a relatively hypocellular center, indicating prolonged tissue degeneration with a central core of demyelination and reduced inflammatory activity, surrounded by ongoing inflammatory and demyelinating activity.

Chronic inactive WM MS lesions are hypocellular throughout, and characterized by a stable state of demyelination and lack of ongoing inflammation (Bø et al., 1994). GM MS lesion microglial activity differ from that of WM MS lesions (Peterson et al., 2001). Active GM lesions exhibit a hypercellular rim and a relatively hypercellular core and adjacent region compared to normal GM tissue (Fig. 1.5 C, D). In chronic active GM MS lesions, there is a hypercellular rim and a core that is either hypocellular or of similar density to normal GM tissue (Fig. 1.5 A, B). Chronic inactive lesions have a cellular density comparable to surrounding normal GM tissue and lack a hypercellular rim (Peterson et al., 2001).

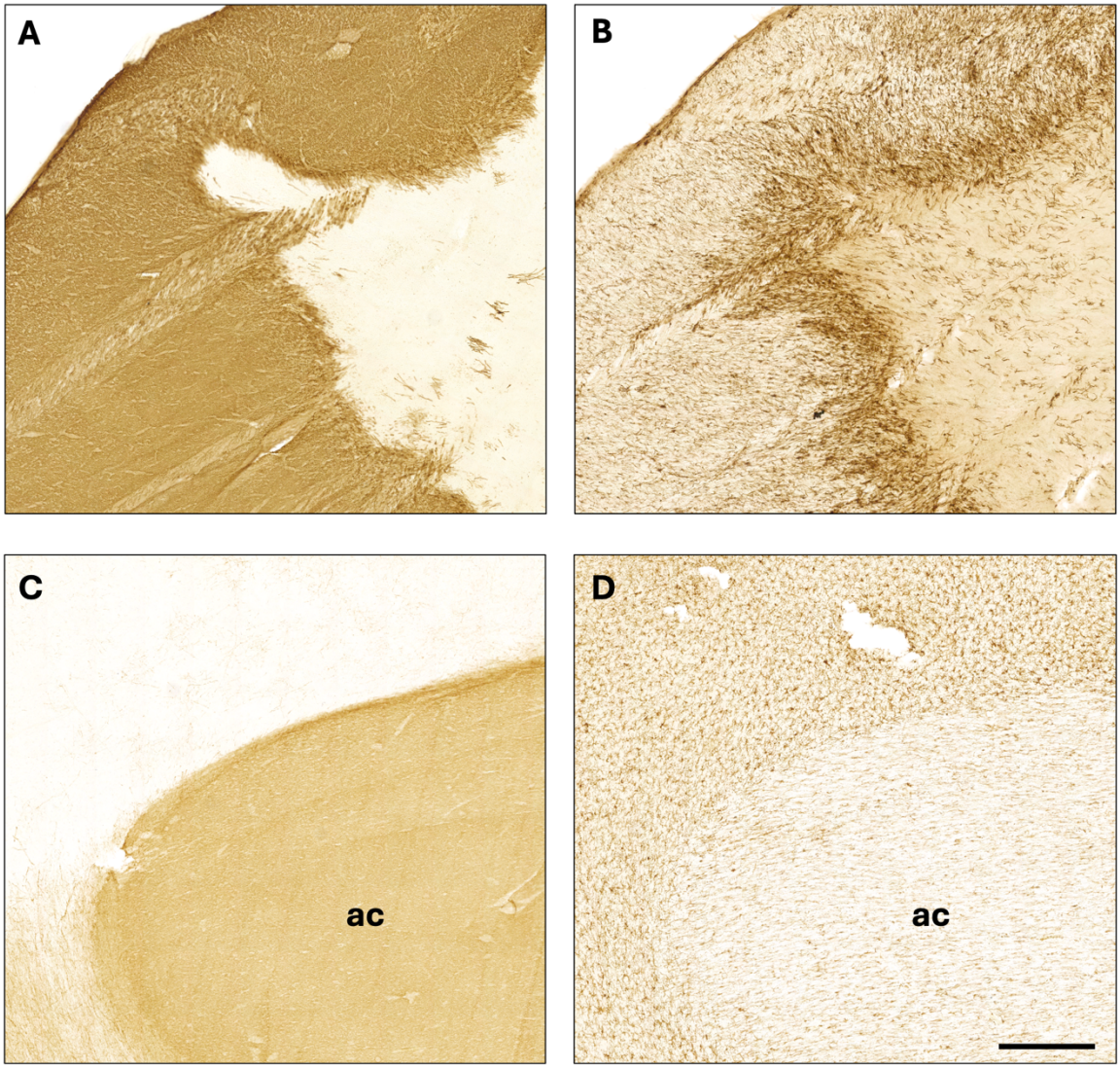

Figure 1.5 Photomicrographs of multiple sclerosis (MS) demyelinated lesions in the pons region of the brainstem (BS; top row) and basal forebrain (BF; bottom row) region adjacent to the anterior commissure (ac). Adjacent sections were immunohistochemically stained for myelin basic protein (MBP; left column) to elucidate regions of demyelination and Iba1 for microglia (right column). The demyelinated MS lesion in the BS (A, B) demonstrated chronic active MS lesion category characteristics, displaying a hypercellular rim and relatively hypocellular center. The demyelinated MS lesion in the BF (C, D) surrounding the ac demonstrated active MS lesion category characteristics, exhibiting microglial hypercellularity within the borders of the lesion. Scale bar = 500µm.

1.2. The Cholinergic System

The cholinergic system is a complex network within the nervous system that uses the neurotransmitter acetylcholine (ACh) to transmit signals between neurons and their target cells (English & Jones, 2012; Hampel et al., 2018). ACh is synthesized from choline and acetyl coenzyme A by the enzyme choline acetyltransferase (ChAT) expressed in neurons. Once synthesized, ACh is packaged into synaptic vesicles by vesicular ACh transporter (vAChT) and released into the synaptic cleft in response to an action potential arriving at the presynaptic neuron. Once released, ACh is available to bind to one of two types of receptors: muscarinic (mAChR) and nicotinic (nAChR) receptors (Dani & Bertrand, 2007; M. Ishii & Kurachi, 2006). mAChRs are G-protein coupled receptors located on the postsynaptic membrane of target cells such as neurons, smooth and cardiac muscle cells, endothelial, immune, and pancreas and salivary glandular cells (Fryer et al., 2012). mAChRs are present in the central nervous system (CNS) and the parasympathetic nervous system (PNS), where they regulate neuronal excitability and autonomic functions, respectively (M. Ishii & Kurachi, 2006). There are five subtypes of muscarinic receptors (M1-M5), each with distinct distribution and functions.

nAChRs are ligand-gated ion channels that mediate fast synaptic transmission by responding to the neurotransmitter acetylcholine. These receptors are composed of five subunits and are found in both the central and peripheral nervous systems, as well as in certain non-neuronal tissues such as the adrenal medulla. nAChRs are also present in neurons, endothelial, adrenal glandular cells, and immune cells in the CNS, PNS, the neuromuscular junction, and peripheral regions including the spleen, thymus, and lymph

nodes (Hone & McIntosh, 2018). nAChRs in neurons facilitate rapid, excitatory neurotransmission crucial for functions like cognitive processes and synaptic signaling between nerves and muscles (Hogg et al., 2003). The cholinergic system is tightly regulated by balance of ACh synthesis, vesicular packaging, vesicular release, hydrolysis by cholinesterases (ChEs), and reuptake into the presynaptic terminal by choline transporters, which transport choline molecules (English & Jones, 2012; Karczmar, 2007). ChEs are serine hydrolases comprising acetylcholinesterase (AChE) and butyrylcholinesterase (BChE), which co-regulate the degradation of ACh into acetic acid and choline (Silver, 1974). Choline can then be recycled and is taken back up into the presynaptic neuron by choline transporters to synthesize new ACh molecules in a continuous cycle, ensuring a steady supply of neurotransmitter for neuronal communication (English & Jones, 2012).

1.2.1. Cholinesterases

ChE's are a class of enzymes crucial for regulating the levels of ACh, a neurotransmitter involved in various physiological processes including arousal, memory, cognition, autonomic, immune, and muscle contraction (English & Jones, 2012). AChE and BChE are serine hydrolases crucial for regulating cholinergic neurotransmission by breaking down ACh (Silver, 1974). Stedman *et al.* (1932) first isolated these enzymes from horse serum in 1932 (Silver, 1974; Stedman et al., 1932). Subsequent research by Mendel and Rudney in 1943 identified two distinct cholinesterase enzymes: one named 'specific' cholinesterase, later identified as acetylcholinesterase, and the other initially termed 'pseudocholinesterase', now known as BChE (Darvesh et al., 2003; Mendel & Rudney, 1943). Initially, AChE was understood to be involved in neural development and

nerve impulse, while BChE's role was overlooked and regarded as a troublesome enzyme because it interfered with results of AChE experiments (Silver, 1974). Further research into ChEs demonstrated that AChE is involved in early development, behaviour, and motor function with the use of AChE knock-out mouse experiments (Duysen et al., 2002). On the other hand, BChE knock-out mice and humans with BChE mutations do not show adverse health effects. Nevertheless, mutations in BChE among humans have been associated with adverse reactions, such as apnea following the administration of succinylcholine during surgery, a muscle relaxant whose action is terminated by BChE (Andersson et al., 2019).

The active site of ChEs is the part of the protein structure which combines with ACh and is responsible for the hydrolysis of the molecule (Silver, 1974). This active site is located in a 20 Å deep active site gorge with a catalytic triad of serine, histidine, and glutamate residues (Nicolet et al., 2003; Sussman et al., 1991). AChE and BChE differ in their substrate specificities, influenced by the number and distribution of aromatic residues lining their active sites. The dimensions and composition of the enzyme gorge play a significant role in determining the selectivity of substrate and inhibitors for ChEs (Nicolet et al., 2003; Saxena et al., 1999; Sussman et al., 1991).

Beyond neurotransmission termination, AChE and BChE serve other physiological purposes. AChE is also known for functions other than ACh hydrolysis, including acting as an adhesion molecule, appears to be involved in synaptogenesis and synaptic maintenance, and neurite outgrowth (De La Escalera et al., 1990; Soreq & Seidman, 2001; Waiskopf & Soreq, 2015). BChE is also capable of detoxifying heroin and cocaine and regulating ghrelin levels (Xing et al., 2021). Both AChE and BChE are

proposed to be involved in amyloid plaque formation, as they have been observed to be associated with these plaques in the brains of individuals with Alzheimer's disease (AD) using histochemical methods (Darvesh, Reid, et al., 2010; Geula & Mesulam, 1989).

Normal AChE and BChE distribution exhibit distinct patterns throughout the brain (Friede, 1967; Mesulam et al., 1983; Mesulam & Geula, 1991). AChE is located within cholinergic neurons and their axons (Friede, 1967; Mesulam et al., 1983). AChE-positive neurons are found throughout the cerebral cortex, hippocampus, and various subcortical structures including the putamen, magnocellular nuclei of the basal forebrain (BF), and brainstem (BS) nuclei such as the pedunculopontine (Ch5) and laterodorsal tegmental nuclei (Ch6; Geula & Mesulam, 1989; Mesulam et al., 1983, 1989). In contrast, BChE-positive neurons are less widespread than AChE and are found in specific neuronal populations in the amygdala, hippocampus, and thalamus (Darvesh & Hopkins, 2003; Reid et al., 2013). Glia, such as microglia and astrocytes, white matter, and endothelial cells are observed to be BChE-positive (Friede, 1967; Mesulam et al., 2002).

ChE function in the brain is altered in neurodegenerative conditions like AD (Darvesh, Reid, et al., 2010; Perry et al., 1978). In AD, AChE activity is decreased while BChE activity is increased in the cerebral cortex, along with the association of cholinesterase activity with Aβ plaques and NFTs throughout the brain (Cash et al., 2021; Darvesh, Reid, et al., 2010; Geula & Mesulam, 1989; Perry et al., 1978). It has been observed that BChE is associated with a subset of predominantly fibrillar Aβ plaques linked to AD, rather than the non-fibrillar Aβ plaques often seen in cognitively normal older adults (Guillozet et al., 2003; Macdonald et al., 2017). Given the increase in BChE activity in the cerebral cortex and its selective association with AD-related pathology,

BChE has been proposed as a diagnostic biomarker for AD (Darvesh, 2016). The significance of ChE expression in AD pathophysiology is further highlighted by the use of ChE inhibitors (ChEIs) such as donepezil, rivastigmine, and galantamine in AD pharmacological treatment to increase ACh availability (Birks, 2006; Giacobini et al., 2022).

1.2.2. Neuroanatomy of the Cholinergic System

The cholinergic innervation of the cerebral cortex and diencephalon primarily originates from six nuclei, which are predominantly composed of ChAT- and AChE-positive neurons, with a relatively sparse presence of BChE-positive neurons in the basal forebrain (BF) and brainstem (BS). These nuclei are designated using 'Ch' nomenclature, for which the prefix Ch denotes the cholinergic nature of these neuron groups (Mesulam et al., 1983). Classified by their anatomical location and projection patterns, BF cholinergic nuclei are categorized into four primary groups: the medial septal nucleus (Ch1), the nucleus of the vertical limb of the diagonal band of Broca (Ch2), the nucleus of the horizontal limb of the diagonal band of Broca (Ch3), and the nucleus basalis of Meynert (Ch4) (Mesulam & Geula, 1988). BS cholinergic nuclei include the pedunculopontine nucleus (Ch5), the laterodorsal tegmental nucleus (Ch6), and the parabigeminal nucleus (Ch8) (Mesulam et al., 1989). For coherence, the Ch7 nucleus corresponds to the medial habenular nucleus (Mufson & Cunningham, 1988).

The Ch1 group is located in the medial septal region, situated at the midline of the brain, dorsal to Ch2 and anterior to the anterior commissure (Horváth & Palkovits, 1987). The Ch1 nucleus contains neurons that are relatively small and generally ovoid (Mesulam et al., 1983). Although designated as a cholinergic nucleus, only about 10% of the

perikaryal in this region are ChAT- and/or AChE-positive, with the remaining being gamma-aminobutyric acid (GABA)-ergic and glutamatergic (Dutar et al., 1995; Mesulam et al., 1983). Tracer experiments in animals identified that Ch1 neurons project largely to the hippocampus (Mesulam et al., 1983; Takeuchi et al., 2021).

The diagonal band of Broca was first described by Pierre Paul Broca in the late 19th century and is a bundle of fibers located within the medial septal area (Broca et al., 1888; Liu & Gentleman, 2021). The nucleus of the diagonal band of Broca is divided into two main components: the vertical limb (Ch2) and the horizontal limb (Ch3). Ch2 contains neurons with axes parallel to the course of the diagonal band, and is located ventral to Ch1 and medio-dorsal to Ch3 (Liu & Gentleman, 2021; Mesulam et al., 1983). The Ch2 group of neurons merge with those found dorsally in Ch1 and ventrally with Ch3 and Ch4. It consists of neurons that are fusiform-to-oval in shape. About 70% of neurons in Ch2 are AChE-positive, with 95-99% of these being also ChAT-positive, while non-cholinergic neurons are GABAergic and glutamatergic (Liu & Gentleman, 2021; Mesulam et al., 1983). Analogous to Ch1, Ch2 neurons also project to the hippocampus (Mesulam et al., 1983).

The Ch3 group is located along the horizontal portion of the diagonal band and ventral to Ch4, parallel to the ventral surface of the BF (Liu & Gentleman, 2021; Mesulam et al., 1983). The dominant morphology of the neurons in this group are fusiform, medium-sized, and hypochromic. Only about 1% of the neurons in Ch3 are AChE- and ChAT-positive. Neurons in this nucleus project to the olfactory bulb (Mesulam et al., 1983).

The main source of cholinergic input for the cerebral cortex is the Ch4 group (Mesulam et al., 1983; Mesulam & Geula, 1988). This group was first discovered toward the end of the 19th century by neuroanatomist Theodore Meynert (Liu et al., 2015). The Ch4 group is located within the substantia innominata, ventral to the anterior commissure, and dorsal to Ch3 (Mesulam et al., 1983). The Ch4 nucleus can be designated as an 'open' nucleus, referring to its indistinct boundaries with surrounding structures, such as Ch2 and Ch3 (Mesulam & Geula, 1988). The neurons in this group are easily recognized by their distinctive magnocellular and hyperchromic features, with mixed morphologies including fusiform, pyramidal, globoid, and multipolar (Mesulam et al., 1983). About 90% of the neurons in Ch4 are AChE- and ChAT-positive. It is the largest of the cholinergic neuron groups, spanning a distance of 13-14 mm antero-posteriorly and 18 mm medio-laterally (Mesulam, 2004; Mesulam & Geula, 1988). Due to its substantial size and its extensive projections to various brain regions, this nucleus can be anatomically subdivided into six distinct subsectors, designated as anteromedial (Ch4am), anterolateral (Ch4al), anterointermediate (Ch4ai), intermedioventral (Ch4iv), interomediodorsal (Ch4id) and posterior (Ch4p) regions (Mesulam et al., 1983).

Ch4am and Ch4al are located at the same rostro-caudal extent and are adjacent, allowing the designation of Ch4am/al to represent the most anterior subsector of this nucleus. In many instances, a vascular structure is present in this subsector and provides a demarcation between Ch4am and Ch4al. The rostral extent of Ch4am/al begins with the landmark of the crossing of the anterior commissure (Table 1.5). Based on tracing experiments in primates, Ch4am/al projects to the medial aspect of the cerebral

hemispheres, frontoparietal opercular region, and to the amygdala (Fig. 1.6; Mesulam et al., 1983).

Just caudal to Ch4am/al is the Ch4ai subsector. This region is unique to humans, as it was introduced to maintain coherence with the anatomy of primate brains, given the more gradual transition from anterior to intermediate subsectors in the human brain (Mesulam & Geula, 1988). Macroscopic anatomical landmarks of this subsector include the division of the globus pallidus (GP) into internal (GPi) and external (GPe) regions by the internal medullary lamina, and the lateral recession of the anterior commissure ventral to putamen and GPe. (Table 1.4; Liu et al., 2015; Mesulam & Geula, 1988). As this subsector is unique to humans and tracing experiments are not feasible, only theoretical conjectures have been formulated regarding its projection regions (Fig. 1.6). Since it is a transitional region between the anterior and the intermediate subdivisions, it is possible that it projects to some or all the regions associated with the anterior and intermediate Ch4 subsectors such as the medial aspects of the cerebral hemispheres, frontoparietal opercular region, amygdala, laterodorsal frontoparietal, peristriate, and midtemporal regions (Liu et al., 2015; Mesulam et al., 1983).

The intermediate subdivision, Ch4i, lies immediately caudal to Ch4ai. Ch4i is characterized by the presence of the white matter fiber bundles of the ansa peduncularis which further divides it into ventral (Ch4iv) and dorsal (Ch4id) subsectors (Table 1.5). Ch4iv and Ch4id are located at the same rostro-caudal extent and are in close proximity and exhibit comparable projection patterns, thus justifying the designation of Ch4iv/id for the intermediate subdivision. Tracing experiments in primates have demonstrated that

Ch4iv/id projects to laterodorsal frontoparietal, peristriate, and midtemporal regions (Figure 1.6; Liu et al., 2015; Mesulam et al., 1983).

The most posterior component of Ch4 is designated as Ch4p. Anatomical landmarks of this region include the lateral anterior commissure located ventrolaterally to the putamen and at the level of the mammillary body (Table 1.5). The neurons in this region abut upon the putamen and amygdala (Mesulam et al., 1983; Mesulam & Geula, 1988). Tracing experiments in primates have demonstrated that Ch4p projects to auditory association areas in the superior temporal and temporal polar regions (Figure 1.6; Mesulam et al., 1983).

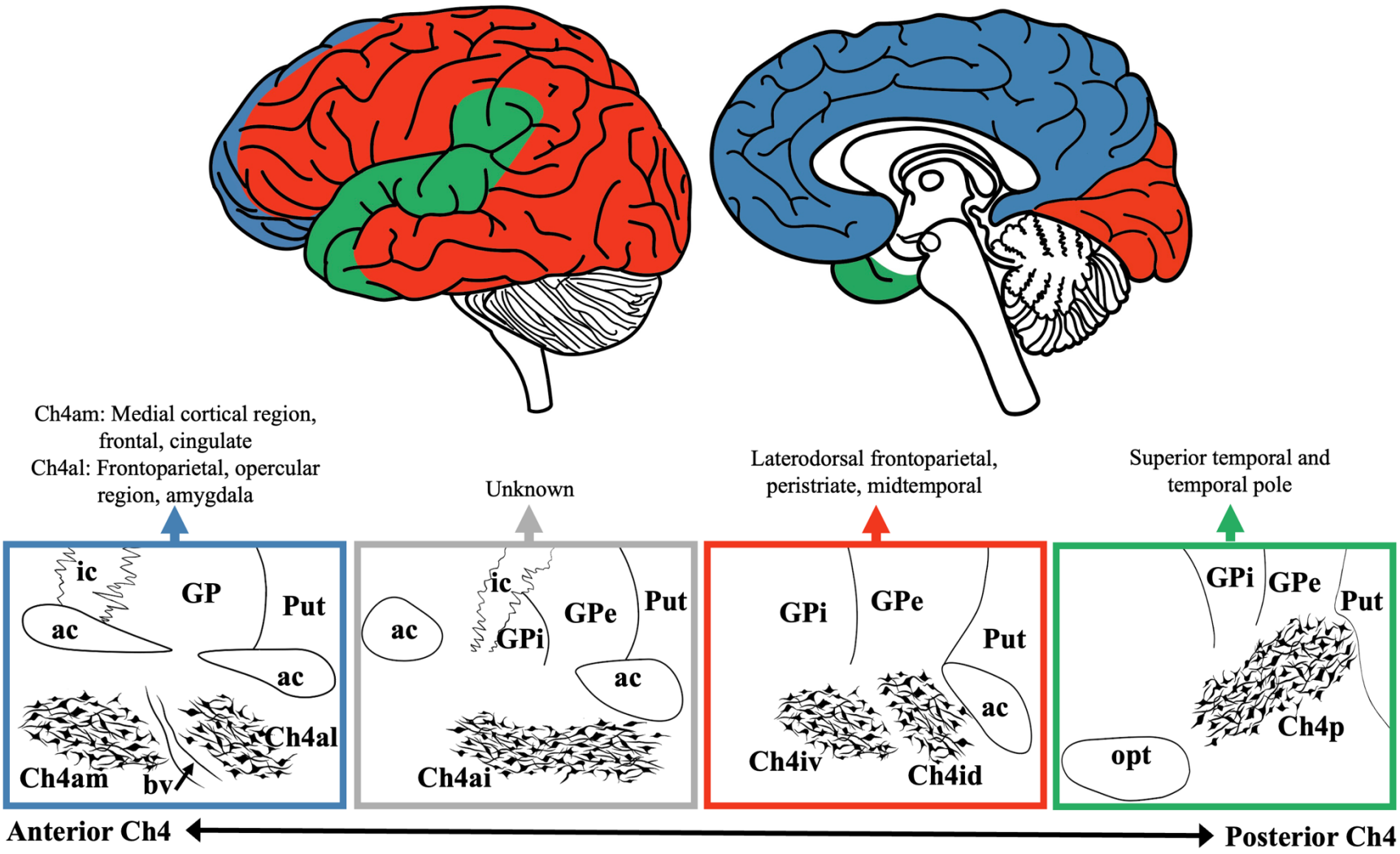
Ch4am: Medial cortical region, frontal, cingulate
Ch4al: Frontoparietal, opercular region, amygdala
Unknown
Laterodorsal frontoparietal, peristriate, midtemporal
Superior temporal and temporal pole
ic
GP
Put
ac
ac
Ch4al
Ch4am
bv
ic
GPi
GPe
Put
ac
ac
Ch4ai
GPi
GPe
Put
ac
Ch4iv
Ch4id
GPi
GPe
Put
Ch4p
opt
Anterior Ch4
Posterior Ch4

Figure 1.6 Diagram illustrating projections from the nucleus basalis of Meynert subsectors. Each subsector is distinguished by the differential distribution of choline acetyltransferase (ChAT) or acetylcholinesterase (AChE) neurons. This figure was based on slides stained for ChAT, with ChAT neurons shown as black neurons in the figure, along with distinctive surrounding landmarks. Abbreviations: ac, anterior commissure; bv, blood vessel; Ch4, nucleus basalis of Meynert; Ch4am, anteromedial subsector of the nucleus basalis of Meynert; Ch4al, anterolateral subsector of the nucleus basalis of Meynert; Ch4ai, anterointermediate subsector of the nucleus basalis of Meynert; Ch4iv, intermedioventral subsector of the nucleus basalis of Meynert; Ch4id, intermediodorsal anteromedial subsector of the nucleus basalis of Meynert; Ch4p, posterior sector of the nucleus basalis of Meynert; GP, globus pallidus; GPe, globus pallidus externus; GPi, globus pallidus internus; ic, internal capsule; opt, optic tract; Put, putamen. Adapted from Liu *et al*. (2015), Mesulam *et al*. (1986).

Table 1.5 Proposed macroscopic and microscopic landmarks for the identification of anterior, intermediate, and posterior subsectors of Ch4

Ch4 Region	**Macroscopic landmark**	**Microscopic landmark**	**Corresponding Ch4 subsectors**
Anterior	Anterior commissure (AC; continuous or split into medial and lateral extents)	Supraoptic nucleus Preoptic area	Ch4am, Ch4al
Anterior-Intermediate	Globus pallidus internus (GPi) Globus pallidus externus (GPe) Lateral AC (receded ventral to putamen and GPe)	Supraoptic nucleus Internal medullary lamina	Ch4ai
Intermediate	Lateral AC (receded ventral to putamen and GPe)	Ansa peduncularis	Ch4iv, Ch4id
Posterior	Lateral AC is receded ventrolateral to putamen Mammillary body (MMB)	Neurons adjacent to putamen and amygdala	Ch4p

The rostral human brainstem contains cholinergic neurons in the oculomotor, trochlear, the pedunculopontine nucleus (Ch5) and the laterodorsal tegmental nucleus (Ch6) within the pontomesencephalic reticular formation, and parabigeminal nucleus (Ch8). In contrast to the cholinergic neurons in the oculomotor, trochlear, and Ch8 nuclei, Ch5 and Ch6 do not have defined boundaries. These two nuclear constellations have neurotransmitter heterogeneity, especially Ch6 neurons which intermingle with the catecholaminergic neurons of the locus coeruleus.

The Ch5 nucleus at its most rostral extent can be observed caudal to the red nucleus and dorsal to the substantia nigra, with its most caudal extent to be located at the mid-pontine level. The optimal visualization of neurons within this nucleus is achieved at the anatomical level corresponding to that of the trochlear motor nucleus. Visible at this level is a dense cluster of cholinergic neurons located laterally to the decussation of fibers within the superior cerebellar peduncles, which is designated as the compact sector of Ch5 (Ch5c). Roughly 90% of Ch5c neurons are ChAT-positive. The diffuse sector of Ch5 (Ch5d), enveloping Ch5c, also comprises ChAT-positive neurons, accounting for approximately 75% of the total neuronal population. All areas containing the ChAT-positive neurons of Ch5 also contained the enzyme nicotinamide adenine dinucleotide phosphate-diaphorase (NADPH-d) in an identical distribution, where 90% of NADPH-d neurons are also ChAT-positive. NADPH-d is an enzyme present in specific neuronal groups co-localized with nitric oxide synthase (NOS), responsible for catalyzing the synthesis of nitric oxide (NO; Dawson et al., 1991; Hope et al., 1991; Mesulam et al., 1989). NO is a neuronal, vascular, and immune messenger molecule found throughout the brain and peripheral tissues (Dawson et al., 1991). Observations of NADPH-d

histochemistry suggests the enzyme to be a helpful technique for identifying cholinergic neurons within the Ch5 region (Mesulam et al., 1989).

Located caudally in the brainstem, relative to Ch5 and the trochlear nucleus, lies the Ch6 nucleus, positioned within the rostral pontine central grey matter. The Ch6 group makes its most rostral appearance at the level of the trochlear nucleus, reaches its peak prominence just caudal to the region of highest density for Ch5, and extends to the mid-to-lower pons. Ch6 is bounded ventrally by the medial longitudinal fasciculus and dorsally by the fourth ventricle. About 80%-90% of neurons within Ch6 are ChAT- and AChE-positive. Due to the absence of clearly defined boundaries of this nucleus, its cholinergic neurons extend into the LC and medial longitudinal fasciculus. The purple ChAT reaction product of Ch6 neurons can be readily differentiated from the brown color and granular appearance of neuromelanin in LC pigmented neurons. Similar to Ch5, within the Ch6 nucleus, nearly all ChAT-positive neurons also exhibit NADPH-d-rich staining. This implies that NADPH-d histochemistry also serves as a reliable method for identifying Ch6 neurons (Mesulam et al., 1989).

Because of the absence of clear boundaries and significant intermingling of neurons between the Ch5 and Ch6 nuclei, the term "Ch5-Ch6" is employed to denote the rostral cholinergic neuron clusters (Mesulam et al., 1989). Collectively, Ch5-Ch6 neurons project to the thalamus, hypothalamus, and cortically-projecting Ch4 neurons, and are involved in the neural circuitry of the reticular activating and extrapyramidal systems (Mesulam et al., 1989).

1.2.3. Sleep and the Cholinergic System

The regulation of the sleep-wake cycle involves the interplay of cholinergic, glutamatergic, GABAergic, and monoaminergic neurotransmitter systems (Scammell et al., 2017). The cholinergic system promotes wakefulness and REM sleep through cortical activation and sensory processing, while its reduced activity during NREM sleep facilitates restorative processes and memory consolidation (Deurveilher & Semba, 2011; Hobson et al., 1975; Kroeger et al., 2017). Cholinergic neurons located in the BF and BS project to widespread areas such as the thalamus, hypothalamus, cerebral cortex, and hippocampus, thereby broadly influencing various aspects of arousal and sleep (Mesulam et al., 1983, 1989; Scammell et al., 2017).

BF cholinergic neurons, particularly those in Ch4, fire in association with fast cortical rhythms during wakefulness and REM sleep, but much less during NREM sleep (Deurveilher & Semba, 2011; M. Xu et al., 2015). Injecting carbachol, a cholinergic agonist, into the BF of the cat increased wakefulness (Baghdoyan et al., 1993). In a study researching mouse cholinergic BF neurons genetically targeted with channelrhodopsin 2, optogenetic activation of these neurons during wakefulness or REM sleep showed sustained cortical activation (Han et al., 2014). Light stimulation of these neurons during NREM sleep facilitated transitions to either wakefulness or REM sleep, suggesting that activation of BF cholinergic neurons facilitates the transition from NREM sleep but does not dictate the direction of the transition (Han et al., 2014). BF cholinergic neurons are well-documented as key promoters of wakefulness and REM sleep, highlighting their dual influence in regulating these distinct states of consciousness.

BS cholinergic neurons, primarily comprising the Ch5 and Ch6 nuclei, project to numerous subcortical regions involved in regulating arousal. These neurons exert their influence by projecting to various subcortical structures involved in sleep-wake regulation, including the thalamus, BF, and hypothalamus (Mesulam et al., 1989). Similar to the basal forebrain, these neurons are most active during wakefulness and REM sleep (Boucetta et al., 2014). BS cholinergic neurons are involved in the modulation and initiation of REM sleep. In fact, selective optogenetic activation of Ch5 and Ch6 cholinergic neurons during NREM sleep is sufficient to induce REM sleep (Van Dort et al., 2015). BS cholinergic neurons play an important role in the modulation and control of sleep-wake states, influencing transitions between wakefulness, NREM sleep, and REM sleep through their widespread projections and neuromodulatory effects. Moreover, Ch5 and Ch6 neurons influence transthalamic processing of sensory information in ways that can modulate complex behavioural states such as arousal and attention (Huerta-Ocampo et al., 2020). Transthalamic processing refers to the relay and integration of sensory and motor information through the thalamus, a central brain structure. This process involves the thalamus receiving input from various sensory pathways, processing this information, and then transmitting it to the appropriate areas of the cerebral cortex for further interpretation and response. The thalamus acts as a crucial hub for modulating and synchronizing neural activity, ensuring coherent and coordinated brain function. These projections have long been linked with initiating and sustaining tonic activation mechanisms within thalamocortical systems, which are crucial for the desynchronization of the electroencephalogram observed during wakefulness and REM sleep (Steriade et al., 1990).

1.2.4. Cholinergic System in Neurodegenerative Disorders

In neurodegenerative disorders (NDDs), pronounced alterations occur in the cholinergic system, contributing to the pathophysiology of these conditions (Davies & Maloney, 1976; Perry et al., 1978). Alzheimer's disease (AD) is perhaps the most extensively studied NDD associated with cholinergic changes and dysfunction, where there is a marked decline in cholinergic neurons, particularly in the BF (Geula et al., 2021; Whitehouse et al., 1981). This neuronal loss leads to a substantial decrease in cortical and hippocampal ACh levels, correlating with deficits in learning, memory, and behaviour (Ballard et al., 2005; Hampel et al., 2018; Mesulam, 2004). The activity of ChAT is notably reduced in AD, further diminishing ACh synthesis (Mesulam et al., 1983). Therapeutic strategies, such as ChEIs, aim to mitigate these deficits by enhancing cholinergic neurotransmission (Birks, 2006). However, these treatments primarily provide symptomatic relief without addressing the underlying neurodegenerative processes (Conti Filho et al., 2023).

Studies have shown that AChE activity is decreased and that BChE activity may be increased or remain stable compared to normal brain tissue (Darvesh, Reid, et al., 2010; Perry et al., 1978). ChEs have been observed to be associated with NFTs and Aβ plaques, the pathological hallmarks of AD (Darvesh, Reid, et al., 2010; Geula & Mesulam, 1995; Mesulam et al., 1989; Perry et al., 1978). AChE and BChE, however, associate with pathology in AD cases, but not the NFTs and Aβ plaques found in cognitively normal older individuals (Macdonald et al., 2017; Mesulam & Geula, 1994). Moreover, visualizing ChE activity associated with NFTs and Aβ plaques requires different experimental conditions than those used to visualize ChE activity in neurons

(Eskander et al., 2005; Geula & Mesulam, 1989). Specifically, a lower pH of 6.8 is optimal for staining ChE activity associated with NFTs and Aβ plaques, whereas a higher pH of 8.0 is ideal for staining normal neuronal ChE activity (Darvesh, Reid, et al., 2010; Geula & Mesulam, 1989). At the present, it is unclear why histochemical ChE activity in pathological conditions differs from that of normal conditions. These findings highlight the predictive value of ChE's, especially BChE, as a biomarker for AD that could facilitate disease diagnosis and management (Darvesh, 2016; DeBay et al., 2017; Macdonald et al., 2017). Understanding the precise mechanisms of cholinergic dysfunction in these disorders is crucial for developing more effective therapeutic interventions.

1.2.5. Neuroinflammation and the Cholinergic System

Inflammation serves as the body's defense mechanism, activating the immune response to eliminate pathogens, remove damaged cells, and initiate tissue repair processes (Lyman et al., 2014). The inflammatory process is marked by the production of pro-inflammatory cytokines, including tumor necrosis factor-alpha (TNF-α), interleukin-1β (IL-1β), and interleukin-6 (IL-6), and other chemokines (Leng & Edison, 2021). Cytokines and chemokines are signaling proteins that regulate immune responses, with cytokines modulating the activity and communication of immune cells and chemokines directing the migration of these cells to sites of inflammation or injury. In the brain, the primary immune cells involved in the inflammatory response are microglia and astrocytes (Kettenmann & Ransom, 2013). Activated microglia and astrocytes release inflammatory mediators, including pro-inflammatory cytokines. Despite its protective intentions, a prolonged or exaggerated inflammatory response can lead to tissue damage and

contribute to disease pathology. Chronic neuroinflammation, primarily driven by activated glia such as microglia, contributes to the progression of inflammatory conditions (Lyman et al., 2014; Reale & Costantini, 2021).

The cholinergic system and neuroinflammation are intricately linked through a complex interplay that significantly impacts the pathophysiology of various NDD such as AD, DLB, and MS (Reale & Costantini, 2021). Acetylcholine (ACh), the primary neurotransmitter of the cholinergic system, is involved in modulating immune responses and inflammatory processes in the central nervous system (CNS). One of the key mechanisms by which the cholinergic system influences neuroinflammation is through the cholinergic anti-inflammatory pathway. The cholinergic anti-inflammatory pathway includes the vagus nerve wherein ACh interacts with alpha-7 nicotinic acetylcholine receptors (α7nAChR) on immune cells such as microglia (Dani & Bertrand, 2007; Hone & McIntosh, 2018). Activation of α7nAChR inhibits the release of pro-inflammatory cytokines, thereby exerting an anti-inflammatory effect (H. Wang et al., 2003).

Cholinergic neurons, particularly in the BF, undergoes significant degeneration in AD, leading to decreased levels of ACh in the brain (Geula et al., 2021). This reduction in ACh diminishes the activation of α7nAChR on microglia, resulting in an unhindered release of pro-inflammatory cytokines and perpetuation of neuroinflammation. The impaired cholinergic system, with reduced ACh levels, fails to adequately regulate the inflammatory responses, leading to a continuous cycle of neuroinflammation and neurodegeneration (Leng & Edison, 2021; Reale & Costantini, 2021).

1.3. Sleep Disturbances in Neurodegenerative Disorders

1.3.1. Normal Sleep-Wake Cycle

The sleep-wake cycle is a complex physiological process that governs the alternating periods of wakefulness and sleep in humans and other animals (Pace-Schott & Hobson, 2013). As defined by Pace-Schott, sleep is defined as a reversible state of reduced responsiveness to external stimuli, marked by characteristic changes in central and peripheral activity and physiology, typically accompanied by altered consciousness, a low level of motor output, and behavioral quiescence (2010). Wakefulness, on the other hand, was defined as a state characterized by high responsiveness to external and internal stimuli, enhanced motor output, and active engagement with the environment, marked by alertness and conscious awareness (Pace-Schott, 2010).

Sleep is broadly categorized into two main types: non-rapid eye movement (NREM) sleep and rapid eye movement (REM) sleep (Stickgold & Walker, 2009). NREM sleep is further subdivided into three stages: NREM1, NREM2, and NREM3. Electroencephalography (EEG) is a neurophysiological monitoring method that records electrical activity of the brain using electrodes placed on the scalp, providing insights into brain function and diagnosing neurological conditions. Brain waveforms, detectable by electroencephalography (EEG), consist of different frequency bands that reflect various states of brain activity (Stickgold & Walker, 2009). Delta waves, ranging from 0.5 to 4 Hz, are associated with deep sleep, such as NREM3 sleep. Theta waves, spanning 4 to 7 Hz, are linked to drowsiness and NREM1 sleep. Alpha waves, found in the 8 to 12 Hz range, are present during relaxed wakefulness and meditative states. Beta waves, between 13 and 30 Hz, indicate active thinking, concentration, and alertness. Finally, gamma

waves, which range from 30 to 100 Hz, are associated with high-level cognitive processing and attention (Stickgold & Walker, 2009). The onset of NREM sleep is gradual and marked by a slowing of brain waves as detected by EEG. This transition slows from beta (14-25 Hz) and gamma (25-80 Hz) frequencies, which are present during wakefulness with eyes open and high attention levels, to alpha (8-13 Hz) frequencies, seen during quiet waking with eyes closed. NREM1, the initial stage of NREM sleep, represents the transition from wakefulness to sleep. During NREM1, theta waves (4-7 Hz) dominate the EEG recordings, accompanied by occasional alpha waves (8-13 Hz). Muscle tone begins to relax, and there may be fleeting sensations or sudden muscle contractions known as hypnic jerks. NREM2 sleep follows NREM1 and constitutes a significant portion of sleep time, typically about 45-55%. This stage is characterized by two distinct waves forms: sleep spindles, brief bursts of rhythmic brain activity (sigma frequencies, 12-14 Hz) and K-complexes, which are large, slow waves. NREM3, also known as slow-wave sleep (SWS), is the deepest stage of NREM sleep, comprising approximately 15-25% of total sleep time. Delta waves (1-3 Hz), which are low frequency and high amplitude waves, predominate the EEG during NREM3, reflecting synchronized neuronal activity. NREM3 plays a crucial role in memory consolidation by facilitating the transfer of information from the hippocampus to the neocortex, thereby promoting long-term memory storage (Born, 2010). The synchronized oscillatory activity during NREM3 supports synaptic plasticity and the reactivation of neural circuits involved in learning, thereby enhancing memory retention and integration (Born, 2010). Finally, REM sleep marks a distinct phase characterized by rapid eye movements, vivid dreaming, skeletal muscle atonia, and heightened brain activity resembling wakefulness

(Scammell et al., 2017; Stickgold & Walker, 2009). REM sleep has historically been referred to as 'paradoxical' sleep due to its EEG pattern closely resembling wakefulness. REM sleep EEG is characterized by fast and random saw-tooth waves. REM sleep typically begins about 90 minutes after falling asleep and recurs cyclically throughout the night, constituting approximately 20-25% of total sleep time in adults. Neurologically, REM sleep involves intricate interactions between brainstem structures—such as the pons and medulla—and higher cortical areas to generate oculomotor muscle movement while suppressing skeletal muscle tone (Stickgold & Walker, 2009).

The organization of the sleep-wake cycle occurs in cycles lasting approximately 90-120 minutes (Stickgold & Walker, 2009). Each cycle progresses through NREM and REM stages, starting with NREM sleep and progressing from N1 to N2, N3, and then into REM sleep. The distribution of these stages varies throughout the night, with more NREM deep sleep occurring in the first half and increased REM sleep in later cycles, reflecting the homeostatic regulation of sleep need and recovery. The early cycles are dominated by slow-wave sleep (NREM3), which is crucial for physical restoration and memory consolidation. As the night progresses, the proportion of REM sleep increases, playing a vital role in emotional regulation, memory processing, and cognitive function. This cyclical pattern ensures that the body and brain receive a balanced mix of restorative processes throughout the night, adapting to the body's immediate needs for recovery and preparation for the next day (Stickgold & Walker, 2009)

1.3.2. Sleep Neuroanatomy

The timing of transition between sleep and waking is regulated by various structures of the brain, including the suprachiasmatic nucleus (SCN) in the ventromedial

region of the hypothalamus, orexin neurons located in the lateral hypothalamus, histaminergic neurons in the posterior hypothalamus, melatonin synthesis by the pineal gland, and the cholinergic neurons in BF and BS (Scammell et al., 2017).

The SCN, located in the anterior hypothalamus, acts as the master circadian rhythm pacemaker, receiving input from light-sensitive cells in the retina via the retinohypothalamic tract (Stickgold & Walker, 2009). The circadian rhythm encompasses a 24 h rhythmic cycle of fluctuations in hormone secretion, body temperature, and the sleep-wake cycle. SCN neurons possess molecular clocks that uphold the circadian rhythm and sleep-wake cycle through interconnected positive and negative feedback mechanisms governing the transcription and translation of genes, such as *CLOCK*, *BMAL1*, *CRY*, and *PER* (Partch et al., 2014). The genes *CLOCK*, *BMAL1*, *CRY*, and *PER* play crucial roles in regulating the circadian rhythm, the internal biological clock that orchestrates daily physiological and behavioral cycles. *CLOCK* and *BMAL1* are transcription factors that form a heterodimer, binding to E-box elements in the promoter regions of target genes, including the Period (*PER*) and Cryptochrome (*CRY*) genes, thereby activating their transcription. The PER and CRY proteins accumulate in the cytoplasm and eventually translocate back to the nucleus, where they inhibit the activity of the *CLOCK-BMAL1* complex, creating a feedback loop that generates the approximately 24-hour cycle of circadian rhythms. This feedback loop is essential for maintaining the proper timing of sleep-wake cycles, hormone release, and other daily biological processes, ensuring that they are synchronized with the environmental light-dark cycle (Partch et al., 2014). This input synchronizes the internal biological clock with the 24-hour day-night cycle, naturally entrained by external stimuli such as light, known

as zeitgebers (German for “time-giver”), physical activity, meal timing, and social interactions (Scammell et al., 2017; Stickgold & Walker, 2009).

Orexin, also known as hypocretin, is a neuropeptide produced in the hypothalamus that plays a important role in regulating wakefulness, arousal, and appetite by modulating the activity of various neural circuits involved in sleep-wake states (Stickgold & Walker, 2009). Orexin neurons are active during wakefulness and decline in activity at sleep onset and remain quiescent during REM. Orexin neurons aim to stabilize the waking state by exciting wake-promoting regions such as other regions in the hypothalamus, BF, cerebral cortex, and BS nuclei such as the locus coeruleus (LC), and dorsal raphe (DR). Orexin neurons are crucial in maintaining wakefulness and preventing inappropriate transitions to sleep states (Stickgold & Walker, 2009). This is highlighted by the link between orexin deficiency and narcolepsy, a condition marked by excessive daytime sleepiness and sudden episodes of muscle weakness, known as cataplexy. The absence or dysfunction of orexin signaling disrupts the stability of wakefulness, leading to the uncontrollable onset of sleep and muscle atonia, emphasizing the importance of orexin in regulating sleep-wake homeostasis and muscle tone. (Stickgold & Walker, 2009). Beyond their role in sleep-wake regulation, orexin neurons also integrate metabolic, circadian, and emotional signals, thereby linking energy homeostasis and arousal states. This integration ensures that wakefulness ensues during periods of high energy demand or emotional stress (Pace-Schott & Hobson, 2013).

The tuberomammillary nucleus (TMN), another region important to sleep located in the posterior hypothalamus, is the sole source of histamine in the brain (Scammell et al., 2017). Histamine acts as a neurotransmitter that promotes wakefulness through its

excitatory effects on various brain regions, including the cerebral cortex and thalamus. Conversely, histamine release decreases during sleep, facilitating the transition from wakefulness to sleep states (Scammell et al., 2017). Certain anti-nausea and allergy medications, such as first-generation antihistamines like dimenhydrinate and promethazine, exert sedative effects by antagonizing histamine receptors in the CNS (Yoshikawa et al., 2021). By blocking histaminergic transmission, these drugs mitigate histamine's wake-promoting effects, leading to sedation, drowsiness, and reduced alertness. This mechanism underlies their clinical use in managing nausea and motion sickness, as well as their off-label use as sleep aids due to their ability to induce calming effects and promote relaxation. Thus, histamine not only regulate sleep but also serve as a target for therapeutic interventions aimed at inducing sedation and alleviating symptoms associated with hyperarousal states (Yoshikawa et al., 2021).

The pineal gland is a small endocrine organ located in the mid-line of the brain, in the epithalamus, outside the blood-brain barrier (BBB) and attached to the roof of the third ventricle by a short stalk (Arendt & Aulinas, 2000). The pineal gland plays a crucial role in the regulation of the sleep-wake cycle through the cyclic production of melatonin, a hormone that promotes sleep. Melatonin synthesis and release is therefore closely linked to the circadian rhythm, which is primarily governed by the SCN. The SCN receives photic information from the retina via the retinohypothalamic tract and, in response to the light-dark cycle, regulates the timing of melatonin secretion by the pineal gland. During the night, the absence of light signals the SCN to stimulate the pineal gland to produce melatonin, which is then released into the bloodstream and cerebrospinal fluid (CSF). Elevated melatonin levels promote sleep by reducing neuronal activity and

lowering core body temperature. Conversely, exposure to light during the day inhibits melatonin synthesis, promoting wakefulness. The secretion of melatonin peaks in the middle of the night and gradually decreases towards morning, helping to regulate the sleep-wake cycle and synchronize it with the external environment (Arendt & Aulinas, 2000).

In addition to the SCN, hypothalamus, and pineal gland, the BF plays a pivotal role in the regulation of the sleep-wake cycle through its diverse neuronal populations and their wide-ranging projections to the cerebral cortex and other brain regions (Lee et al., 2005; Stickgold & Walker, 2009). BF cholinergic neurons are particularly active during wakefulness, help to desynchronize the EEG, and promote REM sleep (Stickgold & Walker, 2009; M. Xu et al., 2015). More specifically, BF cholinergic nuclei involved in the sleep-wake cycle include the Ch1, Ch2, and Ch4 nuclei. The Ch1 and Ch2 nuclei project to the hippocampal region, and have long been purported as key nuclei in the generation of theta oscillations (Boyce et al., 2016; Király et al., 2023; Nuñez & Buño, 2021). The Ch4 nucleus can be parcellated into several subsectors that project to various cortical regions. Out of these, the anterior Ch4 (Ch4a) subsectors are most likely to be involved in the regulation of the sleep-wake cycle based on projections. The Ch4a subsectors project in general to frontal and medial regions, while the intermediate and posterior regions project to anterolateral, occipital, and temporal regions. Frontal brain regions are crucial for sleep due to their circuit connections with subcortical structures involved in promoting REM sleep (Hong et al., 2023). Though most BF neurons are associated with fast EEG activity linked with wakefulness and REM, others are active during NREM (Scammell et al., 2017). These NREM-active neurons are mainly

GABAergic and contribute to the initiation and maintenance of NREM sleep through projections to the neocortex (Scammell et al., 2017). The balance between these excitatory and inhibitory influences in the basal forebrain is crucial for the regulation of sleep architecture, allowing smooth transitions between wakefulness, NREM sleep, and REM sleep. Nevertheless, further research is required to gain a clearer understanding of the specific roles played by cholinergic BF nuclei in the sleep-wake cycle.

The BS is a key component in the regulation of the sleep-wake cycle, containing several key nuclei that orchestrate transitions between wakefulness, NREM sleep, and REM sleep (Stickgold & Walker, 2009). Central to this regulation is the reticular activating system (RAS), a network of interconnected neurons in the BS that promotes arousal and wakefulness and is composed of four main cell groups: Ch5, Ch6, raphe nucleus, and the LC. The RAS exerts its effects via projecting ascending pathways to the thalamus and cerebral cortex. Descending RAS pathways target postural and locomotion systems and controls the atonia characteristic of REM sleep (Stickgold & Walker, 2009).

The Ch5 and Ch6 nuclei are the two major cholinergic cell groups in the BS. Ch5 and Ch6 neurons project to the thalamus, hypothalamus, and cortically-projecting Ch4 neurons (Mesulam et al., 1989), and are involved in the neural circuitry of the reticular activating and extrapyramidal systems, and are involved in the control of REM sleep initiation and maintenance (Boeve et al., 2007; Scammell et al., 2017). These cholinergic BS nuclei also play a crucial role in the initiation and maintenance of REM sleep by activating cortical and thalamic neurons, leading to the characteristic REMs and skeletal muscle atonia observed during this stage (Boeve et al., 2007; Scammell et al., 2017; Stickgold & Walker, 2009).

The LC, situated in the upper dorsolateral pontine tegmentum and one of the primary cell groups of the RAS, is the brain's largest source of norepinephrine. (Benarroch, 2018; Stickgold & Walker, 2009). The LC fires in two distinct modes: tonic and phasic. The switch between these two firing modes regulates the different behavioural states of the individual. Tonic firing is related to the arousal and waking state, which decreases with quiet waking and disengagement with the environment and ceases during REM sleep, while phasic firing is characteristic of focused attention (Benarroch, 2018). During normal REM sleep, skeletal muscle atonia, a near-complete paralysis of voluntary muscles, preventing the physical enactment of dreams, is achieved through concerted efforts by brainstem networks including the coeruleus complex in the pons and the magnocellular nucleus in the medulla oblongata (Ehrminger et al., 2016). The suppression of LC activity during REM sleep disinhibits inhibitory interneurons in the ventromedial medulla, which in turn project to the spinal cord. These interneurons release neurotransmitters such as glycine and GABA that inhibit motor neurons, thereby inducing muscle atonia (Luppi et al., 2011). Lesion experiments in the coeruleus region in cats and rats caused behaviour consistent with REM sleep behaviour disorder (REMBD), a condition marked by the absence of muscle atonia resulting in violent dream enactment (Boeve et al., 2007; Sastre & Jouvet, 1979). In summary, the LC plays a dual role in REM sleep by modulating cortical activation through its suppression of norepinephrine release and facilitating skeletal muscle atonia via inhibitory pathways to spinal motor neurons. This intricate regulation is essential for the maintenance of REM sleep and the prevention of dream enactment, highlighting the importance of the LC in sleep-wake physiology.

The dorsal raphe nucleus (DR), located in the medioventrolateral region of the central grey of the mesencephalon and rostral pons, is the primary source of serotonin (5-HT) in the brain (Monti, 2010). The DR is one of the RAS cell groups influences various physiological and behavioural processes, including sleep architecture and transitions between different sleep stages. The DR exhibits heightened activity during wakefulness, with reduced firing rates during quiet waking, deeper slowing during SWS, and nearly ceasing activity during REM sleep. DR 5-HT released modulates cortical and subcortical activity, promoting arousal, attention, and alertness. The widespread projections of DR neurons to the thalamus, amygdala, hypothalamus, and broad cortical regions facilitate this modulatory role, ensuring a state of vigilance necessary for interaction with the environment. In summary, the DR, through its 5-HT output, exerts a multifaceted influence on the sleep-wake cycle by promoting wakefulness, modulating transitions between sleep stages, suppressing activity during REM sleep (Monti, 2010; Scammell et al., 2017).

1.3.3. Sleep-Wake Cycle Changes in Normal Aging

Aging is associated with notable changes in the sleep-wake cycle, characterized by alterations in sleep architecture and circadian rhythms (Stickgold & Walker, 2009). However, need for sleep remains constant with aging. What actually becomes impaired is the ability to attain quality and restorative sleep. Older adults often experience reduced total sleep time, sleep efficiency, increased sleep fragmentation, advancement of the sleep phase, and a decline in SWS and REM sleep (Stickgold & Walker, 2009; Tatineny et al., 2020). More than 80% of individuals 65 years or older experience some degree of sleep-wake cycle changes (Sterniczuk & Rusak, 2016). In addition, older adults are more likely

to have primary sleep disorders, including circadian rhythm disturbances, insomnia, sleep-related movement disorders like restless legs syndrome (RLS), REM sleep behavior disorder (REMBD), and sleep disordered breathing like obstructive sleep apnea (OSA) (Sterniczuk & Rusak, 2016; Tatineny et al., 2020). These can be additionally affected by sleep disruptions stemming from medical or psychiatric conditions, as well as side effects from medications (Tatineny et al., 2020).

As people age, the circadian rhythm produced by the SCN becomes weaker, desynchronizes, and loses amplitude (Stickgold & Walker, 2009). It is hypothesized that the progressive deterioration of the SCN is a primary underlying cause for aging-related sleep-wake cycle and circadian changes. Melatonin, which acts on the SCN, is also diminished with age and may further exacerbate to the increased prevalence of sleep disturbances with aging. The most common desynchronization pattern observed in older adults is an advancement of the sleep phase, manifesting as an increased drive for sleep between 7 p.m. and 9 p.m. and awakening between 3 a.m. and 5 a.m. (Stickgold & Walker, 2009). Despite older adults spending more time awake in bed, total daily sleep time remains relatively stable at 6.5 to 7 hrs a day in healthy aging (Sterniczuk & Rusak, 2016).

The redistribution of sleep can further influence the transitions between and time spent in each sleep stage, which directly affects sleep quality (Sterniczuk & Rusak, 2016) The time spent in lighter sleep stages (i.e., NREM1 and NREM2) increases with aging, while the time spent in SWS is markedly decreased (Sterniczuk & Rusak, 2016; Stickgold & Walker, 2009). There is also a decreased latency to REM sleep, which may

be considered a direct consequence of an advanced circadian phase (Stickgold & Walker, 2009).

The prevalence of established sleep disorders increases in aging, and commonly include insomnia, sleep-related movement disorders like RLS, REMBD, and sleep disordered breathing including OSA (Sterniczuk & Rusak, 2016; Stickgold & Walker, 2009). Insomnia is defined as difficulty falling sleep (sleep-onset insomnia) or staying asleep (sleep maintenance insomnia) which typically results in daytime consequences such as daytime sleepiness, fatigue, irritability, and memory and concentration problems. Insomnia is habitually comorbid with sleep-related movement disorders like RLS. RLS is characterized by leg dysesthesia during the quiet waking state, which is described as a highly uncomfortable 'creepy crawling' or 'restless' sensation, which is only temporarily relieved from leg movement. Another sleep condition characterized by abnormal movement during sleep is REMBD. REMBD is marked by the absence of skeletal muscle atonia and dream enactment. The movements during REMBD can be particularly violent and may cause injuries to the patient and bed partner. The cause of REMBD is largely unknown, however, idiopathic REMBD is strongly associated with neurodegenerative diseases (NDDs) like dementia with Lewy bodies (DLB) and Parkinson's disease (PD; Boeve et al., 2007; Stickgold & Walker, 2009). Another type of sleep disorder experienced by older adults is sleep-disorders breathing, which encompasses mild to severe snoring (hypopnea) or complete cessation of breathing (apnea). There are two types of sleep-disordered breathing that may produce apnea: central sleep apnea and OSA. Central sleep apnea is linked to a failure of the brain's respiratory control centers, particularly in the BS, to properly signal the muscles that control breathing, leading to

repeated apnea episodes. The second type, OSA, is one of the most common sleep disorders, and is caused by obstruction of the airways from relaxation and subsequent collapse of muscles in the throat. Incidence of OSA is higher in those with obesity, age-related decline in muscle tone, or impaired pharyngeal sensory abilities. OSA typically produces daytime consequences including fatigue, headache, daytime sleepiness, difficulty concentrating, memory loss, and irritability (Sterniczuk & Rusak, 2016; Stickgold & Walker, 2009).

Frailty, described as an increased vulnerability to poor health outcomes as a result of accumulating aging-associated decline in physiological systems is also associated with poor sleep (Sterniczuk & Rusak, 2016). Specifically, frailty is associated with daytime sleepiness, frequent nighttime awakenings, and sleep apnea. Given that sleep disturbances are associated with poorer health, frail individuals, who already are vulnerable to declines in physiological system, may be impacted by poor sleep to a greater extent than older individuals who are not frail. Likewise, frail individuals experiencing sleep disturbances have a higher risk of mortality (Sterniczuk & Rusak, 2016).

In summary, aging-related changes in the circadian rhythm and sleep-wake cycle are characterized by alterations in total sleep time, efficiency, increased sleep fragmentation, and shifts in circadian rhythms, and in sleep architecture. Older individuals also show a higher incidence of sleep disorders. The cumulative impact of these disturbances can significantly affect the overall health, cognitive function, and quality of life of older adults. Getting adequate sleep and maintaining normal daily sleep-wake rhythms are important to sustaining lifelong physical health including proper

immune, metabolic, cognitive function and reducing the risk of disease development (Sterniczuk & Rusak, 2016).

1.3.4. Sleep-Wake Cycle Disturbances in Neurodegenerative Disorders

Sleep disturbances are a prevalent and challenging aspect of various NDDs, notably Alzheimer's disease (AD), dementia with Lewy bodies (DLB), and multiple sclerosis (MS; Sakkas et al., 2019; Sterniczuk & Rusak, 2016; Townsend et al., 2023). Each of these conditions is associated with unique manifestations of sleep disturbances, likely driven by distinct underlying neuropathophysiological mechanisms. In addition, sleep disturbances are associated with an increased risk for NDDs like dementia (Wong & Lovier, 2023).

AD is frequently accompanied by profound sleep disturbances, which significantly impair patients' quality of life, exacerbate pre-existing symptoms, and may accelerate disease progression (Benca et al., 2022). In fact, the level of sleep disturbance is strongly correlated with the severity of the disease (E. Bonanni et al., 2005). Individuals with AD often experience both insomnia and hypersomnia, sundowning, increased awakenings during sleep, leading to fragmented sleep and decreased sleep efficiency and quality (Sterniczuk & Rusak, 2016). The phenomenon of “sundowning”, refers to the observation of increased confusion and agitation in the late afternoon and evening. “Sundowning” can further exacerbate sleep disturbances, creating a cycle of worsening neuropsychiatric symptoms and sleep disruption (Rothman & Mattson, 2012).

The neurodegenerative process in AD, characterized by the accumulation of amyloid-β (Aβ) plaques and tau neurofibrillary tangles (NFTs), disrupts the function of various brain regions, with many being involved in sleep regulation, such as the

hypothalamus, SCN, BF, and BS (Lew et al., 2021; Mirra et al., 1991; Scammell et al., 2017). Disruption to any of these regions may impair the normal expression and 24 h cyclicity of various hormones, neuropeptides, and other transmitters involved in regulating the sleep-wake cycle (Rothman & Mattson, 2012). Additionally, previous research in mice reported that sleep restriction resulted in elevated Aβ production (Kang et al., 2009), and that sleep promoted Aβ clearance via the glymphatic system (Xie et al., 2013). Thus, the restorative function of sleep also includes the enhanced removal and reduced production of potentially neurotoxic waste products that accumulate in the awake central nervous system (CNS).

Medications used to treat AD symptoms including cholinesterase inhibitors (ChEIs) can also impact the sleep-wake cycle (Davis & Sadik, 2006). The administration of ChEIs can cause side effects including frequent awakenings during sleep and reduced sleep time and efficiency. It has been previously reported that ChEI administration before bed tends to result in the most sleep disturbances. It is likely that using ChEIs to enhance acetylcholine levels in the brain, for which its activity is naturally lower during sleep, are the cause for the treatment-related sleep disturbances. The timing of ChEI administration is therefore important to consider (Davis & Sadik, 2006).

DLB is characterized by the presence of α-synuclein aggregates known as Lewy bodies (LBs) and Lewy neurites (LNs) in the brain (McKeith et al., 2017). Sleep disturbances are very common in DLB, with 70-80% of patients experiencing REMBD. In fact, REMBD is a core clinical criterion for DLB diagnosis. Patients also commonly experience frequent awakenings during sleep, insomnia, OSA, RLS, and excessive daytime sleepiness (McKeith et al., 2017; Townsend et al., 2023). The neurodegenerative

process in DLB is characterized by α-synuclein pathology which affects many key regions important to the sleep-wake cycle, including the hypothalamus, thalamus, midbrain, BF, and BS (Boeve, 2019; Townsend et al., 2023). In particular, degeneration of neuromelanin-containing neurons in the substantia nigra and locus coeruleus (LC) is a key neuropathological feature of synucleinopathies such as DLB and PD brains as well as those with idiopathic REMBD (Boeve et al., 2007; Ehrminger et al., 2016). The LC, along with other pontine nuclei such as the pedunculopontine nucleus (Ch5) and the laterodorsal tegmental nucleus (Ch6), are components of the REM sleep circuit and play a role in regulating the skeletal muscle atonia characteristic of REM sleep. These regions vital to REM sleep, particularly in the BS, appear to exert a selective vulnerability to α-synuclein pathology (Boeve et al., 2007). Understanding the selective vulnerability of these brain regions to α-synuclein pathology provides crucial insights into the mechanisms underlying sleep disturbances in DLB, paving the way for targeted therapeutic strategies.

Lastly, MS is a chronic and immune-mediated condition of the central nervous system (CNS) that is characterized by inflammation, demyelination, and neurodegeneration (Bø et al., 1994; MS Canada, 2023a). MS patients commonly experience sleep disturbances, with prevalence estimated to be between 42% and 65% (Sakkas et al., 2019). Example of sleep disturbances commonly experienced by MS patients include insomnia, sleep-related movement disorders including RLS, sleep-related breathing disorders like OSA, and circadian rhythm disturbances (Sakkas et al., 2019). Many MS symptoms like pain, spasticity, and autonomic dysfunction can result in difficulties in initiating or maintaining sleep. As a result, many MS patients experience

difficulties falling and staying asleep, despite fatigue being a primary clinical symptom. Other MS symptoms like depression and anxiety, as well as those brought on by pharmacological treatments can further complicate sleep. The etiology of these sleep disturbances is therefore multifactorial but is largely influenced by the direct effects of demyelinating lesions in key brain regions involved in the sleep-wake cycle (G. Morris et al., 2018). Sleep disturbances thus may vary largely among patients, depending on the neuroanatomical locations of the lesions. Poor sleep may further exacerbate pre-existing symptoms and may also intensify immune activation, thereby potentially reducing quality of life and accelerating the disease process (G. Morris et al., 2018). Sleep disturbances are a prevalent and multifaceted issue in multiple sclerosis (MS), significantly impacting the quality of life and overall health of affected individuals. These disturbances encompass a broad spectrum of disorders, including insomnia, restless legs syndrome (RLS), periodic limb movement disorder (PLMD), narcolepsy, and obstructive sleep apnea (OSA). Insomnia, characterized by difficulty in initiating or maintaining sleep, is frequently reported among MS patients, often exacerbated by pain, spasticity, or nocturia. RLS and PLMD are also common, contributing to fragmented sleep and daytime fatigue. Narcolepsy, although less common, can present with excessive daytime sleepiness and sudden loss of muscle tone (cataplexy). OSA, associated with repeated episodes of upper airway obstruction during sleep, is another significant concern, potentially linked to brainstem lesions that impair respiratory control. The etiology of these sleep disturbances is multifactorial, involving the direct effects of demyelinating lesions in key brain regions, secondary consequences of MS symptoms, and side effects of medications. Demyelination and neurodegeneration within the hypothalamus, thalamus, brainstem, and

spinal cord can disrupt normal sleep-wake cycles and circadian rhythms, while chronic pain, depression, and anxiety further complicate the sleep architecture. Moreover, medications such as corticosteroids, often used in MS management, can have stimulant effects that interfere with sleep. Understanding the complex interplay of these factors is crucial for developing effective interventions to manage sleep disturbances in MS, thereby improving patient outcomes and quality of life.

1.4. Neuroinflammation

1.4.1. Microglia

Microglia are a type of glial cell located throughout the brain and spinal cord, playing a crucial role in maintaining central nervous system (CNS) homeostasis and immune defense (Kettenmann & Ransom, 2013). Originating from the yolk sac during embryogenesis, they comprise 2.5% to 10% of the total CNS cell population depending on the anatomical location (Franco-Bocanegra et al., 2019; Kettenmann & Ransom, 2013). Microglia are involved in a variety of essential functions, including phagocytosis of pathogens and cellular debris, synaptic pruning, and modulation of inflammatory responses (Kettenmann & Ransom, 2013).

Morphologically, microglia are highly dynamic cells characterized by a small soma and numerous, long, and branched processes. Microglial processes are constantly surveying the surrounding environment, detecting any signs of infection, injury, or pathological changes. Upon detection of such signals, microglia undergo a rapid transformation from a resting (ramified) to an activated (hypertrophic) state. Microglia may also exhibit a dystrophic morphology, characterized by degeneration of

ramifications and the formation of spheroidal swellings. This senescent state is frequently linked to chronic inflammation and aging (Streit et al., 2014).

Functionally, microglia are vital for the CNS immune response (Kettenmann & Ransom, 2013). They possess an array of surface receptors that recognize various types of pathogens. Upon activation, microglia secrete various cytokines and chemokines that recruit other immune cells to the site of injury or infection, orchestrating an effective immune response (Leng & Edison, 2021). These cytokines and chemokines include TNF-α, IL-1β, and IL-6. Additionally, microglia are involved in the clearance of apoptotic cells, protein aggregates, and debris through phagocytosis, a process important for preventing secondary damage and promoting tissue repair (Kettenmann & Ransom, 2013).

Microglia also play an essential role in neural development and synaptic plasticity (Kettenmann & Ransom, 2013). During development, microglia participate in synaptic pruning, a process that refines neural circuits by eliminating excess synapses. This process involves extracellular matrix proteins, primarily thrombospondins, which are mainly produced by astrocytes. This is crucial for the proper formation of functional neural networks.

However, dysregulation of microglial function is implicated in various neurodegenerative disorders (NDDs). Chronic activation of microglia related to detection of neuropathology associated with NDDs can lead to a sustained inflammatory response, contributing to the pathogenesis of conditions such as Alzheimer's disease (AD), dementia with Lewy bodies (DLB), Parkinson’s disease (PD), and multiple sclerosis (MS; Reale & Costantini, 2021). In these conditions, microglia may contribute to

neuronal damage through the chronic and excessive release of pro-inflammatory cytokines, reactive oxygen species, and other cytotoxic substances (Kettenmann & Ransom, 2013; Leng & Edison, 2021; Reale & Costantini, 2021). Some studies have additionally found that sleep deprivation can induce microglial activation, and sleep loss is a common symptom observed in many NDDs (Hsu et al., 2003).

1.4.2. Astrocytes

Astrocytes are a type of glia that play a multifaceted and vital role in maintaining CNS homeostasis, supporting neuronal function, and contributing to the overall architecture of the brain and spinal cord (Kettenmann & Ransom, 2013). Originating from neuroepithelium-derived radial glial cells, astrocytes are the most abundant glial cell in the CNS, comprising 20% to 40% of all glia depending on the anatomical location (Preman et al., 2021). Astrocytes are named for their stellate appearance, as their star-shaped morphology, with numerous and long radiating processes, resembles the form of a star. These glia are integral to the formation and maintenance of the blood-brain barrier (BBB), regulation of blood flow, provision of metabolic support to neurons, are involved in synaptic formation and plasticity, as well as in the inflammatory response in injury or disease (Kettenmann & Ransom, 2013).

One of the primary functions of astrocytes is the maintenance of the blood-brain barrier (BBB) (Manu et al., 2023). Astrocytes achieve this through their end-feet, which ensheathe blood vessels and release signaling molecules that promote tight junction formation in endothelial cells. This barrier is crucial for protecting the CNS from toxins and pathogens while regulating the passage of ions, nutrients, and waste products between the blood and the brain (Manu et al., 2023). Astrocytes, through this functional

and anatomical neurogliovascular link between vasculature and the CNS parenchyma, are also able to regulate local blood flow (Lia et al., 2023).

Astrocytes are also essential in the maintenance of the extracellular space, the microenvironment for neurons and glia (Kettenmann & Ransom, 2013). Astrocytes help to regulate its chemical and biophysical properties for the proper functioning of neurons by regulating extracellular ion balance and neurotransmitter homeostasis. They actively uptake excess neurotransmitters, such as glutamate and GABA, from the synaptic cleft through specific transporters. This uptake prevents excitotoxicity and ensures proper synaptic transmission. Additionally, astrocytes regulate extracellular potassium, calcium, sodium, and chlorine levels, which is vital for maintaining the membrane potential of neurons and preventing hyperexcitability (Kettenmann & Ransom, 2013; McNeill et al., 2021).

Glucose is the main energy substrate for the brain, which is a highly metabolically active organ (Kettenmann & Ransom, 2013). Glucose is taken up from the bloodstream via specific transporters at the blood-brain barrier. Astrocytes metabolize glucose through glycolysis, producing lactate, which is shuttled to neurons for adenosine triphosphate (ATP) production via the astrocyte-neuron lactate shuttle. Glycogen, on the other hand, is stored exclusively in astrocytes and serves as an emergency energy reserve that can be mobilized during periods of high metabolic demand or glucose deprivation. This stored glycogen is converted to lactate and supplied to neurons, ensuring continuous energy availability and maintaining neuronal activity and synaptic function. Astrocytes also play a role in the synthesis and release of neurotrophic factors, such as brain-derived

neurotrophic factor and glial cell line-derived neurotrophic factor, which support neuronal survival, growth, and differentiation (Kettenmann & Ransom, 2013).

Astrocytes are actively involved in synaptic formation and plasticity. During development, they secrete extracellular matrix proteins and other molecules that facilitate synaptogenesis. In the mature CNS, astrocytes contribute to synaptic plasticity through the release of gliotransmitters like ATP, D-serine, and glutamate, which modulate synaptic activity and strength. They also participate in the pruning of synapses, a process essential for the refinement of neural circuits.

Astrocytes undergo significant morphological changes characterized by hypertrophy in response to pathogen or injury detection (Kettenmann & Ransom, 2013). In the context of NDDs like AD, the detection of Aβ plaques by astrocytes provokes an activated state, also known as astrogliosis (Li et al., 2011). In an activated state, astrocytes exhibit an enlarged cell body and an increase in the length and thickness of their processes. This response also involves changes in proliferation and the upregulation of intermediate filament proteins such as glial fibrillary acidic protein (GFAP). Like microglia, detection of neuropathology stimulated astrocytes to release pro-inflammatory cytokines and chemokines such as TNF-α, IL-1β, IL-6, and inducible nitric oxide synthase (NOS; Li et al., 2011). Astrocytes often localize to Aβ plaques, and is thought to be an attempt to protect neurons by phagocytosing and degrading Aβ aggregates (Jasiecki et al., 2021). While astrogliosis can be protective by forming a glial scar that limits the spread of damage, it can also impede axonal regeneration and contribute to chronic inflammation. The activated astrocytes at Aβ plaque sites chronically release pro-inflammatory cytokines and chemokines, thereby exacerbating neuronal damage,

dysfunction, and contributing to neurodegeneration (Kettenmann & Ransom, 2013; Li et al., 2011).

1.5. Objectives and Hypothesis

Previous research on the roles of the cholinergic system in the sleep-wake cycle (e.g., Han et al., 2014; Kroeger et al., 2017; Scammell et al., 2017), its characteristic changes in NDDs like AD (e.g., Geula et al., 2021; Whitehouse et al., 1981), its purported roles in neuropathogenesis in various NDDs (e.g., Darvesh, Reid, et al., 2010; Geula & Mesulam, 1995; Thorne et al., 2021), and lastly its involvement in regulation of neuroinflammation (e.g., Hone & McIntosh, 2018; H. Wang et al., 2003) have been reported. However, the intricate relationship between cholinergic, neurodegenerative, neuropathological, and neuroinflammatory changes as potential contributors in regions related to sleep, the BF and BS, remains to be investigated. The objectives of this study were to use immunohistochemical and histochemical staining methods to examine the cholinergic system, neuropathology, and neuroinflammation within the BF and BS in post-mortem AD, DLB, MS, and CN brains.

We hypothesized that cholinergic system changes, increased neuropathological load, and neuroinflammatory processes would be observed within nuclei associated with the regulation of the sleep-wake cycle. Specifically, we expected to observe: 1) a loss of cholinergic neurons, 2) increased neuropathological burden, and 3) increased presence and activation of immune cells indicating neuroinflammation within nuclei involved in sleep-wake cycle regulation. These cholinergic, neuropathological, and neuroinflammatory changes are likely contributors to the progression of

neurodegeneration and the manifestation of sleep disturbances observed in AD, DLB, and MS.

CHAPTER 2. Methods

2.1. Brain Tissues

Post-mortem human brain tissues were obtained from the Maritime Brain Tissue Bank (Halifax, Nova Scotia, Canada) with approval to conduct experiments from the Nova Scotia Health Research Ethics Board. These included age- and sex-matched brains from 5 AD, 5 DLB, 4 MS, and 4 cognitively normal (CN) cases. In this study, AD cases were defined as individuals who fulfilled clinical (McKhann et al., 2011) and neuropathological diagnostic criteria for AD (Montine et al., 2012a), and DLB cases as those who fulfilled clinical and neuropathological (McKeith et al., 2005) diagnostic criteria for DLB, and MS cases as persons who fulfilled clinical and neuropathological (Bø et al., 1994; McDonald et al., 2001) criteria for MS, and CN as those with no clinical history of cognitive impairment. Demographic details of all cases are summarized in Table 2.1., and clinical information relating to sleep disturbances in Table 2.2.

The brains were bisected sagittally at the midline during autopsy, with one hemisphere dedicated to neuropathological diagnosis by a neuropathologist, and the remaining hemisphere sent to the Maritime Brain Tissue Bank. The hemispheres dedicated to the Maritime Brain Tissue Bank were cut coronally into 1-2 cm slabs and immersion fixed in 10% formalin in 0.1 M phosphate buffer (PB; pH 7.4) at 4 ºC for 1-5 days. The slabs were cryoprotected in increasing concentrations of sucrose (10%, 20%, 30%, and 40%) in PB, for approximately 2 days at each concentration. Tissue was stored in 40% sucrose in PB with 0.6% sodium azide at 4 ºC until needed. Note, initially, the study aimed to include three age-matched females and three age-matched males for each group, for a total of 24 brains. However, due to various factors such as brain

Table 2.1 Case demographic details

	Case	Sex	Age (y)	Brain Weight (g)	Cause of Death	Post-Mortem Interval (hrs)	Time in Fix (d)	Braak Stage[b]	CERAD Score[c]
Alzheimer's Disease (AD)	AD1	F	58	1120	Cardiorespiratory Failure	19	2	VI	Frequent
	AD2	F	92	1009	Pneumonia	10	3	IV	Frequent
	AD3	M	58	1470	Cardiorespiratory Failure & Acute Renal Failure	10.75	2.96	VI	Frequent
	AD4	M	72	1344	Respiratory Failure	n/a[a]	1.9	IV	Moderate-Frequent
	AD5	M	95	1215	Pneumonia & Congestive Heart Failure	35	4	V	Frequent
Dementia with Lewy bodies (DLB)	DLB1	F	87	1070	Pneumonia	21	4.25	n/a	Sparse
	DLB2	F	96	1200	n/a	8	3.96	III	Moderate
	DLB3	M	69	1450	Pneumonia	23	2.25	I	n/a
	DLB4	M	81	1317	Pneumonia	n/a	2	I	Sparse
	DLB5	M	89	1312	n/a	24	3	n/a	Sparse
Multiple sclerosis (MS)	MS1	F	63	1357	Cardiovascular Accident	n/a	5	n/a	n/a
	MS2	F	64	1160	Septic Shock	7	2.15	n/a	n/a
	MS3	F	66	1380	n/a	n/a	5	n/a	n/a
	MS4	M	50	1080	n/a	10.83	2	n/a	n/a
Cognitively Normal (CN)	CN1	F	63	1325	Esophageal Carcinoma	15.5	2.02	0	None
	CN2	F	80	1300	Perforated Bowel & Peritoneal Carcinomatosis	9	2.27	1	None
	CN3	F	100	1258	Myocardial Infarct	6	6	IV	Moderate
	CN4	M	104	1249	Cardiorespiratory Arrest	39	2.3	IV	Sparse

[a]n/a = information not available
[b]Braak et al. (2006)
[c]Mirra et al. (1991)

Table 2.2 Clinical information relating to sleep disturbances

	Case	Relevant Clinical Details
Alzheimer' s Disease (AD)	AD1	Rapid eye movement sleep behaviour disorder (REMBD)
	AD2	n/n
	AD3	Insomnia, changes to circadian rhythm, sleep-wake reversal
	AD4	n/n
	AD5	n/n
Dementia with Lewy bodies (DLB)	DLB1	Nightmares, hallucinations
	DLB2	n/a
	DLB3	REMBD
	DLB4	REMBD, possible sleep apnea, Systemic Lupus Erythematosus
	DLB5	n/n
Multiple sclerosis (MS)	MS1	Possible REMBD, poor transitions between wakefulness and sleep, slow brain waves during wake
	MS2	n/n
	MS3	n/a
	MS4	n/n
Cognitively Normal (CN)	CN1	n/n
	CN2	Difficulties with sleep initiation due to pain
	CN3	Sundowning, sleep disturbances not yet diagnosed
	CN4	n/a

n/n = nothing noted with regards to sleep
n/a = no information available

unavailability and imprecise midline bisection cuts, these figures underwent slight modifications, resulting in a total of 18 brains examined in this study. Among the cases examined, certain regions were inaccessible, such as Ch1 for AD3, AD5, DLB1, MS2, MS4, and CN3 due to its fragile nature and did not withstand bisection during autopsy. In addition to the Ch1 region being unavailable for case CN3, the Ch2 and Ch6 regions were additionally inaccessible. The BF, including Ch1, Ch2, Ch4a, and Ch4p regions, were unavailable for case MS3 due to severe freezing artifact resulting in tissue breakdown. It's important to mention that in certain instances, the Ch4a subsector, specifically Ch4am/al, was targeted due to its known projection locations but was not accessible for staining. In such cases, Ch4ai, the neighboring sector of the anterior Ch4, was utilized instead. Considering this, it is appropriate to designate the anterior sector, comprising both Ch4am/al and, where applicable, Ch4ai, should herein be referred to as Ch4a.

The cryoprotected tissue blocks from the BS and BF were cut with a Leica SM2000R microtome (Leica Microsystems Inc., Nussloch, Germany) with a Physitemp freezing stage and BFS-40MPA controller (Physitemp Instruments LLC, Clifton, NJ, United States) in 50 µm serial coronal sections. Sections were stored in 40% sucrose with 0.6% sodium azide in PB at -20 ºC until they were used for staining experiments.

2.2. Immunohistochemical Staining

Standard immunohistochemical techniques were employed using specific primary antibodies (Table 2.3) to detect ChAT-positive neurons, Iba1-positive microglia and GFAP-positive astrocytes to examine inflammation, Aβ plaques, tau NFTs and neuropil threads (NTs), α-synuclein Lewy bodies (LBs) and neurites (LNs), and phosphorylated Tar DNA binding protein 43 (pTDP-43) neuronal cytoplasmic inclusions (NCIs) and

dystrophic neurites (DNs) to detect neuropathology, as done previously (Hamodat et al., 2019; Maxwell et al., 2022; McKeith et al., 2005). In addition, immunohistochemical staining using a primary antibody (Table 2.3) for myelin basic protein was performed to detect demyelinated MS lesions.

Table 2.3 Antibodies used for immunohistochemical staining

Antibody	Host Animal	Dilution	Manufacturer	Catalogue Number
Polyclonal anti-amyloid-β-peptide	Rabbit	1:400	Invitrogen	71-5800
Polyclonal anti-human tau	Rabbit	1:16,000	Dako	A0024
Monoclonal anti-α-synuclein	Mouse	1:200	Invitrogen	18-0215
Polyclonal anti-choline acetyltransferase (ChAT)	Goat	1:1000	Millipore	AB144P
Monoclonal anti-glial fibrillary acidic protein (GFAP)	Mouse	1:2500	New England Biolabs	3670
Polyclonal anti-Iba1	Rabbit	1:2000	Wako	019-19741
Monoclonal anti-myelin basic protein (MBP)	Mouse	1:200	Millipore	AB384
Monoclonal antiTAR DNA-binding protein 43, phosphoSer409/410 (Clone 11-9)	Mouse	1:48,000	Cosmo Bio	CAC-TIP-PTD-M01
Tryptophan hydroxylase	Sheep	1:1000	Millipore	AB1541

All tissues were rinsed in PB for 30 mins. Sections stained for Aβ were subjected to antigen retrieval, starting with a 5 min rinse with 0.5 M PB, followed by a 15 min rinse in distilled water (dH_2O), then were gently agitated in 95% formic acid for 2 mins, succeeded by five 1 min rinses in dH_2O and a final 30 min rinse in PB. All sections were treated with 0.3% hydrogen peroxide (H_2O_2) in phosphate buffer (PB) for 30 min to quench endogenous peroxidase activity, followed by a 30 min rinse in PB. Sections designated for α-synuclein, ChAT, GFAP, and pTDP-43 staining underwent antigen retrieval involving a 30min incubation, while those designated for MBP and Iba1 underwent a 20 min incubation in 0.01 M citrate buffer (pH 6.0) at 80 ºC. All sections were rinsed for 30 minutes in PB after tissue cooled slowly to room temperature. All sections were immersed overnight (16-18 h) in PB containing 0.1% Triton X-100, 1:100 normal goat serum for α-synuclein, Aβ, GFAP, pTDP-43, Iba1, tau, and MBP or normal rabbit serum for ChAT, and the respective primary antibody at room temperature. After a 30 min PB rinse, sections were incubated for 1 h at room temperature in PB containing 0.1% Triton X-100, 1:1000 normal goat serum for α-synuclein, Aβ, GFAP, pTDP-43, Iba1, tau, and MBP or 1:1000 normal rabbit serum for ChAT, and the appropriate biotinylated secondary antibody (1:500). Following another 30 min PB rinse, sections were treated for 1 hour at room temperature with the Vectastain Elite ABC kit (1:182; PK6100, Vector Laboratories, Burlingame, CA, United States) according to the manufacturer's instructions. After a final 30 min PB rinse, sections were developed in 1.39 mM 3,3'-diazobenzidine tetrahydrochloride (DAB) in PB for 5 mins, with the addition of 50 µL of 0.3% H_2O_2 in PB per mL of DAB solution. The reaction was halted by rinsing sections in 0.01 M acetate buffer (pH 3.3) for 30 mins. Control experiments

confirmed the absence of staining when omitting the primary antibody. Finally, all sections were mounted on slides and coverslipped for examination using brightfield microscopy.

2.3. Histochemical Staining

Thionin staining for Nissl substance was used to examine cytoarchitecture of the BF and BS as well as counterstain for immunohistochemically stained α-synuclein and pTDP-43. Mounted sections underwent dehydration through a sequence of ethanol washes (70–100%), were cleared in xylene, and subsequently rehydrated in a series of ethanol washes (100–70%), followed by distilled water (dH2O). The sections were briefly immersed in thionin dye for 3 seconds, then rinsed in dH2O, followed by a series of ethanol washes (70–100%), xylene, and finally coverslipped using an aqueous mounting medium.

Histochemical staining was conducted to visualize the activity of AChE and BChE using a modified (Maxwell et al., 2022) Karnovsky-Roots method (Karnovsky & Roots, 1964). All necessary reagents were procured from Sigma-Aldrich (St. Louis, MO, United States). Tissue sections underwent a 30 min rinsing in 0.1 M maleate buffer (MB; pH 7.4), followed by immersion in 0.15% H_2O_2 in MB for 30 mins to quench endogenous peroxidase activity. After another 30 min rinse in MB, the sections were treated with the Karnovsky-Roots solution for varying durations (between 3 and 48 h), depending on the fixation time of individual cases. The Karnovsky-Roots solution for BChE staining comprised 0.5 mM sodium citrate, 0.47 mM cupric sulphate, 0.05 mM potassium ferricyanide, 0.8 mM butyrylthiocholine iodide (BChE substrate), and 0.01 mM BW 284 C 51 (an AChE-specific inhibitor) in MB at either pH 6.8 or 8.0. Visualization of

cholinesterase activity associated with neuropathological structures used a pH of 6.8, whereas visualization of cholinesterase activity associated with normal neural structures, including neurons and glia, used a pH of 8.0. Subsequently, the sections were rinsed for 30 mins in dH_2O before incubation in 0.1% cobalt chloride in dH_2O for 10 mins. Following another 30 min rinse in PB, the sections were developed by incubation in 1.39 mM DAB in PB for 5 mins, with the reaction initiated by adding 50 µL of 0.15% H_2O_2 in PB per mL of DAB solution. Finally, to halt the reaction, the sections were rinsed in 0.01 M acetate buffer (pH 3.3) for 30 mins.

Histochemical staining protocol for the visualization of AChE activity closely mirrored those used for BChE, with the exception that 0.4 mM acetylthiocholine iodide (the substrate for AChE) was employed alongside 0.06 mM ethopropazine (a BChE-specific inhibitor).

Histochemical staining was performed to visualize the distribution of neurons containing the enzyme NADPH-d, a marker of neuronal nitric oxide synthase. NADPH-d activity is promoted by the catalytic activity of NOS to reduce nitro blue tetrazolium to diformazan, a dark blue-purple precipitate, thereby identifying a subset of neurons containing the enzyme (Hope et al., 1991). All necessary reagents were procured from Sigma-Aldrich (St. Louis, MO, United States). Tissue sections were rinsed for 30 mins in 0.05 M Tris-buffered saline (TBS; pH 7.6), followed by another 30 min rinse in 0.05 M Tris HCl buffer with 0.2% Triton X-100 (pH 8.0). Sections were then incubated in NADPH-d staining solution containing 0.4 mg/mL nitro blue tetrazolium and 0.84 mg/mL reduced β-NADPH-d tetrasodium salt in 0.05 M Tris HCl buffer with 0.2%

Triton X-100 (pH 8.0) in the dark at 37ºC for about an hour. Subsequently, the sections were rinsed for 30 mins in TBS (pH 7.6).

Control experiments were conducted to confirm the specificity of staining for AChE and BChE, following previously performed methods (Darvesh, Reid, et al., 2010). Subsequently, all sections were mounted on slides and covered for examination under brightfield microscopy.

2.4. Data Analysis

Regions of interest were parcellated using sections stained for Nissl substance with thionin, ChAT, tyrosine hydroxylase, and cholinesterase activity at pH 8.0 to identify the nuclei of interest. Nuclei of interest examined within the basal forebrain (BF) included the medial septal nucleus (Ch1), nucleus of the vertical limb of the diagonal band of Broca (Ch2), and anteromedial/anterolateral (Ch4a) and posterior (Ch4p) sectors of nucleus basalis of Meynert (Fig. 2.1). The BF nuclei of interest were parcellated using Nissl, ChAT, and AChE staining, based on the methods established by Mesulam *et al.* (1983). The nuclei were subsequently named according to the 'Ch' nomenclature, also as designated by Mesulam *et al.* (1983). Brainstem (BS) nuclei examined were the pedunculopontine nucleus (Ch5), laterodorsal tegmental nucleus (Ch6), dorsal raphe (DR) nucleus, and locus coeruleus (LC). The Ch5 and Ch6 regions were delineated using Nissl, ChAT, and AChE staining, based on the methods by Mesulam et al. (1983). The DR was identified using tryptophan hydroxylase staining as done by Monti (2010), while the locus coeruleus (LC) was delineated using Nissl staining and recognizing its naturally dark brown, neuromelanin-containing neurons as done by Mesulam *et al.* (1989). The

Ch5 and Ch6 BS nuclei were also named according to the 'Ch' nomenclature designated by Mesulam et al. (1983).

Analysis of the abundance of normal neural elements was performed to determine neuronal counts. Neuronal quantification involved employing various staining techniques, such as thionin for Nissl substance, and methods to visualize AChE-, BChE-, ChAT-, and NADPH-d-positive neurons. Glia, including microglia and astrocytes, were additionally quantified and morphologically characterized using immunohistochemical staining techniques that targeted Iba1 and GFAP proteins, respectively. Next, the abundance, morphology, and distribution of pathology was assessed using staining techniques for Aβ, α-synuclein, tau, pTDP-43, and for AChE and BChE activity at pH 6.8 was examined in the nuclei of interest.

2.4.1. Imaging and Microscopy

Sections from the BF and BS were analyzed using brightfield microscopy and photographed with a Zeiss Axio Scan.Z1 slide scanner with Zen 3.1 Blue Edition software (Carl Zeiss Canada Ltd, Toronto, Canada).

2.4.2. Analysis of Normal Neurons, Microglia, and Astrocytes

Tissue sections stained for normal neural elements including thionin for Nissl substance, and AChE-, BChE-, ChAT-, and NADPH-d-positive neurons were analyzed using brightfield microscopy. Neurons, microglia, and astrocytes within each region of interest were quantified. This involved counting neurons or immune cells within a 500x500μm box positioned within the confines of the nucleus, digitally placed onto the scanned slide section using the Zen 3.1 Blue Edition software. Neuron counts were completed using ImageJ software with the multi-point tool.

Counts for Nissl substance-, AChE-, BChE-, ChAT-, NADPH-d-positive, and lcous coeruleus pigmented neurons were compared between the CN, AD, DLB, and MS groups in each region of interest using Wilcoxon-Mann-Whitney tests. Significant differences between mean neuropathological scores were denoted as follows: *$p<0.05$; **$p<0.01$; ***$p<0.001$.

The morphological characteristics of microglia and astrocytes were also described. Microglia and astrocytes were observed to exhibit various states, including ramified, activated (characterized by swelling of the cell body and processes), or dystrophic (evident as beading/fragmentation of processes, indicating senescence, exhaustion, and/or dysfunction), providing insights into their physiological state.

2.4.3. Neuropathology Analysis

Neuropathological loads for Aβ, tau, pTDP-43, and for AChE and BChE activity at pH 6.8 stains were analyzed using a semi-quantitative score adapted from a modified CERAD neuropathology diagnostic protocol where: 0 = no pathology; 1 = sparse pathology; 2 = moderate pathology; 3 = frequent pathology (Hamodat et al., 2019; Mirra et al., 1991).

Neuropathological density staging for α-synuclein pathology followed a separate diagnostic protocol where: Stage 0 = no pathology; Stage 1 = mild pathology; Stage 2 = moderate pathology; Stage 3 = severe pathology; Stage 4 = very severe pathology (McKeith et al., 2005). In cases where the criteria were partially met for two stages, an intermediate score was assigned. For example, according to McKeith et al. (2005), stage 1 is characterized by sparse Lewy bodies (LBs) or Lewy neurites (LNs), whereas stage 2 is characterized by more than one LB and sparse LNs. In an example scenario where

there is one LB and sparse LNs present, a score of 1.5 would be assigned because the criteria for both stage 1 and stage 2 are partially fulfilled.

Multiple sclerosis (MS) lesions were histologically classified into active, chronic active, and chronic inactive categories based on the density and distribution of microglia (Bø et al., 1994). Active white matter (WM) MS lesions were characterized by hypercellularity throughout. Chronic active WM MS lesions were identified by a hypercellular rim and a relatively hypocellular center. Chronic inactive WM MS lesions were characterized by hypocellularity throughout (Bø et al., 1994). Classification of microglial activity in gray matter (GM) MS lesions differed from that in WM MS lesions (Peterson et al., 2001). GM lesions were designated as active if they exhibited a hypercellular rim and a relatively hypercellular core and adjacent region compared to surrounding normal GM tissue. Chronic active GM MS lesions displayed a hypercellular rim and a core that is either hypocellular or of similar density to surrounding normal GM tissue. GM lesions were classified as chronic inactive if they displayed a cellular density comparable to surrounding normal GM tissue and lacked a hypercellular rim (Peterson et al., 2001).

2.4.4. Statistical Testing

Due to the small sample sizes in this study, where the data cannot reasonably be assumed to follow a normal distribution or have equal variances, a nonparametric test such as the Mann-Whitney rank sum test was utilized to statistically analyze the data (Morgan, 2017). This test was chosen for its robustness and suitability for handling data that do not meet the assumptions required for parametric tests. Specifically, the Mann-Whitney rank sum test was applied to process data related to normal neural elements,

including neuron counts, neuropathological scores, and microglia and astrocyte counts. This approach ensured that the statistical analysis was both appropriate and reliable, given the characteristics of the dataset.

CHAPTER 3. Results

3.1. Parcellation of the Basal Forebrain and Brainstem

Sections stained for AChE activity at pH 8.0 and ChAT immunohistochemistry was used to parcellate the BF (Fig. 3.1) and additionally NADPH-d histochemistry for the BS (Fig. 3.2). Parcellation of the BF in the context of cholinergic neuron distribution has been described in detail by Mesulam *et al.* (Geula et al., 2021; Mesulam et al., 1983, 1986; Mesulam & Geula, 1988). Ch1, also known as the medial septal nucleus, was present in a small proportion of cases, typically with only the most ventral portion intact, as this delicate region is frequently severed during brain bisection. The Ch1 group was located in the medial septal region, positioned along midline of the brain, dorsal to Ch2, and at the rostral extent of the anterior commissure (Fig. 3.1A, D). AChE- and ChAT-positive neurons in this nucleus were notably small and sparse. This nucleus was particularly challenging to identify, especially in the neurodegenerative cases examined.

The Ch2 group (Fig. 3.1A, D), alternatively referred to as the nucleus of the vertical limb of the the diagonal band of Broca, was located ventral to Ch1. AChE- and ChAT-positive neurons in this nucleus were more easily identifiable than those in Ch1 because they were larger and more abundant, as previously described by Mesulam *et al*. (Mesulam et al., 1983). The neuronal axes and neuropil in the Ch2 group was observed to align parallel to the course of the diagonal band. The Ch2 group of neurons were observed to merge with those found dorsally in Ch1 and ventrally with nucleus of the horizontal limb of the diagonal band of Broca (Ch3) and the nucleus basalis of Meynert (Ch4).

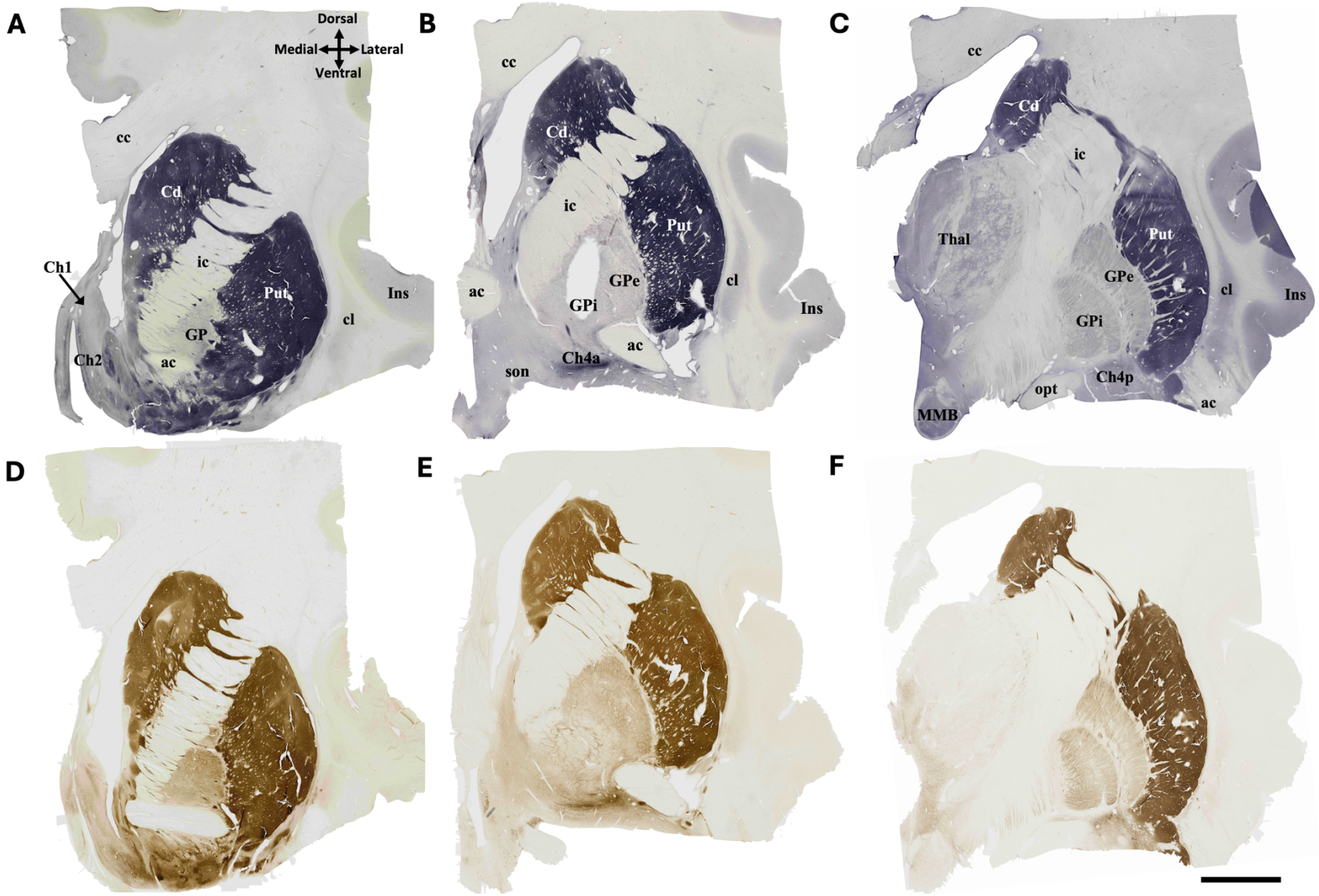
A
Dorsal
Medial
Lateral
Ventral
cc
Cd
ic
Put
Ins
Ch1
cl
GP
Ch2
ac
B
cc
Cd
ic
Put
GPe
cl
Ins
ac
GPi
ac
Ch4a
son
C
cc
Cd
ic
Thal
Put
GPe
cl
Ins
GPi
opt
Ch4p
ac
MMB
D
E
F

Figure 3.1 Representative basal forebrain (BF) sections immunohistochemically stained for choline acetyltransferase (ChAT; top row) and histochemically stained for acetylcholinesterase (AChE; bottom row) in corresponding regions of the medial septal nucleus (Ch1; A, D), nucleus of the vertical limb of the diagonal band of Broca (Ch2; A, D), and anterior (Ch4a; B, E) and posterior (Ch4p; C, F) sectors of the nucleus basalis of Meynert in a cognitively normal case. While denoted as Ch4a to encompass the anterior sector of the Ch4 complex, B and E depict precisely the Ch4ai subsector. Scale bar = 1 cm. Abbreviations: ac, anterior commissure; Cd, caudate nucleus; cc, corpus callosum; cl, claustrum; GP, globus pallidus; GPe, globus pallidus externus; GPi, globus pallidus internus; ic, internal capsule; Ins, insula; MMB, mammillary body; opt, optic tract; Put, putamen; son, supraoptic nucleus; Thal, thalamus.

The neurons of the Ch4 region were easily identifiable because they were magnocellular, hyperchromic, had prominent nucleoli, and were isodendritic as observed in Nissl staining, consistent with descriptions by Mesulam *et al.* (1988). Additionally, Ch4 neurons in CN cases stained intensely for ChAT and AChE, aligning with reports by Mesulam *et al.* (1988). The most anterior portion of the Ch4 complex, comprising the anteromedial/anterolateral subsectors, was denoted as Ch4am/al. This subsector exhibited a high density of ChAT- and AChE-positive neurons, accompanied by abundant neuropil, positioned ventral to the anterior commissure, consistent with descriptions by Mesulam *et al.* (1988). At this level, the anterior commissure was beginning to decussate, with Ch4am/al persisting caudally as the lateral recession of the anterior commissure began. In nearly all cases, a blood vessel was observed to project vertically that delineated Ch4am from Ch4al subsectors.

Just caudal to Ch4am/al, lies the anterointermediate subsector of the Ch4 complex, denoted as Ch4ai (Fig. 3.1B, E). This subsector was demarcated by macroscopic anatomical landmarks of this subsector include the division of the globus pallidus (GP) into internal (GPi) and external (GPe) regions by the internal medullary lamina, and the lateral recession of the anterior commissure ventral to putamen (Put) and external globus pallidus (GPe; Table 1.5). This region also exhibited a high density of easily identifiable magnocellular and hyperchromic neurons that stained intensely for ChAT and AChE, accompanied by abundant neuropil.

The most caudal subsector of the Ch4 complex, the posterior subsector, was denoted as Ch4p (Fig. 3.1C, F). Anatomical landmarks of this region included the lateral anterior commissure positioned ventrolateral to the putamen and at the level of the

mammillary body (Table 1.5). This subsector also contained many AChE- and ChAT-positive neurons and neuropil. These neurons abutted upon the putamen.

Parcellation of the BS in the context of cholinergic neuron distribution has also been described in detail by Mesulam *et al.* (Mesulam et al., 1989). The pedunculopontine nucleus (Ch5) was optimally observed around the anatomical level corresponding to that of the trochlear nucleus. Ch5 was delineated by the presence of intensely stained AChE-, ChAT-, and NADPH-d-positive neurons and neuropil. Ch5 neurons were observed to exhibit perikaryal heteromorphism, were isodendritic, and lacked a common orientation, as well as extended beyond arbitrary cytoarchitectural boundaries of its nucleus (Mesulam et al., 1989). Relative boundaries used to delineate the Ch5 nucleus included the medial longitudinal fasciculus, the decussation of the superior cerebellar peduncles, and the substantia nigra. A dense cluster of Ch5 neurons, referred to as the compact sector of Ch5 (Ch5c), was observed, with diffuse Ch5 neurons surrounding it, designated as the diffuse sector of Ch5 (Ch5d).

The laterodorsal tegmental nucleus (Ch6) was located caudal relative to Ch5 (Fig. 3.2D, E, F). This nucleus was optimally observed at the anatomical level corresponding to the mid-rostral-caudal extent of the locus coeruleus (LC) and positioned within the rostral pontine central grey. Ch6 was bounded ventrally by the medial longitudinal fasciculus and dorsally by the fourth ventricle. However, this nucleus contains no clear delineation of boundaries, for which its AChE-, ChAT-, and NADPH-d-positive neurons extended into the adjacent LC and medial longitudinal fasciculus. Similar to Ch5, nearly all ChAT-positive neurons also exhibited NADPH-d activity staining. Though, Ch6 was observed to have a smaller density of neurons than Ch5. Like Ch5 neurons, Ch6 neurons

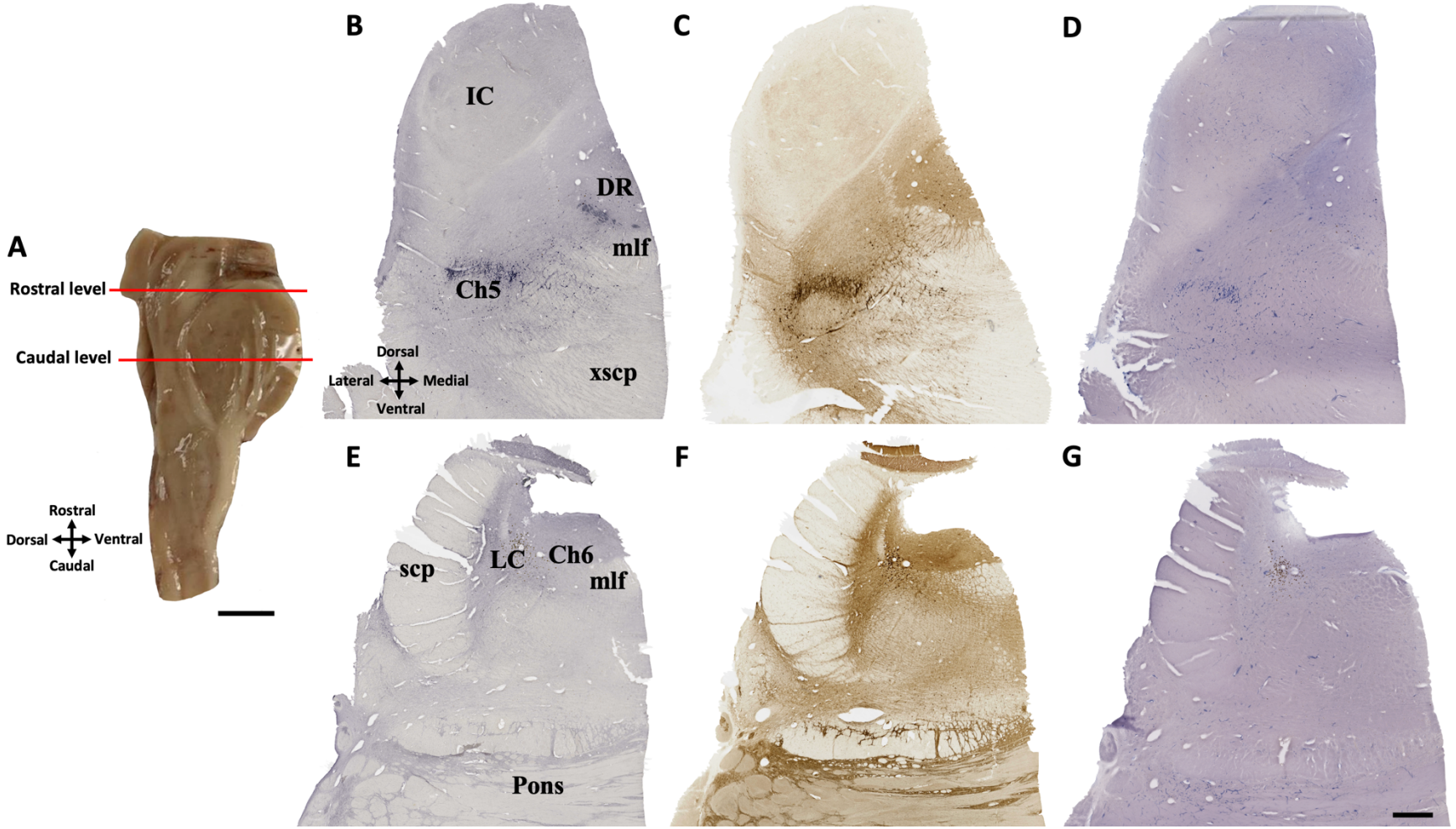
A
Rostral level
Caudal level
Rostral
Dorsal
Ventral
Caudal
B
IC
DR
mlf
Ch5
xscp
Dorsal
Lateral
Medial
Ventral
C
D
E
scp
LC
Ch6
mlf
Pons
F
G

Figure 3.2 Representative sections containing the nuclei of interest at two rostral-caudal extents of the brainstem (A) in a cognitively normal case. Corresponding sections at the rostral extent (B, C, D) contain the pedunculopontine nucleus (Ch5) and dorsal raphe nucleus (DR), while the sections at the caudal extent (E, F, G) contain the laterodorsal tegmental nucleus (Ch6) and locus coeruleus nucleus (LC). Sections were immunohistochemically stained for choline acetyltransferase (ChAT; B, E) and histochemically stained for acetylcholinesterase (AChE; C, F) and NADPH-diaphorase (NADPH-d; D, G). Scale bar in (A) = 1 cm, in (B, C, D, E, F, G) = 1 mm. Abbreviations: IC, inferior colliculus; mlf, medial longitudinal fasciculus; scp, superior cerebellar peduncle; xscp, decussation of the superior cerebellar peduncles.

were also observed to exhibit perikaryal heteromorphism, were isodendritic, and lacked a common orientation, as well as extended beyond indiscriminate cytoarchitectural boundaries of its nucleus (Mesulam et al., 1989).

The dorsal raphe nucleus (DR; Fig. 3.2A, B, C), predominantly containing serotonergic (5-HT) neurons, was situated in the ventral region of the central gray matter spanning the mesencephalon and rostral pons, was instead identified through tryptophan hydroxylase immunohistochemistry (Koutcherov et al., 2004). Although not inherently cholinergic, occasional presence of AChE-, ChAT-, BChE-, and NADPH-d-positive neurons was noted.

Finally, the LC (Fig. 3.2D, E, F) was readily identified by its naturally dark brown neuromelanin-containing neurons. Neuromelanin is contained within granules inside the neurons, producing a characteristic granular appearance that allowed for identification despite the presence of brown precipitate in certain stains used in this study. This nucleus was located within a relatively large rostral-caudal extent of the pons and lied rostrally in the caudal portion of the inferior colliculus and caudally at the level of the motor nucleus of the trigeminal nucleus. The LC was optimally observed at the mid-lower pontine level and situated in the lateral portion of the central grey matter, and bordered laterally by the superior cerebellar peduncle, ventrally by the medial longitudinal fasciculus, and medially by Ch6. This optimal rostral-caudal extent was use for all analyses in this study.

3.2. Neurodegenerative Changes

3.2.1. Cholinergic Changes

The loss of cholinergic neurons has long been documented across various neurodegenerative conditions, especially in the dementias such as Alzheimer's disease

(AD) and dementia with Lewy bodies (DLB; Geula et al., 2021). Evaluating relative neuronal counts provides insight into the extent of cholinergic and/or cholinoceptive alterations. Neurons positive for the acetylcholine-synthesizing enzyme choline acetyltransferase (ChAT), as well as for cholinesterases such as acetylcholinesterase (AChE) and butyrylcholinesterase (BChE), were quantified in regions of interest within the BF and BS within AD (Table 3.1), DLB (Table 3.2), multiple sclerosis (MS; Table 3.2), and cognitively normal (CN; Table 3.1) brains. A figure illustrating ChAT and AChE neuron differences between groups in corresponding regions of the Ch4a region in the BF is presented in Figure 3.3.

The Mann-Whitney statistical analysis for ChAT neuron counts across various brain regions of interest in the BF and BS comparing CN and AD brains revealed significant differences in specific areas (Table 3.1). In the Ch4a region, the mean count was 69.8 (± 5.2) ChAT neurons for CN brains, which was significantly higher than a mean of 30.4 (± 16.3) ChAT neurons for AD brains, with a p-value of 0.016. The Ch2, Ch4p, Ch6, DR, and LC regions did not show significant differences for mean ChAT neuron counts. For AChE neurons, significant differences were observed in the Ch4p region, where the mean neuron count in CN brains was 27.8 (± 2.4) which was significantly higher than 12.2 (± 6.5) for AD brains, yielding a p-value of 0.008. Other regions, including Ch1, Ch2, Ch4a, Ch5, Ch6, DR, and LC, did not demonstrate significant differences in ChAT or AChE neurons. Analysis of BChE neuron (Fig. 3.4) counts indicated no significant differences between CN and AD brains across all regions examined.

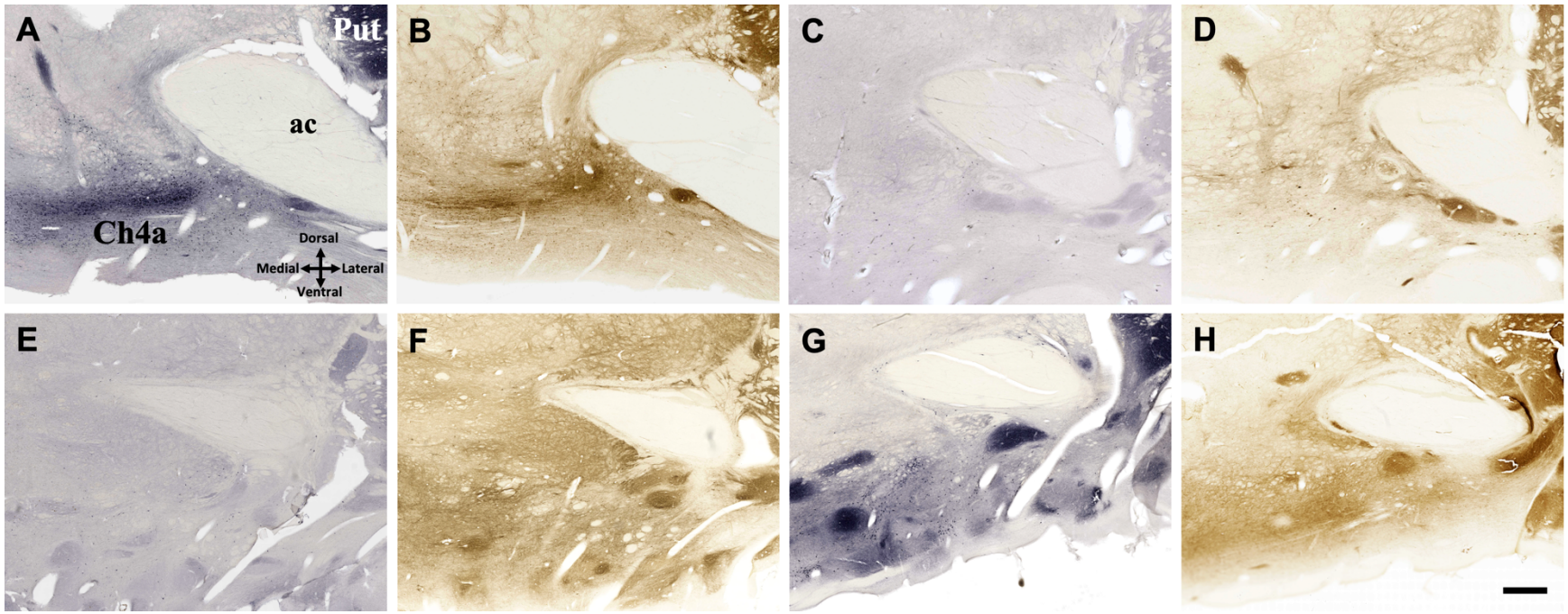

Figure 3.3 Differences in choline acetyltransferase (ChAT; A, C, E, F) and acetylcholinesterase (AChE; B, D, F, H) staining in the Ch4a region between cognitively normal (CN; A, B), Alzheimer's disease (AD; C, D), dementia with Lewy bodies (DLB; E, F), and multiple sclerosis (MS; G, H) groups. Note the loss of ChAT and AChE staining, particularly in the region containing the Ch4a neurons and surrounding cholinergic regions such as the putamen. Abbreviations: ac, anterior commissure; Ch4a, anterior sector of the nucleus basalis of Meynert; Put, putamen. Scale bar = 1mm.

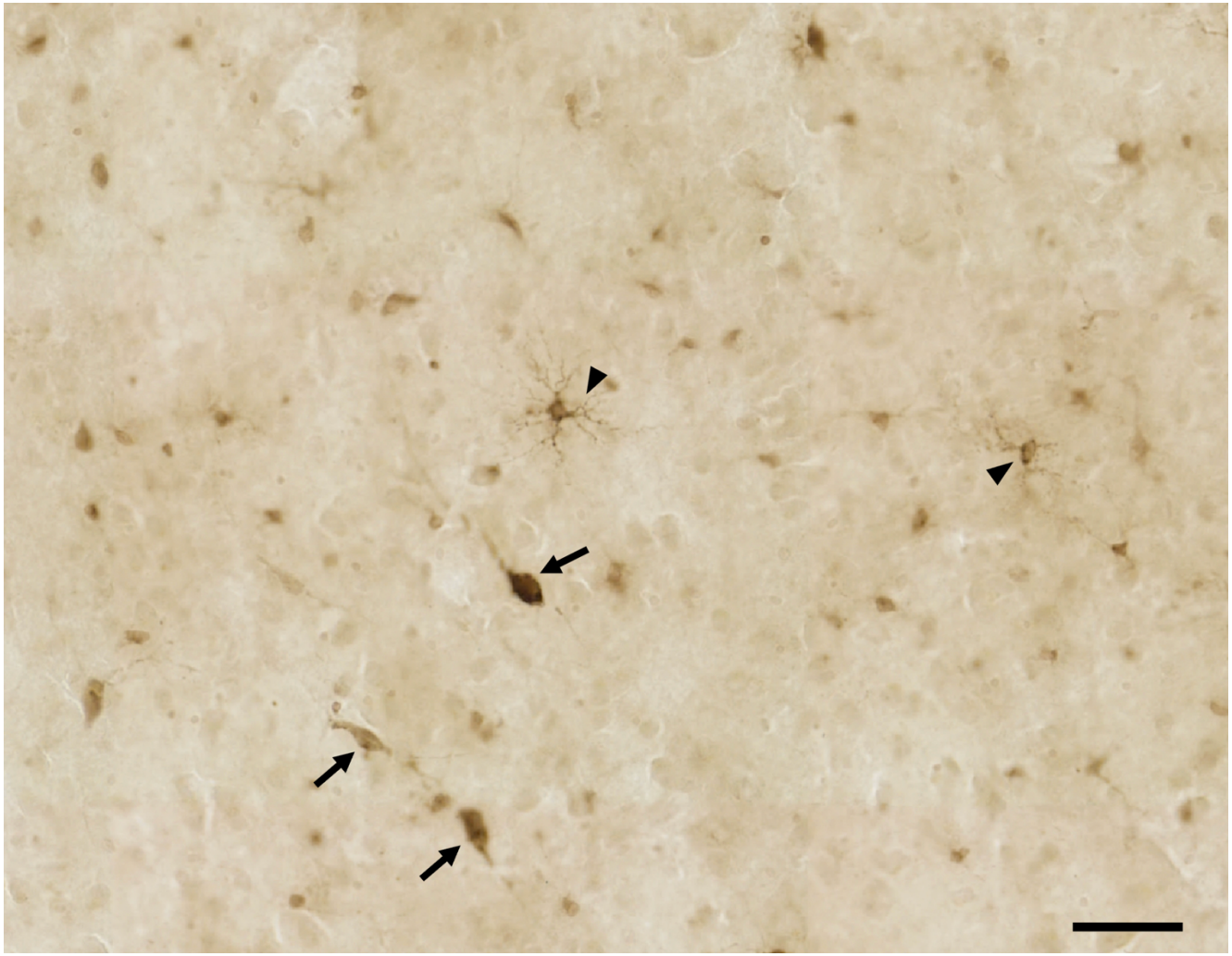

Figure 3.4 Butyrylcholinesterase (BChE)-positive neurons (arrows) and microglia (arrowheads) in the nucleus of the vertical limb of the diagonal band of Broca in a cognitively normal case. Note the larger size of the soma and axons of BChE neurons as compared to microglia. These microglia appear to be in a resting state, based on their ramified appearance. Scale bar = 50μm.

Table 3.1 Mann-Whitney statistical analysis of cholinergic neuron counts in regions of interest related to sleep comparing cognitively normal (CN) and Alzheimer's disease (AD) brains

	Cognitively Normal (CN)				Alzheimer's Disease (AD)				
	N	Mean	St. Dev.	Median	N	Mean	St. Dev.	Median	p value
ChAT neurons									
Region									
Ch1	2	10.5	0.7	10.5	1	3.0	n/a	3.0	n/a
Ch2	3	47.3	18.9	39.0	4	14.8	7.0	12.0	0.057
Ch4a	4	69.8	5.2	69.0	5	30.4	16.3	35.0	0.016*
Ch4p	4	42.3	18.2	38.0	5	19.2	16.7	14.0	0.071
Ch5	4	41.8	24.9	40.0	5	17.6	13.6	11.0	0.191
Ch6	3	6.7	7.2	3.0	5	7.4	6.9	5.0	0.714
DR	4	2.0	2.5	1.5	5	0.2	0.5	0	0.286
LC	4	5.3	3.9	3.5	5	4.4	6.1	2.0	0.452
AChE neurons									
Region									
Ch1	2	10.5	3.5	10.5	2	4.5	3.5	4.5	0.333
Ch2	3	18.3	11.9	13.0	5	14.0	6.2	13.0	0.857
Ch4a	4	30.8	12.5	29.5	5	16.6	9.9	13.0	0.111
Ch4p	4	27.8	2.4	27.0	5	12.2	6.5	10.0	0.008**
Ch5	4	22.8	4.5	21.5	5	14.4	8.0	11.0	0.286
Ch6	3	8.7	6.0	8.0	5	8.4	7.3	5.0	0.839
DR	4	1.5	1.0	2.0	5	0.2	0.5	0	0.087
LC	4	5.5	5.2	3.5	5	1.3	1.5	1.0	0.171
BChE neurons									
Region									
Ch1	2	0	0	0	2	0	0	0	1
Ch2	3	2.0	1.7	1.0	5	1.8	1.3	1.0	1
Ch4a	4	4.5	3.5	4.5	5	2.8	1.8	3.0	0.564
Ch4p	4	2.5	3.0	1.0	5	1.4	0.6	1.0	1
Ch5	4	4.8	2.9	5.5	5	2.0	1.9	2.0	0.214
Ch6	3	8.0	3.5	10.0	5	1.8	2.2	1.0	0.071
DR	4	1.0	1.4	0.5	5	0	0	0	0.167
LC	4	5.5	4.8	4.5	5	2.2	1.9	2.0	0.262

n/a = values not available

Next, the Mann-Whitney statistical analysis for ChAT neuron counts comparing CN and DLB brains indicated significant differences in several regions (Table 3.2). In the Ch2 region, the mean ChAT neuron count for DLB brains (10.6 ± 5.9) was significantly lower compared to CN brains (47.3 ± 18.9), with a p-value of 0.036. Ch4a region also showed a significant reduction in ChAT neuron count for DLB brains (24.6 ± 15.7) as compared to CN brains (69.8 ± 5.2), with a p-value of 0.016. Similar significant reductions were observed in the Ch4p region (10.2 ± 6.8 for DLB vs. 42.3 ± 18.2 for CN, p = 0.016). The other regions analyzed, including Ch1, Ch5, Ch6, DR, and LC, did not show significant differences. Significant differences were found in the Ch4p region for AChE neuron counts, where the mean in DLB brains (9.8 ± 6.0) was significantly lower compared to CN brains (27.8 ± 2.4), yielding a p-value of 0.016. The Ch5 region also demonstrated significant differences in AChE neuron counts, with an average of 13.0 (± 5.2) neuron for DLB compared to 22.8 (± 4.5) neurons for CN, giving a p value of 0.024. The other regions, Ch6, DR, and LC, did not show significant differences. For BChE neuron counts, the analysis revealed significant differences only in the Ch6 region, where the mean neuron count in DLB brains of 1.2 (± 0.5) BChE neurons was significantly lower an average of 8.0 (± 3.5) BChE neurons n in CN brains, with a p-value of 0.018. The remaining regions of interest did not show significant differences for BChE neuron counts. According to Geula *et al.* (2021), there is evidence that BF cholinergic neurons are also vulnerable to degeneration in DLB, though further investigation is required. Consistent with this, the results from this study relating to ChAT and AChE neuron counts suggest that this region is particularly vulnerable to the loss of cholinergic neurons.

Table 3.2 Mann-Whitney statistical testing of cholinergic neuron counts in regions of interest related to sleep comparing cognitively normal (CN), dementia with Lewy bodies (DLB), and multiple sclerosis (MS) brains

	Dementia with Lewy bodies (DLB)					Multiple sclerosis (MS)				
	N	Mean	St. Dev.	Median	p value	N	Mean	St. Dev.	Median	p value
ChAT neurons										
Region										
Ch1	3	3.0	1.7	3.0	0.437	0	n/a	n/a	n/a	n/a
Ch2	5	10.6	5.9	9.0	0.036*	3	27.3	24.8	23.0	0.400
Ch4a	5	24.6	15.7	21.0	0.016*	3	53.3	8.1	52.0	0.057
Ch4p	5	10.2	6.8	7.0	0.016*	3	71.3	43.3	81.0	0.629
Ch5	5	10.8	7.9	8.0	0.064	4	35.3	24.0	35.0	0.343
Ch6	5	5.0	3.1	5.0	0.893	4	9.0	10.0	6.5	0.857
DR	5	0.4	0.6	0	0.528	4	2.0	2.8	1.0	1
LC	5	6.0	3.3	5.0	0.573	4	9.0	3.7	8.5	0.171
AChE neurons										
Region										
Ch1	3	1.7	1.5	2.0	0.200	0	n/a	n/a	n/a	n/a
Ch2	5	13.0	5.7	16.0	0.964	3	28.0	14.8	35.0	0.400
Ch4a	5	20.0	13.6	15.0	0.127	3	29.3	12.0	30.0	0.971
Ch4p	5	9.8	6.0	10.0	0.016*	3	28.7	7.2	25.0	0.571
Ch5	5	13.0	5.2	11.0	0.024*	4	19.8	4.3	18.0	0.257
Ch6	5	5.6	1.7	6.0	0.446	4	9.8	2.4	9.0	0.886
DR	5	1.2	1.8	0	0.810	4	0.3	0.5	0	0.143
LC	5	6.6	3.6	6.0	0.516	4	4.3	2.2	5.0	1
BChE neurons										
Region										
Ch1	3	0.3	0.6	0	1	0	n/a	n/a	n/a	n/a
Ch2	5	2.6	2.1	2.0	0.750	3	3.3	2.5	3.0	0.700
Ch4a	5	2.4	0.9	3.0	0.675	3	4.3	1.5	4.0	1
Ch4p	5	2.2	2.7	1.0	1	3	2.0	1.0	2.0	0.657
Ch5	5	2.0	1.4	3.0	0.143	4	3.3	1.7	3.5	0.514
Ch6	5	1.2	0.5	1.0	0.018*	4	2.0	0.8	2.0	0.057
DR	5	0.2	0.5	0	0.405	4	0.5	0.6	0.5	1
LC	5	3.0	3.1	3.0	0.437	4	2.8	2.2	3.0	0.486

n/a = values not available

In the analysis of MS brains, no significant differences were observed in the ChAT, AChE, and BChE neuron counts across all regions when compared to CN brains (Table 3.2).

3.2.2. Nicotinamide Adenine Dinucleotide Phosphate-Diaphorase Neurons

Nicotinamide adenine dinucleotide phosphate-diaphorase (NADPH-d) neurons were identified by an intense dark blue-purple staining of the neuronal soma and axons (Fig. 3.5) and quantified in each region of interest across all groups (Fig. 3.6; Table 3.3). Overall, NADPH-d neuron counts in AD brains were generally lower than in CN brains across most regions (Fig. 3.6; Table 3.3). In region Ch1, there were 0 NADPH-d neurons on average in AD while CN brains had an average of 1.0 ($p = 0.100$). Region Ch2 in AD cases showed a mean count of 1.4 NADPH-d neurons versus 6.3 in CN cases ($p = 0.143$). For Ch4a, the mean was 3.2 compared to 5.0 in CN cases ($p = 0.246$), and Ch4p had a mean of 1.0 compared to 8.8 in CN cases ($p = 0.135$). The Ch5 region had a mean of 8.6 ($\pm$ 15.6) versus 36.3 ($\pm$ 29.3) in CN brains ($p = 0.056$). The Ch5 region in both AD and CN cases demonstrated the highest standard deviation amongst the regions examined. Region Ch6 had a mean of 6.2 compared to 9.7 in CN ($p = 0.375$). The DR region was significantly different from that of CN brains and had no neurons in AD ($p = 0.048$), whereas CN had a mean of 3.0 NADPH-d neurons. The LC region showed a mean count of 3.0 in AD and 2.5 in CN ($p = 0.714$).

Overall, NADPH-d neuron counts in DLB brains were also generally lower, however, none were significantly different compared to those in CN brains (Table 3.3). In region Ch1, the mean count was 1.3 compared to 1.0 in CN ($p = 1$). Ch2 displayed a mean of 5.4 versus 6.3 in CN ($p = 0.875$). For Ch4a, the mean was 5.6 compared to

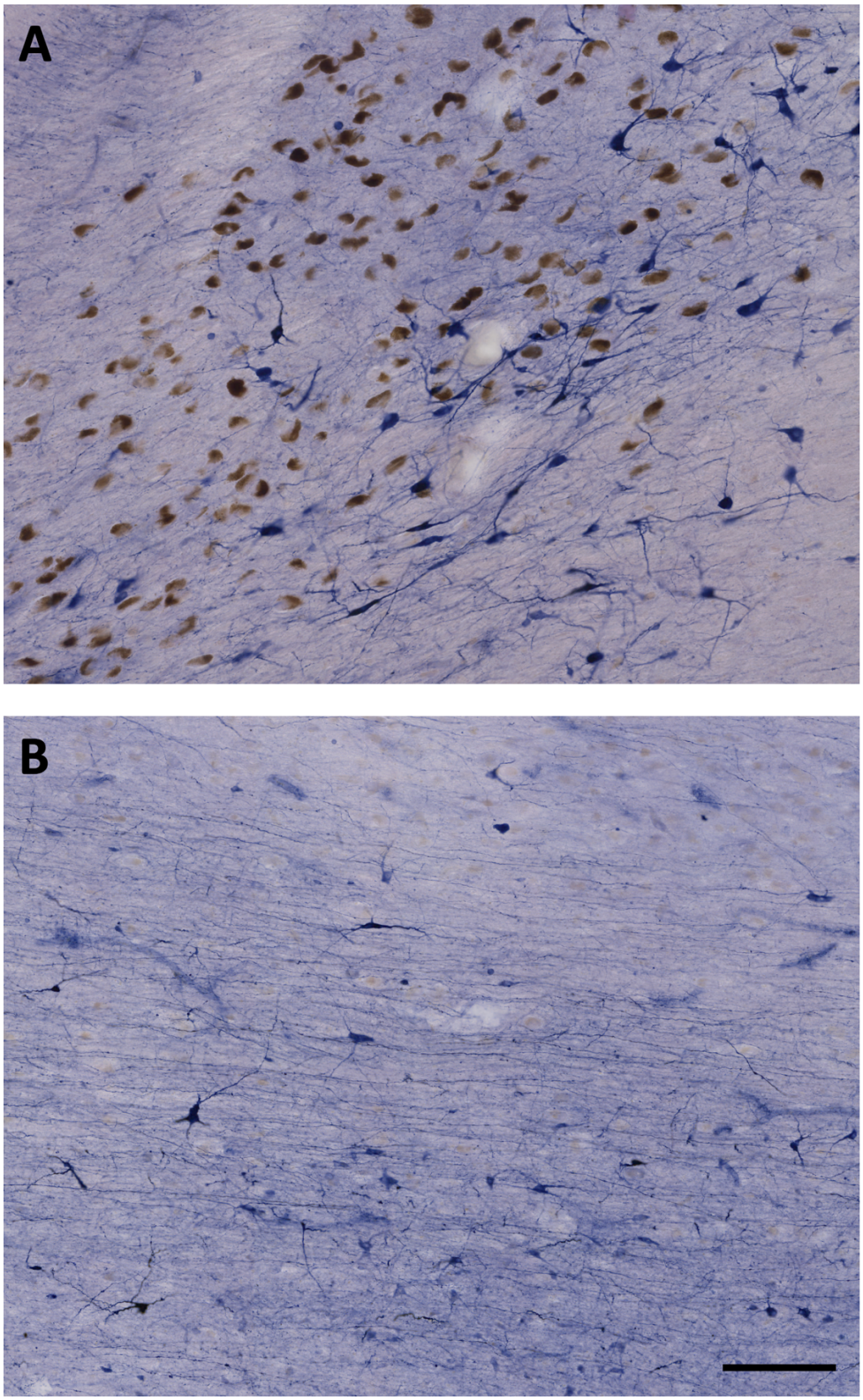

Figure 3.5 Photomicrographs of dark blue-purple NADPH-diaphorase neurons in the brainstem (A) contrasted by dark brown neuromelanin-containing locus coeruleus neurons, and in the basal forebrain (B) within the anterior nucleus basalis of Meynert. Scale bar = 200μm.

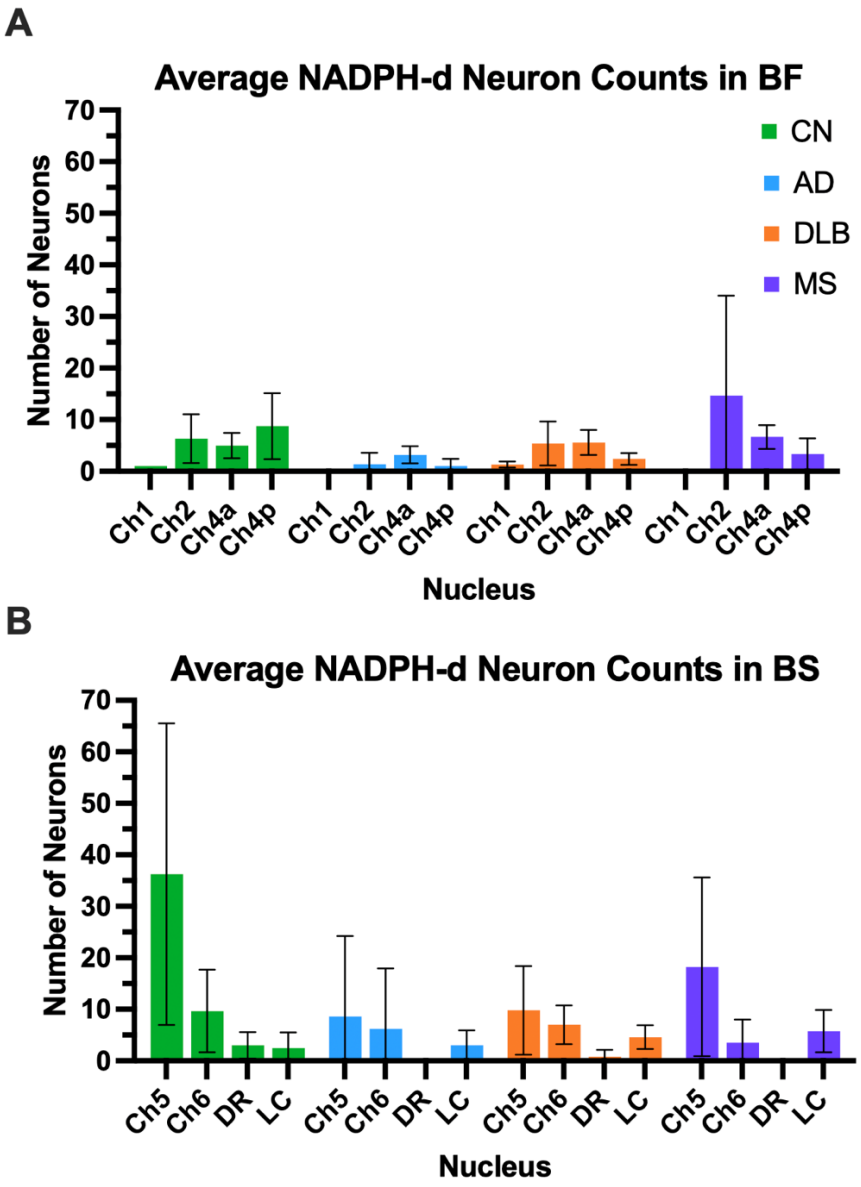

Figure 3.6 Average NADPH-diaphorase neuron counts in cognitively normal (CN), Alzheimer's disease (AD), dementia with Lewy bodies (DLB), and multiple sclerosis (MS) groups in the basal forebrain (BF; A) and brainstem (BS; B). Values are mean ± SD.

Table 3.3 Mann-Whitney statistical testing of average NADPH-diaphorase neurons in regions of interest related to sleep comparing cognitively normal (CN), Alzheimer's disease (AD), dementia with Lewy bodies (DLB), and multiple sclerosis (MS) brains

Cognitively Normal (CN)					
	N	Mean	St. Dev.	Median	
Region					
Ch1	2	1.0	0	1.0	
Ch2	3	6.3	4.7	8.0	
Ch4a	4	5.0	2.5	5.5	
Ch4p	4	8.8	6.4	10.5	
Ch5	4	36.3	29.3	37.5	
Ch6	3	9.7	8.0	9.0	
DR	4	3.0	2.6	3.0	
LC	4	2.5	3.0	2.0	
Alzheimer's disease (AD)					
	N	Mean	St. Dev.	Median	p value
Region					
Ch1	3	0	0	0	0.100
Ch2	5	1.4	2.2	0	0.143
Ch4a	5	3.2	1.6	3.0	0.246
Ch4p	5	1.0	1.4	0	0.135
Ch5	5	8.6	15.6	0	0.056
Ch6	5	6.2	11.8	0	0.375
DR	5	0	0	0	0.048*
LC	5	3.0	2.9	2.0	0.714
Dementia with Lewy bodies (DLB)					
	N	Mean	St. Dev.	Median	p value
Region					
Ch1	3	1.3	0.6	1.0	1
Ch2	5	5.4	4.3	4.0	0.875
Ch4a	5	5.6	2.4	5.0	0.762
Ch4p	5	2.4	1.1	2.0	0.254
Ch5	5	9.8	8.6	5.0	0.127
Ch6	5	7.0	3.7	6.0	0.732
DR	5	0.8	1.3	0	0.206
LC	5	4.6	2.3	5.0	0.278
Multiple sclerosis (MS)					
	N	Mean	St. Dev.	Median	p value
Region					
Ch1	0	n/a	n/a	n/a	n/a
Ch2	3	14.7	19.4	4.0	1
Ch4a	3	6.7	2.3	8.0	0.314
Ch4p	3	3.3	3.1	4.0	0.257
Ch5	4	18.3	17.4	16.5	0.343
Ch6	4	3.5	4.5	2.0	0.400
DR	4	0	0	0	0.143
LC	4	5.8	4.1	5.5	0.257

n/a = values not available

5.0 in CN ($p = 0.762$), and Ch4p had a mean count of 2.4 versus 8.8 in CN cases($p = 0.254$). Region Ch5 had a mean of 9.8 (± 8.6) NADPH-d neurons compared to 36.3 in CN ($p = 0.127$), and this region was also characterized by the highest standard deviation amongst the regions examined. Region Ch6 had a mean count of 7.0 in DLB cases versus 9.7 in region Ch6 in CN ($p = 0.732$) cases. The DR region had a mean of 0.8 in DLB compared to 3.0 in CN ($p = 0.206$), and the LC region had a mean count of 4.6 compared to 2.5 in CN ($p = 0.278$).

In MS brains, NADPH-d neuron counts were relatively comparable to those in CN brains (Fig. 3.6; Table 3.3). In the Ch1 region, data was not available. Ch2 had a mean count of 14.7 compared to 6.3 in CN ($p = 1$). For Ch4a, the mean NADPH-d neuron count was 6.7 in MS cases compared to 5.0 in CN cases ($p = 0.314$), while Ch4p showed a mean count of 3.3 NADPH-d neurons in MS cases compared to 8.8 in CN ($p = 0.257$). The Ch5 region had a mean of 18.3 (± 17.4) compared to 36.3 in CN ($p = 0.343$), and once again, demonstrating the highest standard deviation in this region. Ch6 showed a mean count of 3.5 compared to 9.7 in CN ($p = 0.400$). The DR region had no neurons in MS ($p = 0.143$), whereas CN had a mean of 3.0. The LC region showed a mean count of 5.8 NADPH-d neurons in MS compared to 2.5 in CN ($p = 0.257$).

In CN brains, region Ch1 had a mean count of 1.0, Ch2 had a mean of 6.3, Ch4a showed a mean of 5.0, and Ch4p had a mean of 8.8 NADPH-d neurons. Region Ch5 had a high mean count of 36.3 (± 29.23) while Ch6 displayed a mean of 9.7 NADPH-d neurons. The DR region had a mean of 3.0, and the LC region showed a mean count of 2.5 NADPH-d neurons.

3.2.3. Locus Coeruleus Pigmented Neurons

Locus coeruleus (LC) pigmented neurons, distinguished by the presence of dark brown neuromelanin-containing granules within the neurons (Fig. 3.7), were quantified in several control sections from each case within every group (Fig. 3.8). AD brains showed a mean of 27.8 (± 24.5, $p < 0.001$), while DLB brains had a mean of 7.7 (± 3.3, $p < 0.001$), both significantly lower than CN brains, with a of 56.8 (± 18.2). MS brains did not differ statistically from CN brains, with a mean of 61.8 (± 15.7, $p = 0.456$). Many LC pigmented neurons in AD and DLB cases displayed signs of degeneration, evident not only through reduced neuron counts but also with the observation of neuromelanin fragments scattered throughout the nucleus (Fig. 3.9).

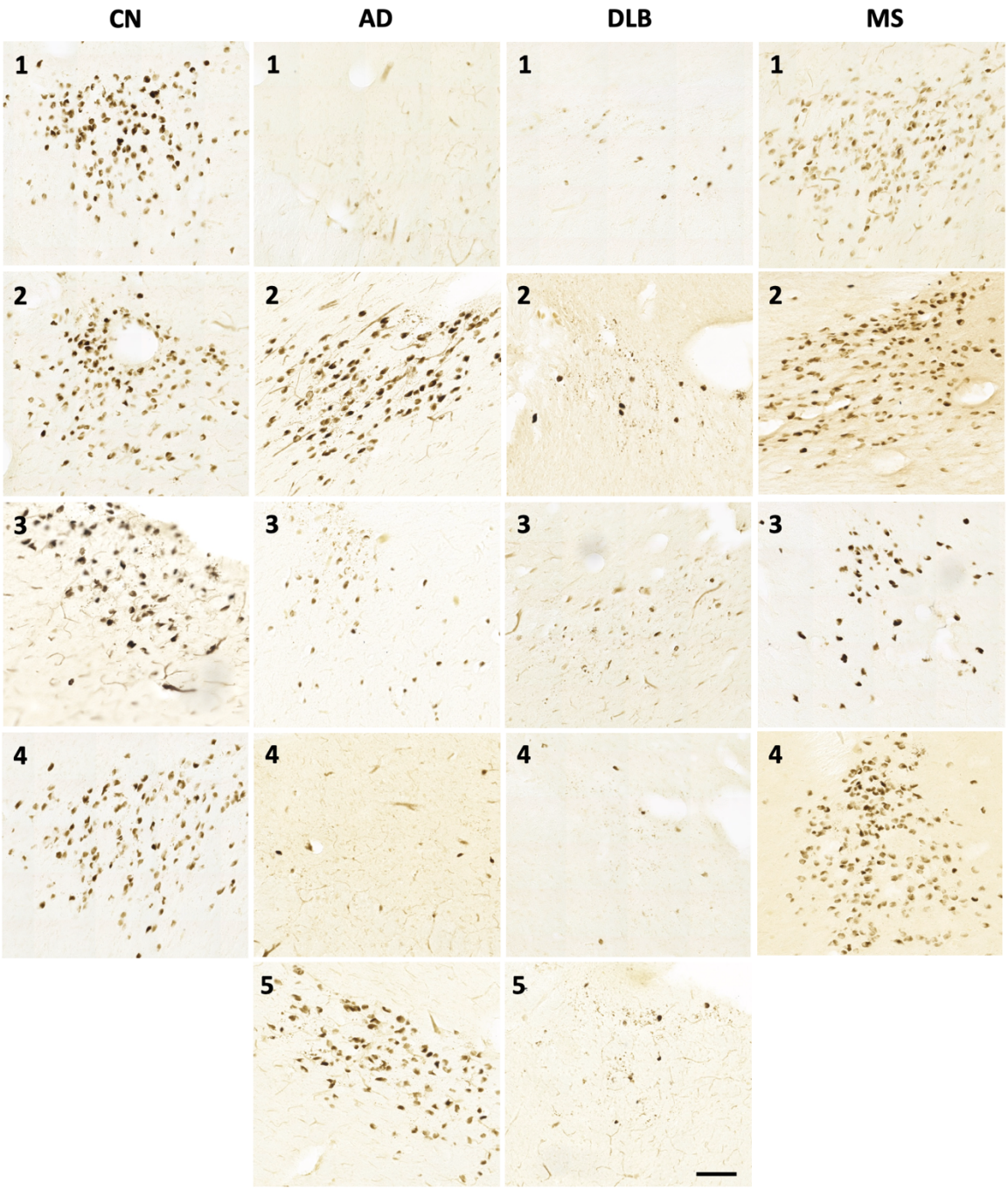

Figure 3.7 Photomicrographs of the locus coeruleus nucleus in negative control immunohistochemical stain sections comparing cognitively normal (CN; first column), Alzheimer's disease (AD; second column), dementia with Lewy bodies (DLB; third column), and multiple sclerosis (MS; fourth column) brains. The numbers in each column correspond to the case number (Table 2.1). Scale bar = 200µm.

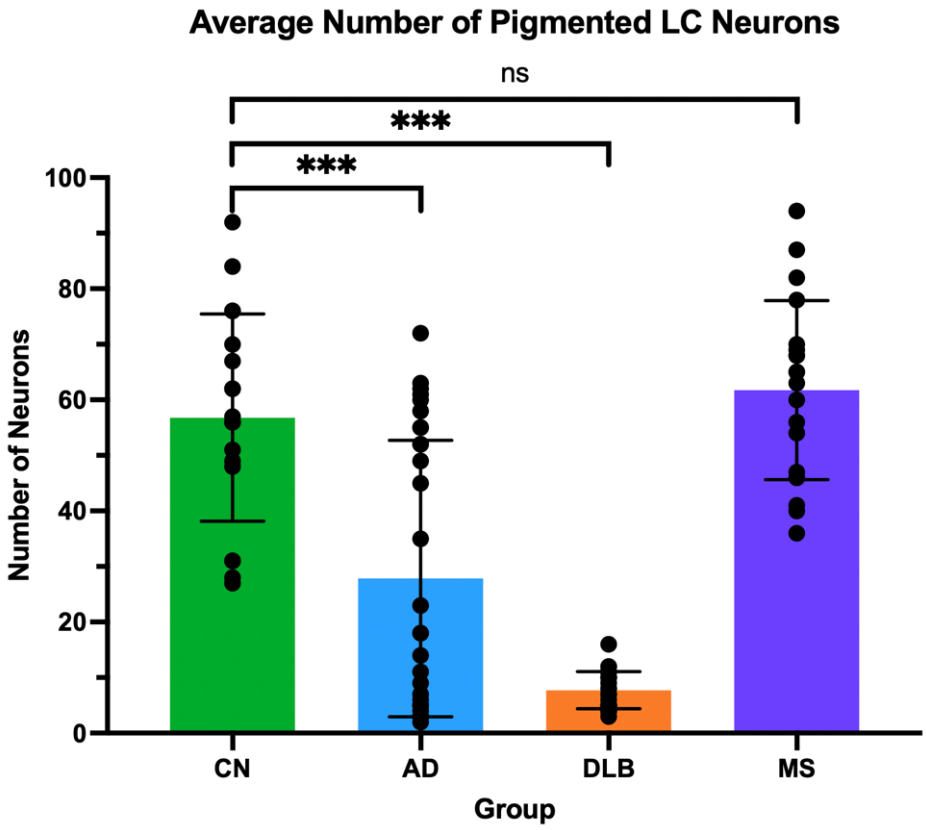

Figure 3.8 Locus coeruleus pigmented neuron counts in cognitively normal (CN), Alzheimer's disease (AD), dementia with Lewy bodies (DLB), and multiple sclerosis (MS) brains in control stain sections. Note the significant reductions in AD and DLB groups as compared to CN brains, as well as the comparable values between CN and MS brains. Values are mean ± SD. Statistical analysis by Mann-Whitney test, ns = not significant, ***$p<0.001$.

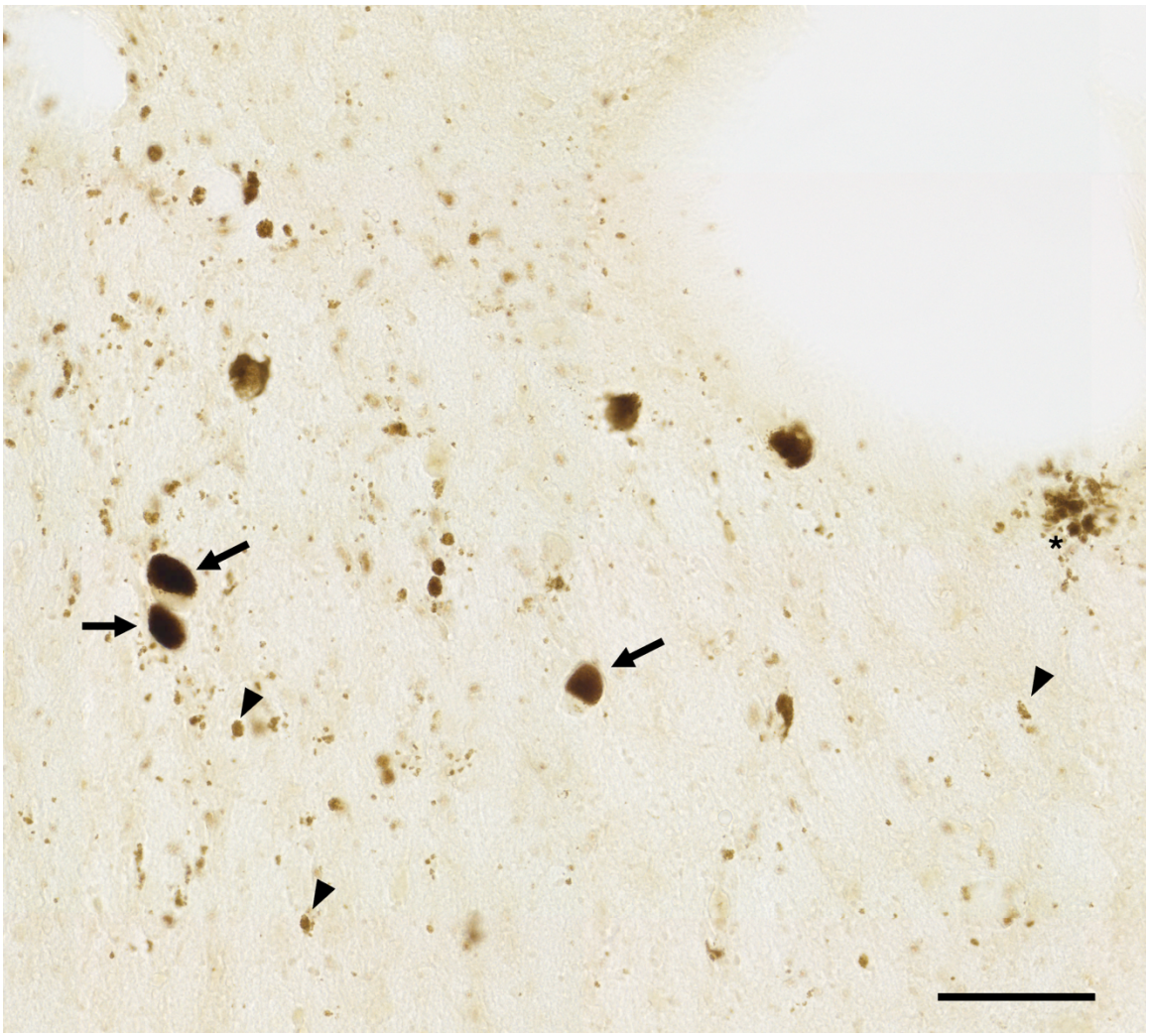

Figure 3.9 Example of degenerated locus coeruleus (LC) pigmented neurons in a negative control Iba1 stain section of a dementia with Lewy bodies case. Arrows indicate intact LC pigmented neurons. Arrowheads point to neuromelanin fragments, and the asterisk marks a cluster of neuromelanin fragments in the extracellular space, from degenerated LC pigmented neurons. Scale bar = 100µm.

3.3. Neuropathological Changes

Standard immunohistochemical techniques were employed using specific primary antibodies to detect Aβ plaques, tau NFTs and neuropil threads (NTs), α-synuclein Lewy bodies and neurites, and phosphorylated Tar DNA binding protein 43 (pTDP-43) neuronal cytoplasmic inclusions (NCIs) and dystrophic neurites (DNs). Histochemical methods used to examine pathological (pH 6.8) AChE and BChE expression. Neuropathological loads for Aβ, tau, pTDP-43, and for AChE and BChE activity at pH 6.8 stains were analyzed using a semi-quantitative score adapted from a modified CERAD neuropathology diagnostic protocol where: 0 = no pathology; 1 = sparse pathology; 2 = moderate pathology; 3 = frequent pathology (Hamodat et al., 2019; Mirra et al., 1991). Neuropathological density staging for α-synuclein pathology followed a separate diagnostic protocol where: Stage 0 = no pathology; Stage 1 = mild pathology; Stage 2 = moderate pathology; Stage 3 = severe pathology; Stage 4 = very severe pathology (McKeith et al., 2005).

Overall, a frequent abundance of Aβ plaques was observed in AD cases, with the greatest deposition of plaques observed in the BF in Ch2, Ch4a, and Ch4p and in the BS in Ch5, DR, and LC regions, and a lesser deposition in Ch1 in the BF and Ch6 in the BS (Fig. 3.10A, B). The regions in AD brains exhibiting significantly different Aβ plaque abundance scores compared to CN brains were: Ch2 ($p = 0.018$), Ch5 ($p = 0.008$), Ch6 ($p = 0.018$), DR ($p = 0.008$), and LC ($p = 0.008$; Table 3.4). Other regions, such as Ch1, Ch4a, Ch4p, and Ch5, did not show significant differences in Aβ plaque abundance between the groups. Tau NFTs were observed at a moderate-to-frequent abundance overall in AD cases. The highest abundance was seen in the Ch4a and Ch4p regions of

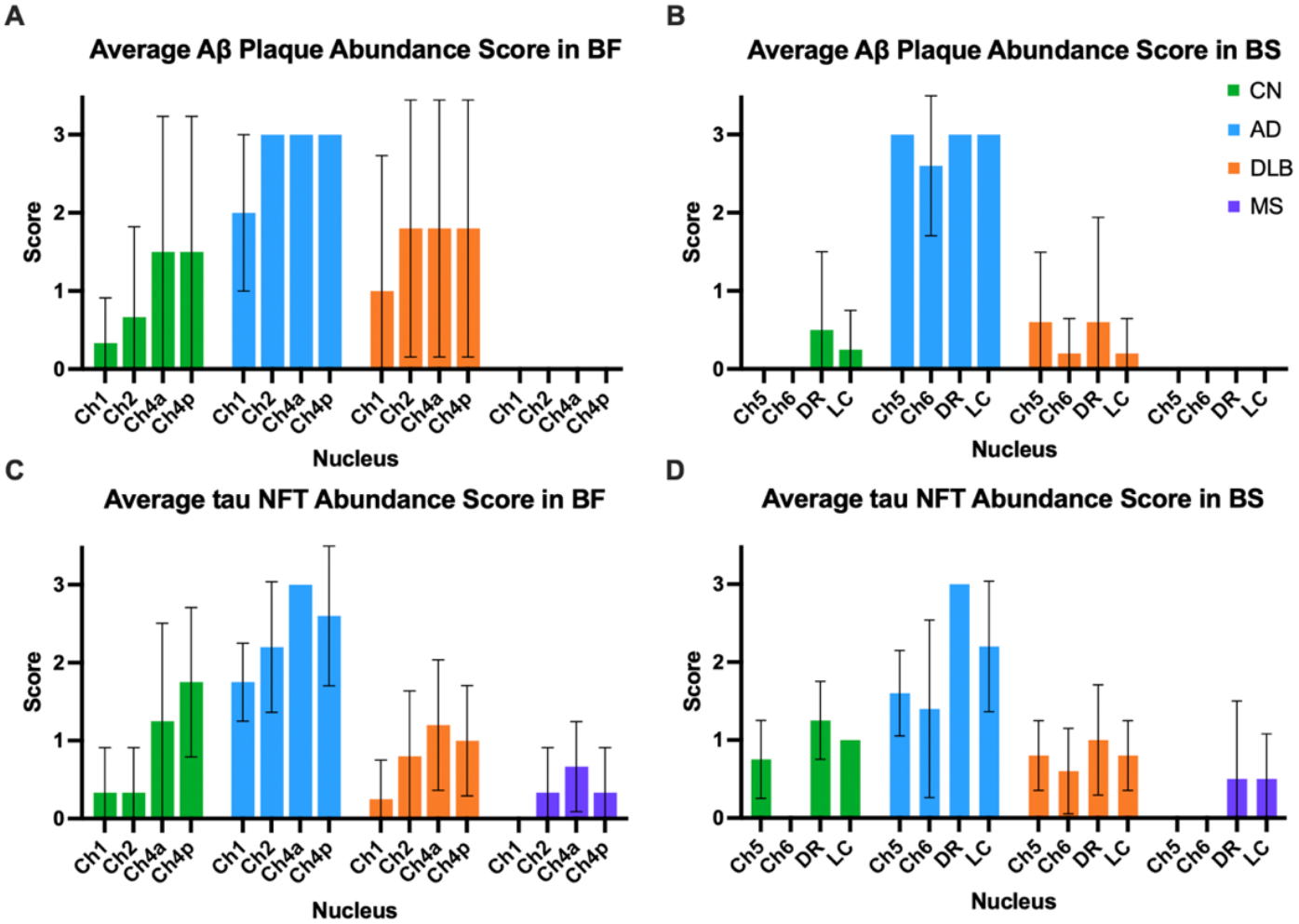

Figure 3.10 Average amyloid-β (Aβ) plaque abundance score in the basal forebrain (BF; A) and brainstem (BS; B) and average tau neurofibrillary tangle (NFT) abundance score in the basal forebrain (BF; C) and brainstem (BS; D) in cognitively normal (CN), Alzheimer's disease (AD), dementia with Lewy bodies (DLB), and multiple sclerosis (MS) brains. Scores: 0 = no pathology; 1 = sparse pathology; 2 = moderate pathology; 3 = frequent pathology (Hamodat et al., 2019; Mirra et al., 1991). Values are mean ± SD.

Table 3.4 Mann-Whitney statistical testing of average Aβ plaque, tau NFT, and α-synuclein pathology abundance scores in regions of interest related to sleep comparing cognitively normal (CN) and Alzheimer's disease (AD) brains

	Cognitively Normal (CN)				Alzheimer's Disease (AD)				
	N	Mean	St. Dev.	Median	N	Mean	St. Dev.	Median	p value
Amyloid-β (Aβ) plaques									
Region									
Ch1	3	0.3	0.6	0	3	2.0	1.0	2.0	0.200
Ch2	3	0.7	1.2	0	5	3.0	0	3.0	0.018*
Ch4a	4	1.5	1.7	1.5	5	3.0	0	3.0	0.167
Ch4p	4	1.5	1.7	1.5	5	3.0	0	3.0	0.167
Ch5	4	0	0	0	5	3.0	0	3.0	0.008**
Ch6	3	0	0	0	5	2.6	0.9	3.0	0.018*
DR	4	0.5	1.0	0	5	3.0	0	3.0	0.008**
LC	4	0.3	0.5	0	5	3.0	0	3.0	0.008**
Tau neurofibrillary tangles (NFTs)									
Region									
Ch1	3	0.3	0.6	0	4	1.8	0.5	2.0	0.086
Ch2	3	0.3	0.6	0	5	2.2	0.8	2.0	0.071
Ch4a	4	1.3	1.3	1.0	5	3.0	0	3.0	0.048*
Ch4p	4	1.8	1.0	1.5	5	2.6	0.9	3.0	0.286
Ch5	4	0.8	0.5	1.0	5	1.6	0.6	2.0	0.119
Ch6	3	0	0	0	5	1.4	1.1	1.0	0.107
DR	4	1.3	0.5	1.0	5	3.0	0	3.0	0.008**
LC	4	1.00	0	1.0	5	2.2	0.8	2.0	0.048*
α-synuclein pathology									
Region									
Ch1	3	0	0	0	3	0.3	0.6	0	1
Ch2	3	0	0	0	5	0.2	0.5	0	1
Ch4a	4	0	0	0	5	0.4	0.9	0	1
Ch4p	4	0	0	0	5	0.3	0.7	0	1
Ch5	4	0	0	0	5	0.2	0.5	0	1
Ch6	3	0	0	0	5	0.2	0.5	0	1
DR	4	0	0	0	5	0.3	0.7	0	1
LC	4	0	0	0	5	0.2	0.5	0	1

Table 3.5 Mann-Whitney statistical testing of average Aβ plaque, tau NFT, and α-synuclein pathology abundance scores in regions of interest related to sleep comparing cognitively normal (CN), dementia with Lewy bodies (DLB), and multiple sclerosis (MS) brains

	Dementia with Lewy bodies (DLB)					Multiple sclerosis (MS)				
	N	Mean	St. Dev.	Median	p value	N	Mean	St. Dev.	Median	p value
Amyloid-β (Aβ) plaques										
Region										
Ch1	3	1.0	1.7	0	1	0	n/a	n/a	n/a	n/a
Ch2	5	1.8	1.6	3.0	0.250	3	0	0	0	1
Ch4a	5	1.8	1.6	3.0	1	3	0	0	0	0.429
Ch4p	5	1.8	1.6	3.0	1	3	0	0	0	0.429
Ch5	5	0.6	0.9	0	0.444	4	0	0	0	1
Ch6	5	0.2	0.5	0	1	4	0	0	0	1
DR	5	0.6	1.3	0	1	4	0	0	0	1
LC	5	0.2	0.5	0	1	4	0	0	0	1
Tau neurofibrillary tangles (NFTs)										
Region										
Ch1	3	0.3	0.5	0	1	0	n/a	n/a	n/a	n/a
Ch2	5	0.8	0.8	1.0	0.679	3	0.3	0.6	0	1
Ch4a	5	1.2	0.8	1.0	1	3	0.7	0.6	1.0	0.771
Ch4p	5	1.0	0.7	1.0	0.286	3	0.3	0.6	0	0.171
Ch5	5	0.8	0.5	1.0	1	4	0	0	0	0.143
Ch6	5	0.6	0.6	1.0	0.196	4	0	0	0	1
DR	5	1.0	0.7	1.0	0.762	4	0.5	1.0	0	0.143
LC	5	0.8	0.5	1.0	1	4	0.5	0.6	0.5	0.429
α-synuclein pathology										
Region										
Ch1	3	1.0	0	1.0	0.029*	0	n/a	n/a	n/a	n/a
Ch2	5	1.1	0.2	1.0	0.018*	3	0	0	0	1
Ch4a	5	1.1	0.2	1.0	0.008**	3	0	0	0	1
Ch4p	5	1.5	1.1	1.0	0.048*	3	0	0	0	1
Ch5	5	1.4	0.4	1.5	0.008**	4	0	0	0	1
Ch6	5	1.6	0.9	1.0	0.018*	4	0	0	0	1
DR	5	2.3	1.0	2.0	0.016*	4	0	0	0	1
LC	5	1.9	0.2	2.0	0.016*	4	0	0	0	1

the BF, and the DR region of the BS, while the lowest abundance was found in the Ch1 and Ch2 regions of the BF, as well as the Ch5, Ch6, and LC regions of the BS (Fig. 3.10C, D). The regions in AD brains exhibiting significantly different tau NFT abundance scores compared to CN brains were: Ch4a ($p = 0.048$), DR ($p = 0.008$), and LC ($p = 0.048$; Table 3.4). The Ch1, Ch2, Ch4p, Ch5, and Ch6 regions did not show significant differences between the two groups, although there was a trend towards higher mean scores in AD brains. Tau neuropil threads (NTs) were also observed to have an average abundance of moderate-to-frequent, with a similar distribution pattern as NFTs in the BF but were instead observed to be consistently more frequent throughout the BS. α-synuclein pathology was assessed using a different scoring system than the one used for Aβ, tau, AChE- and BChE-positive, and pTDP-43 pathology (McKeith et al., 2005). α-synuclein pathology was detected in only one AD case (AD2) and showed an average stage of 1.5 (mild-to-moderate) in all regions examined (Fig. 3.11A, B). This case therefore demonstrated mixed neuropathology. However, AD brains did not show significant differences in α-synuclein staging scores compared to CN brains in any of the regions of interest (Table 3.4).

DLB cases showed an overall sparse-to-moderate deposition of Aβ plaques, with the highest abundance in the Ch2, Ch4a, and Ch4p BF regions, and a reduced abundance in Ch1 in the BF and all BS nuclei of interest (Fig. 3.10A, B). However, DLB brains did not show significant differences in tau NFT abundance scores compared to CN brains in any region of interest (Table 3.5). In the analysis of tau NFTs, DLB cases had an overall sparse abundance of NFTs and NTs throughout the BF and BS (Fig. 3.10C, D). Though, DLB brains did not show significant differences in tau NFT abundance scores compared

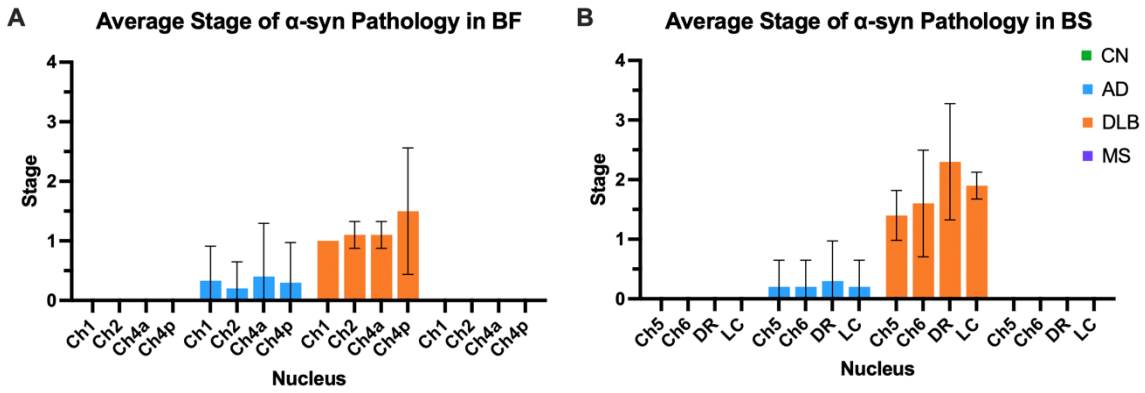

Figure 3.11 Average α-synuclein pathology stage in cognitively normal (CN), Alzheimer's disease (AD), dementia with Lewy bodies (DLB), and multiple sclerosis (MS) brains in the basal forebrain (BF; A) and brainstem (BS; B). Stage 0 = no pathology; Stage 1 = mild pathology; Stage 2 = moderate pathology; Stage 3 = severe pathology; Stage 4 = very severe pathology (McKeith et al., 2005). Values are mean ± SD.

to CN brains in any region of interest (Table 3.5). α-synuclein deposition in DLB showed an overall average severity stage of 1 (mild) throughout the BF and 1.5 (mild-to-moderate) throughout the BS, with the highest severity staging of 2 (moderate) observed in the DR and LC BS nuclei (Fig. 3.11A, B). All regions of interest in DLB cases were significantly different from those in CN brains: Ch1 ($p = 0.029$), Ch2 ($p = 0.018$), Ch4a ($p = 0.008$), Ch4p ($p = 0.048$), Ch5 ($p = 0.008$), Ch6 ($p = 0.018$), DR ($p = 0.016$), and LC ($p = 0.016$; Table 3.5).

Analysis of MS cases showed no Aβ plaques in any BF or BS regions (Fig. 3.9A, B), and none of the regions examined showed significant differences in Aβ plaque abundance scores compared to CN brains (Table 3.5). In MS cases, NFTs showed a sparse abundance in Ch2, Ch4a, and Ch4p BF regions and DR and LC BS regions. Though, MS brains did not show significant differences in tau NFT abundance scores compared to CN brains in any region of interest (Table 3.5). NTs shared a similar BF distribution and abundance, meanwhile NTs were sparsely observed throughout all BF nuclei in MS brains. No α-synuclein pathology was observed in any MS case, and none of the regions showed significant differences in α-synuclein staging scores when compared (Table 3.5).

Analysis of CN cases showed an overall sparse-to-moderate Aβ plaques abundance in CN cases, with the highest abundance in Ch4a and Ch4p BF regions, and the sparsest abundance in Ch1 and Ch2 in the BF, and the DR and LC regions in the BS (Fig. 3.9A, B). It should be noted that Aβ plaques were only observed in cases CN3 and CN4, who were 100 and 104 years old at the time of death, respectively (Table 2.1). Overall, NFTs were sparsely abundant in CN cases. NFTs, however, were not observed

in Ch6 in the BS. NTs were observed to have a similar distribution and abundance. It should be noted that cases CN3 and CN4 also demonstrated a slightly higher NFT and NT abundance compared to the other CN cases.

pTDP-43 pathology, observed only as sparse neuronal cytoplasmic inclusions (NCIs), was present in only one AD case (AD5) within the Ch4p nucleus and was not statistically different from CN brains.

Cholinesterases (ChEs) have previously been known to associate with AD Aβ plaques and NFTs (Perry et al., 1978). ChE-positive plaque abundance was examined using the same scoring protocol as Aβ plaques and tau NFTs. AChE- and BChE-positive plaque load score throughout the BF and BS regions of interest was not remarkably different within the AD group (Fig. 3.12). The Ch4a region in the BF and DR in the BS consistently showed a frequent ChE-positive plaque score. The remaining nuclei demonstrated a rather consistent moderate-frequent ChE-positive plaque abundance score. For AChE plaques, AD brains show significant differences compared to CN brains in regions Ch2, Ch5, Ch6, DR, and LC with p-values of 0.036, 0.016, 0.018, 0.008, and 0.016, respectively (Table 3.6). In the case of BChE plaques, significant differences were observed in AD brains compared to CN brains in regions Ch5, Ch6, DR, and LC, with p-values of 0.016, 0.036, 0.048, and 0.008, respectively (Table 3.6). Some AD cases showed ChE-positive NFTs, often at a sparse abundance within some BF and BS regions of interest.

DLB cases exhibited an overall sparse ChE-positive plaque abundance in the BF and very sparse plaque abundance in the BS (Fig. 3.12). DLB brains were not significantly different CN brains in AChE or BChE plaque abundance (Table 3.7)

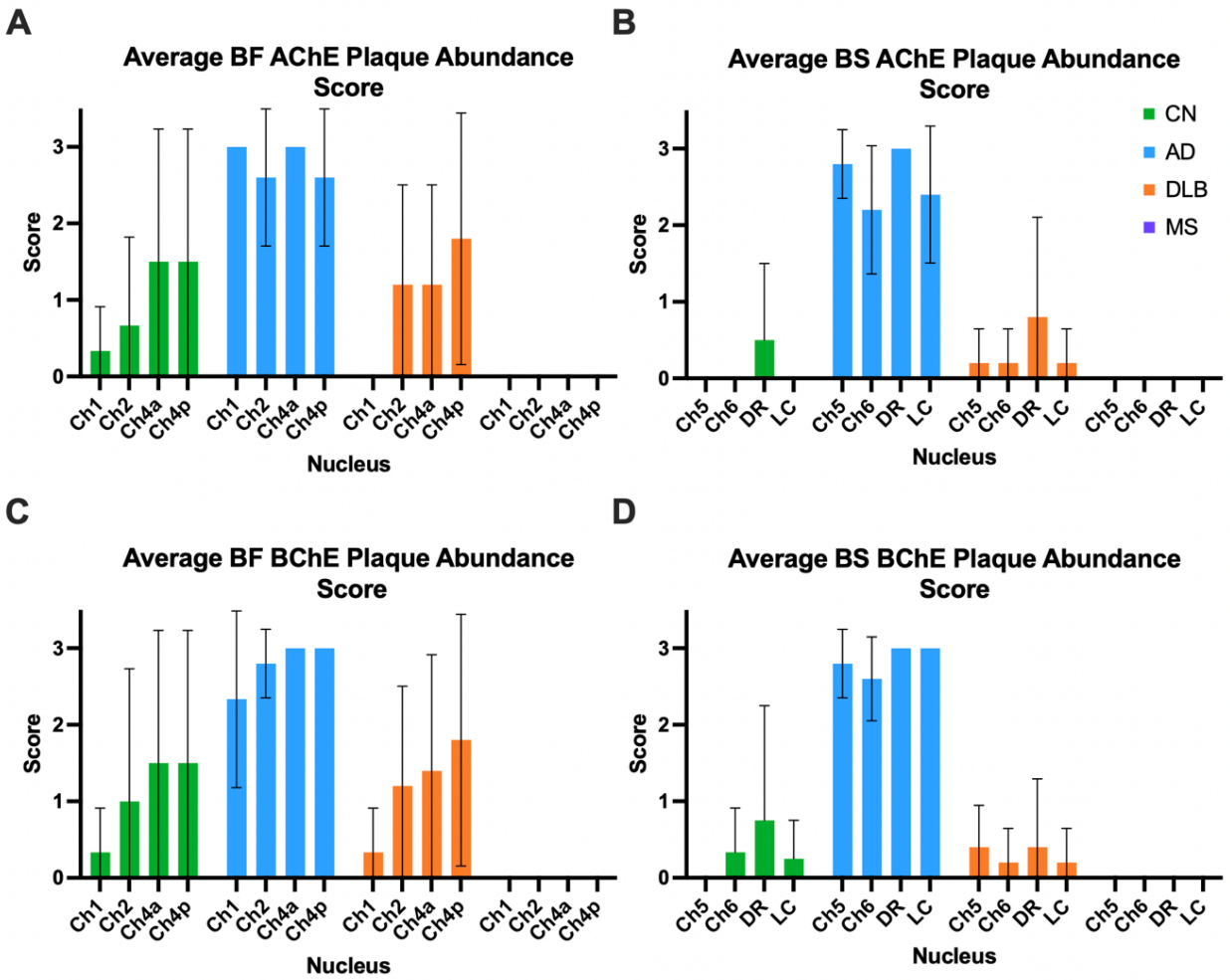

Figure 3.12 Average AChE- (top row) and BChE-positive (bottom row) plaque abundance score in the basal forebrain (BF; A, C) and brainstem (BS; B, D) in cognitively normal (CN), Alzheimer's disease (AD), dementia with Lewy bodies (DLB), and multiple sclerosis (MS) groups. Values are mean ± SD. Scores: 0 = no pathology; 1 = sparse pathology; 2 = moderate pathology; 3 = frequent pathology.

Table 3.6 Mann-Whitney statistical testing of average AChE- and BChE-positive plaque abundance scores in regions of interest related to sleep comparing cognitively normal (CN) and Alzheimer's disease (AD) brains

	Cognitively Normal (CN)				Alzheimer's Disease (AD)				
	N	Mean	St. Dev.	Median	N	Mean	St. Dev.	Median	p value
Acetylcholinesterase (AChE) plaques									
Region									
Ch1	3	0.3	0.6	0	3	3.0	0	3.0	0.200
Ch2	3	0.7	1.2	0	5	2.6	0.9	3.0	0.036*
Ch4a	4	1.5	1.7	1.5	5	3.0	0	3.0	0.167
Ch4p	4	1.5	1.7	1.5	5	2.6	0.9	3.0	0.286
Ch5	4	0	0	0	5	2.8	0.5	3.0	0.016*
Ch6	3	0	0	0	5	2.2	0.8	2.0	0.018*
DR	4	0.5	1.00	0	5	3.0	0	3.0	0.008**
LC	4	0	0	0	5	2.4	0.9	3.0	0.016*
Butyrylcholinesterase (BChE) plaques									
Region									
Ch1	3	0.3	0.6	0	4	2.3	1.2	3.0	0.200
Ch2	3	1.0	1.7	0	5	2.8	0.5	3.0	0.286
Ch4a	4	1.5	1.7	1.5	5	3.0	0	3.0	0.167
Ch4p	4	1.5	1.7	1.5	5	3.0	0	3.0	0.167
Ch5	4	0	0	0	5	2.8	0.5	3.0	0.016*
Ch6	3	0.3	0.6	0	5	2.6	0.6	3.0	0.036*
DR	4	0.8	1.5	0	5	3.0	0	3.0	0.048*
LC	4	0.3	0.5	0	5	3.0	0	3.0	0.008**

Table 3.7 Mann-Whitney statistical testing of average AChE- and BChE-positive plaque abundance scores in regions of interest related to sleep comparing cognitively normal (CN), dementia with Lewy bodies (DLB), and multiple sclerosis (MS) brains

	Dementia with Lewy bodies (DLB)					Multiple sclerosis (MS)				
	N	Mean	St. Dev.	Median	p value	N	Mean	St. Dev.	Median	p value
Acetylcholinesterase (AChE) plaques										
Region										
Ch1	3	0	0	0	0.429	0	n/a	n/a	n/a	n/a
Ch2	5	1.2	1.3	1.0	0.750	3	0	0	0	1
Ch4a	5	1.2	1.3	1.0	1	3	0	0	0	0.429
Ch4p	5	1.8	1.6	3.0	1	3	0	0	0	0.429
Ch5	5	0.2	0.5	0	1	4	0	0	0	1
Ch6	5	0.2	0.5	0	1	4	0	0	0	1
DR	5	0.8	1.3	0	0.841	4	0	0	0	1
LC	5	0.2	0.5	0	1	4	0	0	0	1
Butyrylcholinesterase (BChE) plaques										
Region										
Ch1	3	0.3	0.6	0	1	0	n/a	n/a	n/a	n/a
Ch2	5	1.2	1.3	1.0	0.929	3	0	0	0	1
Ch4a	5	1.4	1.5	1.0	1	3	0	0	0	0.429
Ch4p	5	1.8	1.6	3.0	1	3	0	0	0	0.429
Ch5	5	0.4	0.6	0	0.444	4	0	0	0	1
Ch6	5	0.2	0.5	0	1	4	0	0	0	1
DR	5	0.4	0.9	0	0.722	4	0	0	0	1
LC	5	0.2	0.5	0	1	4	0	0	0	1

n/a = values not available

ChE-positive NFTs were very sparse, appearing in only two cases and positive only for BChE, not AChE.

MS cases did not exhibit any ChE-positive plaques, and did no significant differences were identified in any regions (Table 3.7). However, one MS case showed sparse ChE-positive NFTs in the DR and LC regions in the BS.

In the CN group, ChE-positive plaques were sparsely observed throughout the BF. AChE-positive plaques were very sparsely observed only in the DR, while BChE-positive plaques were very sparsely observed in Ch6, DR, and LC in the BS (Fig. 3.12). Interestingly, NFTs associated with ChE activity were observed in three cases, showing positivity only for BChE, and were found in varying regions of the BF and BS including Ch2, Ch4a, Ch5, Ch6, and DR regions in sparse abundance.

MS demyelinated lesions within relevant regions were characterized for each individual case. In MS1, an active demyelinating lesion was observed lateral to Ch2, consistent with a periventricular lesion. However, Ch2 exhibited minimal demyelination despite the presence of activated microglia. Ch4a was largely spared of demyelination with the exception of three small, demyelinated lesions within the anterolateral (Ch4al) subsector, and an evident caudal continuation of the periventricular lesion observed in the Ch2 section, which abutted upon the medial anterior commissure (Fig. 1.5). No demyelination was observed in Ch4p, although there was evident microglial activation and proliferation. In the BS, a small active demyelinated lesion was found in the dorsal portion of the periaqueductal grey, sparing the DR. Another active demyelinated lesion was observed within the LC and appeared to be associated with a blood vessel.

In MS2, active demyelination was observed in various regions medioventral and dorsolateral to Ch2, with a ventral portion of Ch2 being involved, and appeared to be consistent with periventricular lesions. Although an active demyelinated lesion was located lateral to the anterolateral portion of Ch4 (Ch4al), Ch4a remained unaffected. Ch4p was nearly entirely involved in an active demyelinating lesion. No demyelinated lesions were observed in the BS, however, there were various regions marked by phagocytic and activated microglia, including within the DR, LC, and some areas outside of the nuclei of interest including the superior cerebellar peduncle and pons.

In MS3, Only the BS was available for analysis. Partial demyelination was observed in the periaqueductal grey, affecting the dorsal portions of the DR and Ch6 regions, with evidence of activated microglia in these areas. It should also be noted that multiple regions within the ventrolateral pons were infiltrated by activated and phagocytic microglia and displayed a prominent hypercellular rim.

MS4 demonstrated scattered regions of active demyelination within and surrounding Ch2, particularly in the medioventral Ch2 and peri-ventricular regions. The Ch4 region remained unaffected by demyelination; however, a large active demyelinated lesion was present throughout the entire periventricular area, as well as an active demyelinated lesion lateral to Ch4p. The BS in this case was nearly entirely demyelinated (Fig. 3.13A, C) by a large lesion with regions marked by active and chronic active activity (Fig. 3.13B, D). This lesion affected all BS nuclei of interest, namely Ch5, Ch6, DR, and LC.

In addition to its normal functions in white matter, neurons, and glial cells, as well as its proposed role in AD pathogenesis, BChE appears to significantly influence the

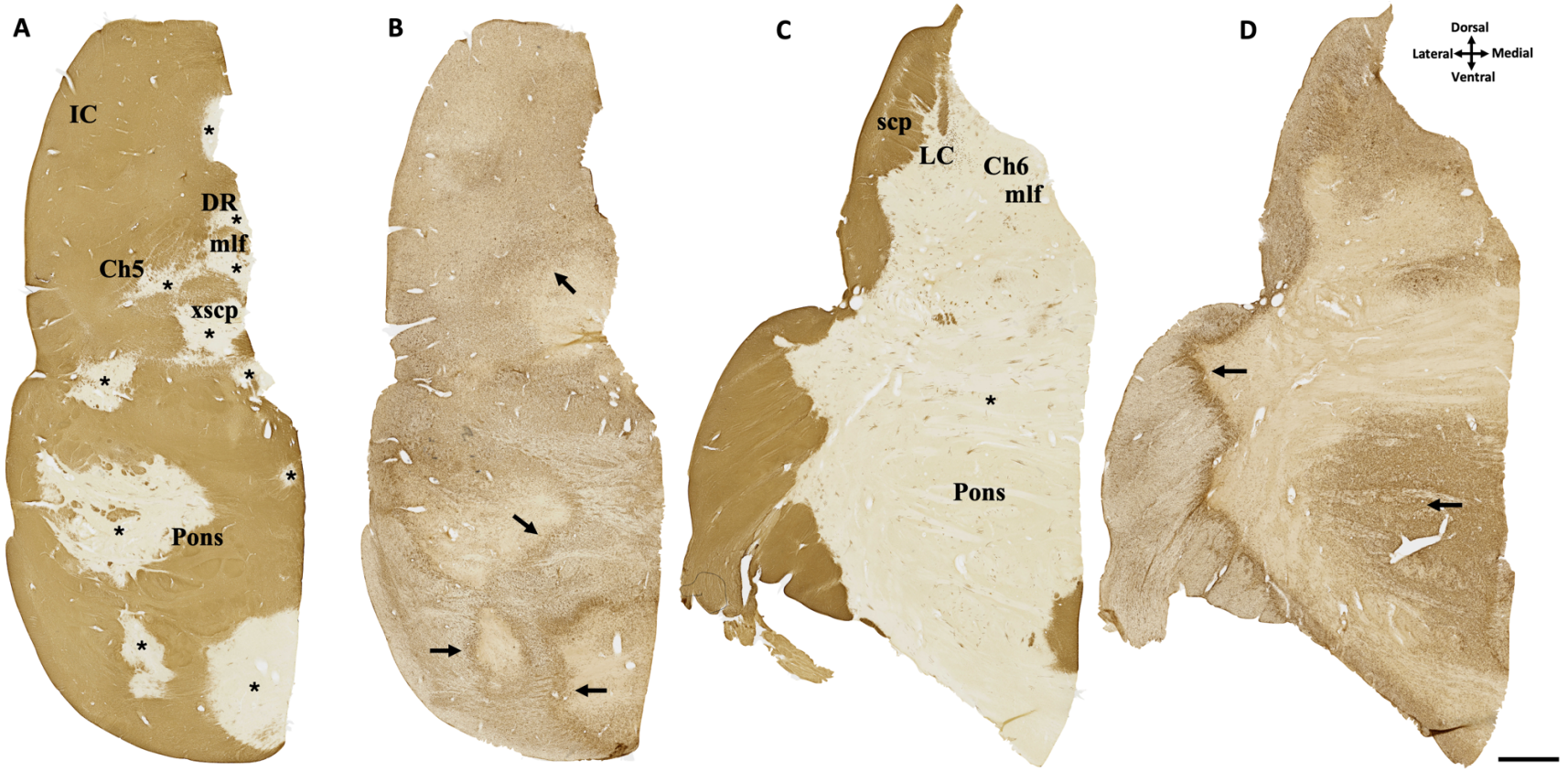

Figure 3.13 Example of multiple sclerosis demyelinated lesions in corresponding sections in the brainstem in case MS4, revealed with myelin basic protein (A, C) and iba1 (B, D) immunohistochemistry. Regions of demyelination are demarcated by asterisks. Note the regions of microglial infiltration in the Iba1 sections (arrows), particularly at the borders of demyelinated regions, which is indicative of active demyelination. Scale bar = 2 mm. Abbreviations: Ch5, pedunculopontine nucleus; Ch6, laterodorsal tegmental nucleus; DR, dorsal raphe nucleus; IC, inferior colliculus; LC, locus coeruleus nucleus; mlf, medial longitudinal fasciculus; scp, superior cerebellar peduncle; xscp, decussation of the superior cerebellar peduncles.

pathology of MS by affecting glial cell activity in active demyelinating lesions (Darvesh, LeBlanc, et al., 2010; Roessmann & Friede, 1966; Thorne et al., 2021). Previous research by Darvesh *et al.* (2010) and Thorne *et al.* (2021) has shown that BChE staining is altered in MS lesions, specifically exhibiting a loss of staining within demyelinated regions, potentially linked to the loss of the enzyme through the loss of glial cells such as oligodendrocytes. Furthermore, BChE was found to stain activated microglia, but not astrocytes, in both active and chronic active MS lesions. These findings support the involvement of BChE in the neuroinflammatory and demyelinating processes that occur in MS (Darvesh, LeBlanc, et al., 2010; Thorne et al., 2021). However, in the cases examined in this study, many active and chronic active lesions within the regions of interest did not follow this trend. Although this study examined subcortical and deep grey matter regions, in contrast to the cortical and white matter regions studied by Darvesh et al. (2010) and Thorne et al. (2021), only a mild presence of activated microglia was observed in BChE stains in active and chronic active MS lesions. The results for BChE staining varied greatly between MS cases and often did not align with the trends described in previous studies. This inconsistency was observed even in cases where BChE staining appeared to have functioned correctly, as evidenced by the surrounding microglial and normal neuronal staining. Consequently, classification of MS lesions, as done in previous studies (Darvesh, LeBlanc, et al., 2010; Thorne et al., 2021), was not feasible in this project.

3.4. Neuroinflammatory Changes

Microglia and astrocytes were quantified, and their morphology described to assess their activity. The analysis of microglia and astrocyte counts across different regions of the brain revealed distinct patterns when comparing cognitively normal (CN) individuals to those with Alzheimer's disease (AD), dementia with Lewy bodies (DLB), and multiple sclerosis (MS).

When comparing CN and AD brains, the mean microglial counts were generally higher in AD brains across most regions. Specifically, in the Ch2 region, AD brains had a mean count of 104.2 microglia compared to 58.7 microglia on average in CN brains (Fig. 3.14). In the Ch4a region, AD brains showed a mean count of 96.0 microglia versus 72.5 microglia in CN brains. microglia Lastly, in the Ch6 region, AD brains had a mean count of 123.8 microglia compared to 61.0 microglia in CN brains. However, none of these differences were statistically significant (Table 3.7). However, it is noteworthy that many microglia appeared dystrophic and highly degenerated, often presenting only the cell body. Microglial dystrophy was particularly pronounced in cases with the longest disease durations and highest neuropathological burden, which is consistent for the other NDD groups as well. Otherwise, microglia in AD cases exhibited an activated morphology, marked by swelling of the cell body and processes, and retraction of processes (Fig. 3.15B). It should also be noted that microglial counts in both AD and CN exhibited a high standard deviation. When comparing astrocyte counts, the results showed less pronounced differences between CN and AD groups. For example, in Ch2, the mean count of 54.3 astrocytes was higher in the CN group compared to the AD group which had on average 47.6 astrocytes, but the p-value was 1, indicating no

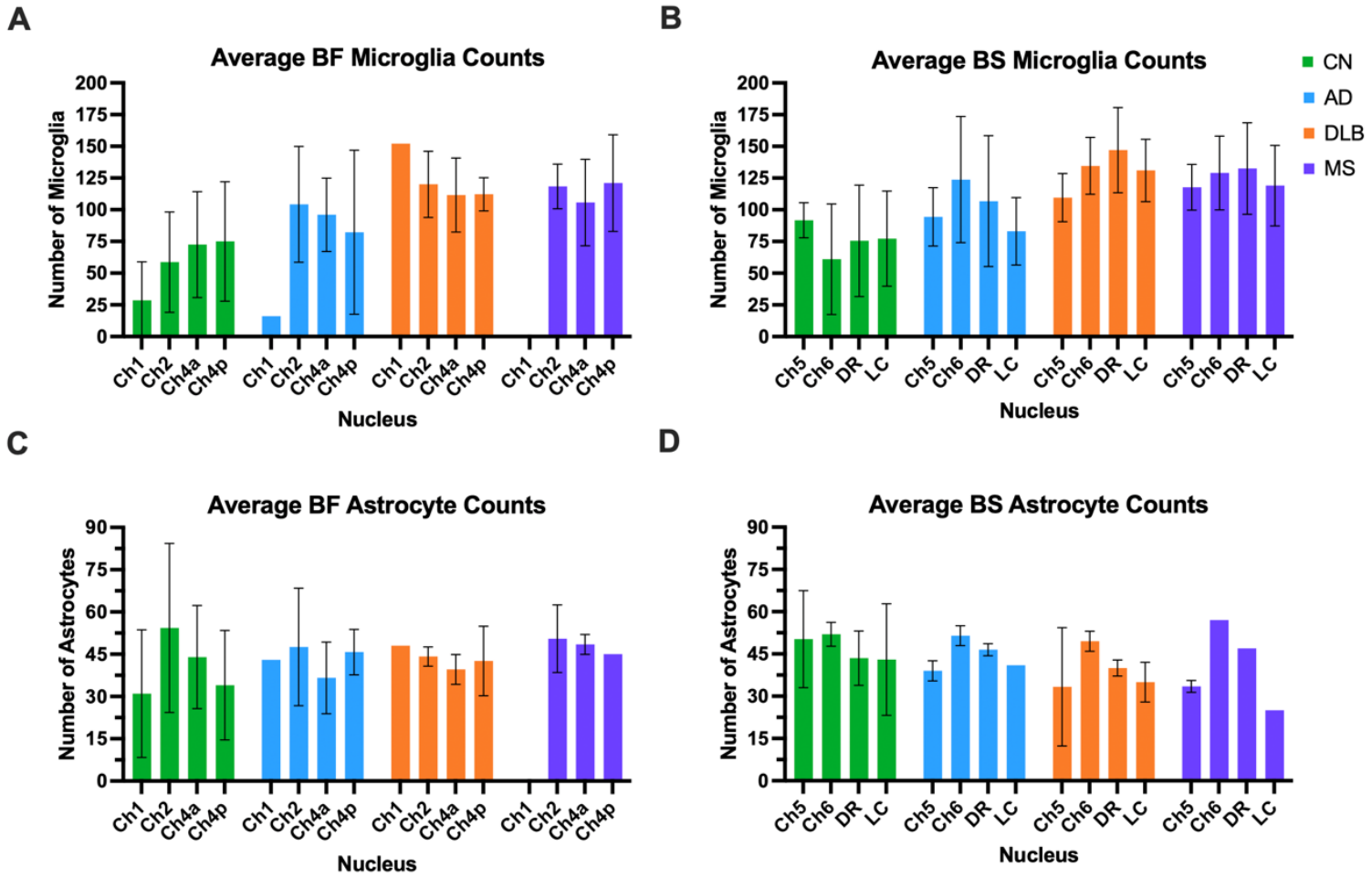

Figure 3.14 Comparison of average microglia counts in the basal forebrain (BF; A) and brainstem (BS; B) and average astrocyte counts in the basal forebrain (BF; C) and brainstem (BS; D) between cognitively normal (CN), Alzheimer's disease (AD), dementia with Lewy bodies (DLB), and multiple sclerosis (MS) groups. Note the overall increase in microglial counts in AD, DLB, and MS groups as compared to CN (A, B). Also note the overall stability in astrocyte counts between groups (C, D). Values are mean ± SD.

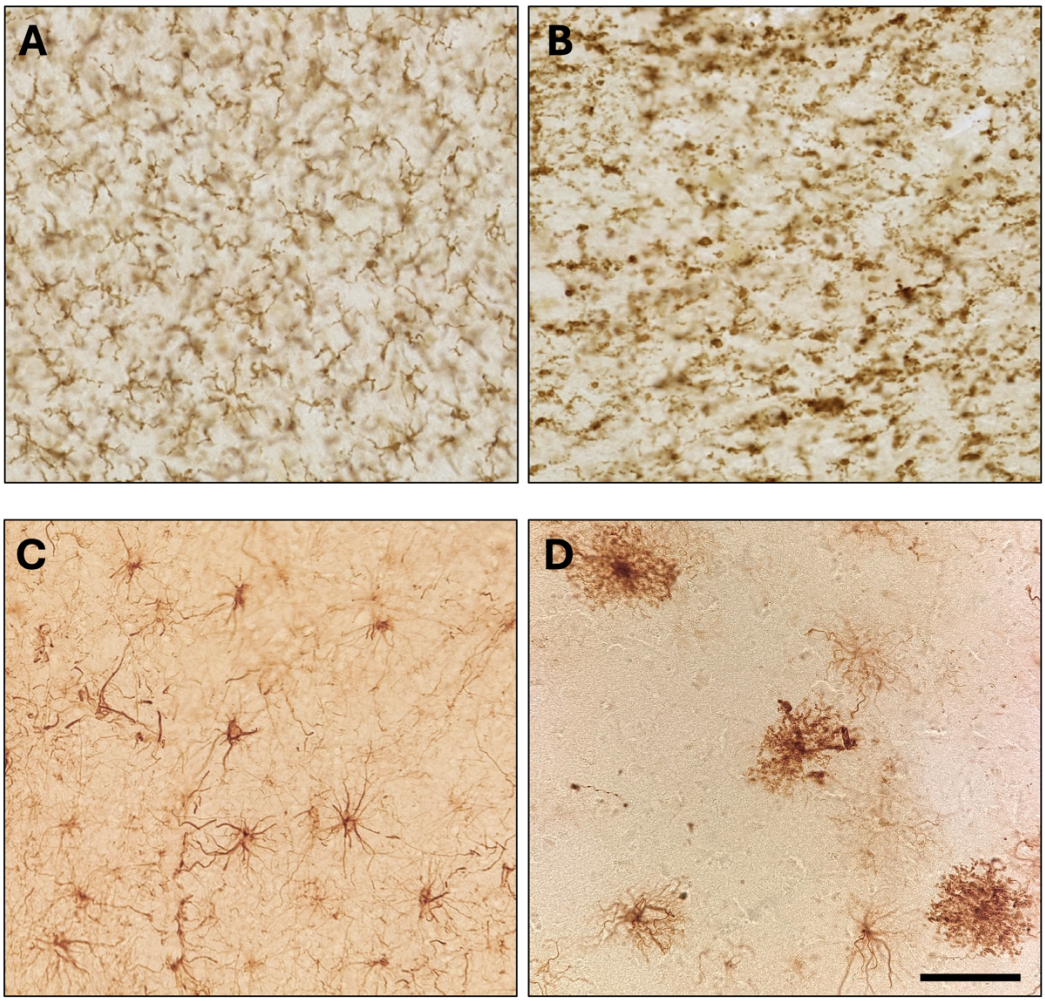

Figure 3.15 Immunohistochemical stains for Iba1-positive microglia (top row) and GFAP-positive astrocytes (bottom row) in a cognitively normal (A, C) versus Alzheimer's disease (B, D) case. Note the ramified morphology of microglia and astrocytes in the cognitively normal case (A, C). Also note the activated, dystrophic, and degenerated microglia (B), with often only the cell body remaining. Note the activated and dystrophic (beaded) morphology of certain astrocytes, while the others appear ramified in the Alzheimer's disease case (D). Scale bar for A and B is 50µm, and 200µm in C and D.

Table 3.8 Mann-Whitney statistical testing of average microglia and astrocyte counts in regions of interest related to sleep comparing cognitively normal (CN) and Alzheimer's disease (AD) brains

	Cognitively Normal (CN)				Alzheimer's Disease (AD)				
	N	Mean	St. Dev.	Median	N	Mean	St. Dev.	Median	p value
Microglia									
Region									
Ch1	2	28.5	30.4	28.5	1	16.0	n/a	16.0	n/a
Ch2	3	58.7	39.6	80.0	5	104.2	45.6	111.0	0.143
Ch4a	4	72.5	41.7	83.0	5	96.0	28.9	86.0	0.730
Ch4p	4	75.0	47.1	78.0	5	66.8	65.8	70.0	0.691
Ch5	4	91.8	13.8	94.0	5	94.4	23.0	95.0	0.905
Ch6	3	61.0	43.6	72.0	5	123.8	49.7	109.0	0.143
DR	4	75.5	43.9	81.0	5	106.8	51.6	89.0	0.556
LC	4	77.3	37.5	86.5	5	83.0	26.5	77.0	1
Astrocytes									
Region									
Ch1	2	31.0	22.6	31.0	1	43.0	n/a	43.0	n/a
Ch2	3	54.3	30.0	48.0	5	47.6	20.9	58.0	1
Ch4a	4	44.0	18.3	45.0	5	36.6	12.7	42.0	0.556
Ch4p	4	34.0	19.4	37.0	4	45.8	8.1	43.5	0.486
Ch5	4	50.3	17.2	52.5	5	39.0	3.5	40.0	0.318
Ch6	2	52.0	4.2	52.0	2	51.5	3.5	51.5	1
DR	4	43.5	9.6	41.5	2	46.5	2.1	46.5	0.800
LC	2	43.0	19.8	43.0	1	41.0	n/a	41.0	n/a

n/a = values not available

Table 3.9 Mann-Whitney statistical testing of average microglia and astrocyte counts in regions of interest related to sleep comparing cognitively normal (CN), dementia with Lewy bodies (DLB), and multiple sclerosis (MS) brains

	Dementia with Lewy bodies (DLB)					Multiple sclerosis (MS)				
	N	Mean	St. Dev.	Median	p value	N	Mean	St. Dev.	Median	p value
Microglia										
Region										
Ch1	1	152.0	n/a	152.0	n/a	0	n/a	n/a	n/a	n/a
Ch2	5	120.0	26.1	118.0	0.036*	3	118.3	17.5	118.0	0.100
Ch4a	5	111.6	29.2	105.0	0.191	3	105.7	34.1	109.0	0.629
Ch4p	5	112.2	13.1	107.0	0.286	3	121.0	38.2	125.0	0.400
Ch5	5	109.6	19.0	102.0	0.318	4	117.8	18.0	118.0	0.114
Ch6	5	134.6	22.4	132.0	0.018*	4	129.0	29.0	135.0	0.114
DR	5	147.0	33.5	136.0	0.040*	4	132.5	36.1	135.0	0.114
LC	5	131.0	24.5	135.0	0.032*	4	119.0	31.7	131.0	0.200
Astrocytes										
Region										
Ch1	1	48.0	n/a	48.0	n/a	0	n/a	n/a	n/a	n/a
Ch2	5	44.2	3.4	45.0	0.714	2	50.5	12.0	50.5	1
Ch4a	5	39.6	5.3	39.0	0.556	2	48.5	3.5	48.5	0.800
Ch4p	5	42.6	12.3	44.0	0.460	1	45.0	n/a	45.0	n/a
Ch5	3	33.3	21.0	26.0	0.229	3	44.0	18.3	33.5	0.533
Ch6	2	49.5	3.5	49.5	0.667	1	57.0	n/a	57.0	n/a
DR	2	40.0	2.8	40.0	1	1	47.0	n/a	47.0	n/a
LC	2	35.0	7.1	35.0	1	1	25.0	n/a	25.0	n/a

n/a = values not available

significant difference. Across most regions, the astrocyte counts in AD brains did not significantly differ from those in CN brains, with p-values well above the 0.05 threshold, indicating a lack of statistical significance. Activated astrocytes, characterized by increased arborization and swelling of both cell body and processes, were observed consistently throughout the regions of interest in AD.

In DLB cases, microglial counts were also elevated as compared to CN brains (Fig. 3.14). In DLB brains, microglial counts were significantly higher in Ch2 ($p = 0.036$), Ch6 ($p = 0.018$), DR ($p = 0.040$), and LC ($p = 0.032$) regions as compared to CN brains (Table 3.10). Microglial morphology in DLB cases was predominantly activated, with some cases showing dystrophy. Microglial counts in DLB cases also showed high standard deviation, albeit lesser than that in CN cases. The astrocyte counts in DLB brains did not show significant differences from CN brains across most regions, like the patterns observed in AD brains. Activated astrocytes were observed throughout the regions of interest in DLB brains.

MS cases also exhibited increased microglial counts as compared to CN cases (Fig. 3.14), however, none were statistically significantly different than CN cases (Table 3.10). Microglia in active demyelinating lesions showing an activated morphology, often displaying a phagocytic phenotype characterized by a rounded, enlarged cell body and retracted processes at the active lesion borders. Some regions outside areas of demyelination additionally displayed microglia activation, particularly with a phagocytic phenotype. Astrocyte counts in MS brains did not differ significantly from CN brains (Table 3.9). Activated astrocytes displayed a similar distribution as microglia, distributed

in and around active demyelinating lesions, with scattered instances of astrocytic dystrophy observed (Fig. 3.15D).

CN cases generally exhibited ramified microglia (Fig. 3.15A), although some cases displayed evidence of activated microglia, particularly in the oldest individuals with concurrent neuropathology (i.e., CN3 and CN4).

CHAPTER 4. Discussion

The present study aimed to investigate the cholinergic, neuropathological, and neuroinflammatory changes in BF and BS nuclei that regulate the sleep-wake cycle and compared these changes in AD, DLB, and MS to CN brains. This comparative approach was undertaken to better understand the brain changes that might contribute to the sleep disturbances commonly observed in these conditions. Sleep problems significantly impact the quality of life of patients with these conditions, yet the specific brain mechanisms responsible for these disturbances remain poorly understood. By analyzing and contrasting the pathological features in key sleep-wake regulatory regions, this study provides valuable insights into how these changes correlate with sleep dysfunction in AD, DLB, and MS. The findings revealed distinct and overlapping patterns of cholinergic neuron loss, neuropathological, and neuroinflammatory changes, shedding light on their potential neuroanatomical, neuropathological, and neurochemical changes that underlie sleep-wake disturbances in these NDDs.

4.1. Summary of Key Findings

4.1.1. Summary of the Parcellation of the Basal Forebrain and Brainstem

First, a summary of the results will be presented, followed by a discussion of their implications. The BF and BS was parcellated by examining the distribution of cholinergic neurons that were AChE- and ChAT-positive, as well as NADPH-d-positive neurons for BS parcellation. These results were generally consistent with previous research (e.g., Mesulam et al., 1983, 1989), albeit with some slight discrepancies. In the BF, the Ch1 region exhibited very sparse and relatively small ChAT and AChE neurons in CN cases, aligning with literature (Mesulam et al., 1983). In contrast, the Ch2 region had ChAT and

AChE neurons that were slightly larger in size and were more abundant, which is in accordance with descriptions of this region in established studies by Mesulam *et al.* (1983). Also consistent with previous research (Mesulam & Geula, 1988), the Ch4 region was marked by relatively abundant numbers of ChAT and AChE neurons. Further, these neurons appeared magnocellular, hyperchromic, isodendritic, and had prominent nucleoli based on Nissl stains, and stained intensely for ChAT and AChE. Mesulam *et al.* (1983) described the presence of a blood vessel that delineated the anteromedial (Ch4am) from the anterolateral (Ch4al) subsectors in Ch4. This feature was observed in many cases and served as a reliable landmark for identifying the anterior Ch4 region. The ChAT and AChE neurons located in the Ch4p region exhibited similar morphology and staining characteristics to those observed in the Ch4a region, albeit with a slightly lower abundance.

The BS was parcellated using ChAT, AChE, and NADPH-d staining. In the BS, the Ch5 and Ch6 regions were marked by the presence of ChAT-, AChE-, and NADPH-d-positive magnocellular neurons. These markers for Ch5 and Ch6 neurons were consistent with reports by Mesulam *et al.* (1989). As highlighted by Mesulam *et al.* (1989), NADPH-d staining proved to be a useful tool in identifying Ch5 and Ch6 neurons. It was noted that only Ch5 and Ch6 neurons stained positively for NADPH-d. Also in agreement with Mesulam *et al.* (1989), not all cholinergic neurons exhibited NADPH-d positivity. This was apparent from the absence of NADPH-d staining in the cholinergic neurons of the trochlear motor and parabigeminal nuclei within the same sections as Ch5 and Ch6. Therefore, this supports the validity of NADPH-d staining as a characteristic feature of Ch5 and Ch6 neurons. Another observation in this study was that

the DR, which is predominantly serotonergic, occasionally contained ChAT, AChE, and NADPH-d neurons. This could be attributed to the fact that the adjacent cholinergic nuclei (i.e., Ch5 and Ch6) do not have distinct boundaries, appearing to allow its neurons to extend into the DR. Similarly, this phenomenon was observed in the LC, which is predominantly noradrenergic. The LC was readily identified by its characteristic dark brown neuromelanin-containing neurons and did not require any staining to be visible. These findings underscore the complexity and variability in the distribution of ChAT, AChE, and NADPH-d neurons within the BF and BS, providing a detailed anatomical framework that aligns with and expands upon existing literature.

4.1.2. Summary of Neurodegenerative Changes

The findings of this study provided insights into the cholinergic deficits associated with NDDs and their potential contribution to sleep disturbances commonly experienced by patients. By comparing quantifications of ChAT-, AChE-, and BChE-positive neurons in various nuclei in the BF and BS among AD, DLB, MS, and CN brains, the results revealed significant changes specific to certain types of neurons and regions associated with the regulation of the sleep-wake cycle. Comparative analyses revealed significant reductions in ChAT neuron counts in specific brain regions when comparing AD and CN brains. The Ch4a region exhibited a marked decrease in ChAT neurons in AD brains. This finding reflects the underlying feature that led to the cholinergic hypothesis of AD, which suggests that a decline in the levels of acetylcholine, a key neurotransmitter involved in learning and memory, contributes considerably to the cognitive deficits observed in the disease (Bartus, 2000). The Ch2, Ch4p, Ch6, DR, and LC regions did not show significant differences in ChAT neuron counts. Research by

Mesulam and Geula *et al.* (1988) indicated that the Ch4p region in AD cases experience substantial AChE neuron loss, ranging from 80% to 88%, while the Ch4a region shows losses between 29% and 54% compared to CN brains. In this study, the Ch4p region exhibited a 56% loss of AChE neurons in AD brains compared to CN brains, and the Ch4a region showed a 46% loss. Congruently, AChE neuron counts were significantly lower in the Ch4p region of AD brains compared to CN brains. These findings aligned with the literature, confirming the trend of greater AChE neuronal loss in the Ch4p region than in Ch4a, although the exact percentages observed here are lower for Ch4p but within the reported range for Ch4a. The other regions of interest examined did not demonstrate significant differences. BChE neuron counts showed no significant differences across all examined regions between AD and CN brains. It is important to mention that as far as we know, quantification of BChE-positive neurons in these BF and BS regions of human brain tissue has not been reported. Consequently, it becomes difficult to compare BChE neuron counts in the regions of interest examined in this study.

When comparing DLB and CN brains, significant reductions in ChAT neuron counts were observed in the Ch2, Ch4a, and Ch4p regions of DLB brains. These regions also exhibited significant decreases in AChE neuron counts, with additional differences noted in the Ch5 region. For BChE neurons, only the Ch6 region showed significant reductions in DLB brains compared to CN brains. The findings suggest that BF cholinergic neurons are particularly vulnerable to degeneration in DLB, consistent with existing literature (Colloby et al., 2017; Geula et al., 2021; Tiraboschi et al., 2002). In MS brains, no significant differences were observed in ChAT, AChE, or BChE neuron counts as compared to CN brains. These results supported our hypothesis that changes in the

cholinergic system would be observed within nuclei associated with the regulation of the sleep-wake cycle, specifically with a loss of cholinergic (i.e., ChAT-, AChE-, and BChE-positive) neurons. However, this observation was significant only in AD and DLB cases and specifically with ChAT- and AChE-positive neurons.

This study also quantified NADPH-d neurons across the AD, DLB, MS, and CN groups within nuclei of interest in the BF and BS to examine if these neurons were also compromised. Consistent with literature, all BF regions exhibited relatively very sparse NADPH-d neurons in CN brains (Geula et al., 1993). NADPH-d counts in the BS in CN brains were detailed earlier, and were also in line with existing literature (Mesulam et al., 1989).

In AD brains, NADPH-d neuron counts were generally lower than in CN brains across most regions. There were significant reductions observed in the DR and Ch4p regions as compared to counts in corresponding regions in CN brains. These results, especially those in the Ch4 complex, do not align with the literature, which indicates a surplus of NADPH-d neurons in this region in AD cases (Benzing & Mufson, 1995). Other research suggests these neurons are selectively spared (Tao et al., 1999). The contrasting results from this study instead suggests that NADPH-d neurons in the AD cases examined were degenerated. Another notable finding was that the Ch5 region in AD brains exhibited the greatest variability in neuron counts among the regions examined.

DLB brains also showed generally lower NADPH-d neuron counts compared to CN brains, although the differences were not statistically significant. The Ch5 region again showed significant variability for NADPH-d neuron counts in DLB brains. In MS

brains, NADPH-d neuron counts were relatively comparable to those in CN brains, with no significant differences observed. The Ch5 region, again, demonstrated considerable variances in NADPH-d neuron counts. These findings highlight the loss of NADPH-d in AD and DLB brains. The consistency in NADPH-d neuron counts in MS brains compared to CN brains suggests different underlying neuropathological mechanisms in MS.

The quantification of pigmented neurons in the LC across AD, DLB, MS, and CN brains provides significant insights into the neuropathological changes associated with these conditions. Another important finding regarding the LC pigmented neurons is the degree of standard deviation within AD, MS, and CN groups, except for DLB. This finding is consistent with literature indicating that LC pigmented neurons are particularly vulnerable to α-synuclein pathology, and their loss is a characteristic neuropathological feature of DLB and other synucleinopathies, such as Parkinson's disease (Boeve et al., 2007; Ehrminger et al., 2016). Overall, these findings demonstrate a notable reduction and degeneration of LC pigmented neurons in AD and DLB brains, while MS brains maintain a neuron count comparable to that of CN brains. This highlights distinct patterns of neuronal integrity across different neurodegenerative conditions.

4.1.3. Summary of Neuropathological Changes

Standard immunohistochemical techniques were utilized to detect amyloid-beta (Aβ) plaques, tau neurofibrillary tangles (NFTs) and neuropil threads (NTs), α-synuclein Lewy bodies (LBs) and neurites (LNs), and phosphorylated Tar DNA binding protein 43 (pTDP-43) neuronal cytoplasmic inclusions (NCIs) and dystrophic neurites (DNs). Histochemical methods were also used to examine pathological AChE and BChE

expression. Pathological loads for these markers were analyzed in all groups using semi-quantitative scoring adapted from established neuropathology diagnostic protocols.

AD cases exhibited an overall frequent abundance of Aβ plaques was observed, with the greatest deposition in BF Ch2, Ch4a, and Ch4p regions, and in the BS regions of Ch5, DR, and LC. Statistical analysis revealed significant differences in Aβ plaque abundance between AD and CN brains in Ch2, Ch5, Ch6, DR, and LC regions. Tau NFTs were observed to be moderately-to-frequently abundant, particularly in Ch4a, Ch4p, and DR, with NTs following a similar pattern. These results align with literature describing the neuropathological deposition patterns of Aβ plaques and tau NFTs in more advanced AD cases, which correspond to the Thal phases (Thal et al., 2002) and Braak stages (Braak et al., 2006) in the AD cases included in this study outlined in Table 2.1. α-synuclein pathology was rare in AD cases, detected in only one instance, indicating mixed neuropathology. This reflects that while α-synuclein pathology can occur in AD, it is not a predominant neuropathological feature, and it did not significantly differ from CN brains in this study. This feature has been previously reported, with as many as 50% of AD cases exhibit α-synuclein pathology (Hamilton, 2000). Additionally, only one case examined, AD5, showed sparse pTDP-43 pathology in the Ch4p region. In fact, while pTDP-43 aggregates are primarily associated with frontotemporal dementia (Cairns et al., 2007), amyotrophic lateral sclerosis (Neumann et al., 2006), and limbic-predominant age-related pTDP-43 encephalopathy (Nelson et al., 2019), pTDP-43 aggregates may be seen in up to 57% of AD cases, and is often correlated with an increased severity of cognitive impairment (Meneses et al., 2021). AChE and BChE activities associate with a subset of plaques typically associated with AD (Darvesh, Reid, et al., 2010; Geula & Mesulam,

1989, 1995; Macdonald et al., 2017). This phenomenon highlights the potential for ChEs, in particular BChE, as a sensitive biomarker for AD diagnosis and management (Macdonald et al., 2017). This study, AChE- and BChE-positive plaque loads showed frequent abundance in Ch4a and DR, with overall moderate-to-frequent scores in other regions. Significant differences in AChE-positive plaque scores between AD and CN brains were observed in several regions, including Ch2, Ch5, Ch6, DR, and LC. Similarly, significant differences in BChE-positive plaque scores were noted in the Ch5, Ch6, DR, and LC regions. It has also been reported that AChE and BChE associate with NFTs, but for only a small fraction of NFTs (Geula & Mesulam, 1995; Hamodat et al., 2019). In this study, some AD cases showed the presence of ChE-positive NFTs, although these were often sparse throughout some of the regions examined.

Although DLB is characterized predominantly by α-synuclein pathology (McKeith et al., 2005), mixed neuropathological presentations may occur. Many DLB cases exhibit concurrent AD pathology, including Aβ plaques and tau NFTs (Schumacher et al., 2021). DLB cases showed sparse-to-moderate Aβ plaque and sparse tau NFT deposition, but these values were not significantly different from those in corresponding regions in CN brains. α-synuclein deposition in DLB showed an overall mild-to-moderate severity, with the highest staging in DR and LC regions. All regions of interest in DLB cases were significantly different from those in CN brains regarding α-synuclein pathology. ChE-positive plaques and NFTs were sparse, with very sparse abundance in the BS. This suggests that ChE-positive plaques typically associated with AD appear to also be seen in other NDDs like DLB. However, there were no significant differences in ChE-positive plaque abundance between DLB and CN brains.

MS cases did not exhibit any Aβ plaques or α-synuclein pathology but showed sparse NFTs and NTs in specific regions. ChE-positive plaques were not present, but sparse ChE-positive NFTs were noted in one case. This indicated that while ChE pathology is generally absent in MS, isolated instances may occur. This feature may be related to pathological changes associated with aging, such as the accumulation of tau NFTs (Ziontz et al., 2019), and further implies involvement of ChEs in pathology in NDDs outside of AD. Demyelination was observed in various BF and BS regions throughout the MS cases examined, with active demyelinating processes marked by microglial activation (Bø et al., 1994). The role of BChE in MS demyelination was also investigated, building on previous research that linked BChE activity with neuroinflammatory and demyelinating processes in MS (Darvesh, LeBlanc, et al., 2010; Thorne et al., 2021). The BChE staining results varied greatly between cases and did not consistently align with trends reported in previous research. This discrepancy was evident even when BChE staining appeared to function correctly, as indicated by surrounding microglial and normal neuronal staining. Consequently, classification of MS lesions based on BChE activity, as previously established, was not feasible in this project.

In CN brains, Aβ plaques were observed in a sparse-to-moderate abundance, primarily in the oldest cases examined. This is consistent with findings that roughly 30% of CN adults over the age of 65 have Aβ plaques in their brain (Katzman et al., 1988), and sometimes exhibiting a burden comparable to that of AD cases (Macdonald et al., 2017). Tau NFTs were sparsely abundant, with NTs following a similar pattern. Tau pathology may also be found in CN adults, where it can be found in virtually all above the age of 70 (Ziontz et al., 2019). ChE-positive plaques were sparsely observed

throughout the BF. AChE-positive plaques were very sparsely observed only in the DR, while BChE-positive plaques were very sparsely observed in Ch6, DR, and LC in the BS. The presence of ChE-positive plaques in CN brains, particularly in the centenarians examined, indicates that pathological changes in ChE activity may be analogous to that of Aβ plaques as part of the aging process. Interestingly, ChE activity associated with NFTs were sparsely observed in three CN cases, showing positivity only for BChE.

These findings highlight the distinct neuropathological features across AD, DLB, MS, and CN brains, with variations in the distribution and abundance of Aβ plaques, tau NFTs, α-synuclein pathology, pTDP-43 pathology, ChE-positive plaques and NFTs, as well as demyelination in MS cases. This analysis provides an overview of the neuropathological landscape in these conditions, offering insights into the specific patterns of pathology. These results support our hypothesis that increased neuropathological load would be observed within nuclei associated with the regulation of the sleep-wake cycle. An increased neuropathological burden was observed in all NDD cases, typically corresponding to their hallmark pathology type.

4.1.4. Summary of Neuroinflammatory Changes

An analysis of microglial and astrocytic activity across different brain regions in CN individuals and those with AD, DLB, and MS, was performed. The findings reveal distinct patterns of microglia and astrocyte counts and morphological changes that offer insights into the neuroinflammatory processes associated with these conditions. Microglial counts were generally higher in AD brains compared to CN brains across most regions. Although these differences were not statistically significant, the elevated microglial presence suggests an ongoing neuroinflammatory response in AD. This

reflects the fact that AD is universally known as a neuroinflammatory condition (Kettenmann & Ransom, 2013; Leng & Edison, 2021). However, it is noteworthy that many microglia appeared dystrophic and highly degenerated, often presenting only the cell body, which posed challenges for accurate counting and likely resulted in lower counts than typically observed in AD, a condition marked by pronounced neuroinflammation (Leng & Edison, 2021). Microglial dystrophy is a phenomenon described in the literature and is typically associated with chronic inflammatory responses (Streit et al., 2014). This microglial dystrophy was particularly pronounced in cases with prolonged disease durations and higher neuropathological burden, indicating a potential correlation between disease progression and microglial degeneration, consistent with literature (Streit et al., 2014). The activated microglial morphology observed in AD, characterized by cell body swelling and retraction of processes, underscores the chronic inflammatory state in these brains.

In DLB cases, microglial counts were significantly higher in several regions, including Ch2, Ch6, DR, and LC, compared to CN brains. This suggests a pronounced microglial and neuroinflammatory response in DLB, with a predominant activated morphology. DLB is also known as condition marked by neuroinflammation (Loveland et al., 2023). Some dystrophic microglia were also observed, indicating that, like AD, DLB involves significant microglial activation and occasionally degeneration (Streit et al., 2014). The high standard deviation in microglial counts in DLB cases, though lower than in CN cases, reflects the variability in neuroinflammatory response among individuals.

MS is universally recognized as an inflammatory condition (Kettenmann & Ransom, 2013; Thompson et al., 2018). MS cases exhibited increased microglial counts

in cases compared to CN cases, particularly in active demyelinating lesions where microglia showed an activated, phagocytic phenotype. This is indicative of their role in clearing myelin debris and mediating inflammatory responses at the lesion borders (Kettenmann & Ransom, 2013). Additionally, some regions outside demyelinated areas also displayed activated microglia, suggesting a widespread neuroinflammatory state in MS. The presence of phagocytic microglia in these regions further highlights their active involvement in the destruction of myelin in the disease process.

Astrocytes are also universally acknowledged in their role in the inflammatory process in AD (Kettenmann & Ransom, 2013). In AD, astrocytes often exhibit an activated morphology, characterized by increased arborization and swelling of the cell body and processes, as well as an upregulation of GFAP. They frequently show signs of hypertrophy and reactivity, indicating their response to the disease's pathological environment. In AD cases in this study, astrocyte counts did not significantly differ between AD and CN brains across most regions. However, activated astrocytes, characterized by increased arborization and swelling of both cell body and processes, were consistently observed throughout the regions of interest in AD brains. This activation indicates a reactive astrogliosis response to ongoing neurodegeneration and inflammation.

Consistent with observations for microglia, DLB brains also show astrocyte activation as part of the inflammatory process (Kettenmann & Ransom, 2013; Loveland et al., 2023). In DLB brains, astrocyte counts were similarly not significantly different from CN brains. Activated astrocytes were nonetheless present throughout the regions of interest.

Despite its inflammatory profile, astrocyte counts in MS brains also did not differ significantly from CN brains. However, activated astrocytes were observed in and around active demyelinating lesions, displaying a distribution pattern like that of activated microglia. Instances of astrocytic dystrophy were also noted, indicating that, like microglia, astrocytes can also display a senescent morphology.

It should be noted that counting astrocytes in NDD cases was particularly challenging due to several factors: the highly arborized processes obscured the cell bodies, background staining was often dark, and the high cell density within the nuclei complicated identification. These issues contributed to smaller sample sizes.

These results support our hypothesis that increased neuroinflammatory processes would be observed within nuclei associated with the regulation of the sleep-wake cycle. An increased presence of microglia, but not astrocytes, was observed in all NDD cases, with all demonstrating an activated morphology indicative of neuroinflammation. This activated morphology was also observed in some CN cases.

4.2. Clinicopathological Correlations

This study aimed to investigate the cholinergic, neuropathological, and neuroinflammatory changes in the BF and BS nuclei involved in the regulation of the sleep-wake cycle, comparing these changes across AD, DLB, MS, CN brains. The results provided insights into the neuropathological underpinnings of sleep disturbances commonly observed in these NDDs. It can be inferred that cholinergic, neuropathological, and neuroinflammatory changes within a given region can impact its normal functioning and lead to dysfunction in its corresponding roles in sleep-wake regulation. It should be noted that clinicopathological correlations described here are

inherently inferential. Therefore, these correlations are hypothesized based on available information and should be interpreted with caution.

Weakening of the cholinergic system associated a loss of cholinergic (i.e., ChAT, AChE, BChE) neurons, degeneration of NADPH-d and LC pigmented neurons, along with an abundance of neuropathology and neuroinflammation would impair the proper functioning of the sleep-wake cycle. Weakening of the cholinergic system results in impaired cholinergic neurotransmission, which disrupts communication between cholinergic sleep-regulating regions. This impaired communication is central to the cholinergic hypothesis of AD (Bartus, 2000).The loss of NADPH-d neurons, which play a crucial role in producing nitric oxide (NO) by associating with nitric oxide synthase, can lead to disrupted NO signaling pathways in sleep-related brain regions. Additionally, NO's role in vasodilation and neuroprotection means its deficiency could potentially contribute to neuroinflammation and oxidative stress, further impairing proper functioning of regions involved in sleep (Hope et al., 1991). The loss of LC pigmented neurons is understood to be a feature associated with sleep disturbances (Boeve et al., 2007; Kelly et al., 2017; Van Egroo et al., 2022). Neuropathology disrupts the proper functioning of several biological neuronal processes, including synaptic communication, and also elicits a neuroinflammatory response (National Institute on Aging, 2024). While inflammation aims to protect neurons, excessive and chronic inflammation can lead to neuronal death (Kettenmann & Ransom, 2013), thus serving as another mechanism of impairment in brain regions related to the sleep-wake cycle. These findings highlight the potential mechanisms by which neurodegenerative changes in NDDs disrupt sleep-wake

regulation, contributing to the sleep disturbances commonly experienced by these patients.

Such mechanisms underlying sleep-wake cycle disturbances in the AD group can be linked to the cholinergic, neuropathological, and neuroinflammatory changes outlined in the results. These findings provide a general understanding of how sleep disturbances may arise from significant pathological changes observed in the AD group as a whole. However, specific clinicopathological correlations can be deduced based on the available clinical information for the AD cases. The clinical profile of AD cases revealed varying reports of sleep-wake disturbances. AD1 experienced REMBD, while AD3 experienced insomnia, circadian rhythm disturbances, and sleep-wake reversal. REMBD in AD1 can be associated with changes observed in several brain regions implicated in REM sleep regulation. Regions such as Ch4a in the BF, and multiple BS nuclei including Ch5, Ch6, DR, and LC, are all involved in REM sleep processes. This case exhibited significant losses of cholinergic neurons, NADPH-d-positive neurons, and LC pigmented neurons compared to both CN brains and other AD cases. Notably, AD1 had the lowest average count of LC pigmented neurons among all cases, averaging only 4.2 neurons in the LC. The LC plays a crucial role in regulating REM sleep and the skeletal muscle atonia associated with it. Neuropathologically, AD1 showed an overall frequent abundance of Aβ plaques and tau NFTs in all regions examined, consistent with severe AD pathology. Microglial cells in AD1 were highly fragmented and degenerated, indicating chronic neuroinflammation. Astrocytes also demonstrated morphologies consistent with activation. The duration of disease in this case was 14 years, aligning with this observed inflammatory profile of the brain tissue. The extensive cholinergic, NADPH-d, and LC

neurodegeneration, significant AD-related neuropathology, and chronic neuroinflammation observed in AD1 likely contributed to the severe sleep disturbances, particularly REMBD. Next, AD3 experienced insomnia, circadian rhythm disturbances, and sleep-wake reversal. Cholinergic neuron loss (i.e., ChAT, AChE, and BChE neurons) in AD3 was not as profound as in other AD cases; nevertheless, counts were overall reduced compared to CN brains. NADPH-d and LC pigmented neurons also demonstrated a notable loss, which is likely to impair their respective signaling pathways. This case exhibited a frequent burden of Aβ plaques and tau NFTs in both the BF and BS. Interestingly, AD3 showed elevated microglial counts compared to CN brains and even other AD cases. Intense neuropathological burden typically evokes an intense inflammatory response, and microglia in AD3 demonstrated an activated morphology without evidence of dystrophy, and astrocytes also appeared activated. The activated microglial and astrocytic morphology suggests a robust neuroinflammatory response, which, without the dystrophy seen in longer-duration cases, indicates ongoing but perhaps less chronic inflammation. This is consistent with the shorter disease duration of 4 years of this case. This feature highlights the utility of examining microglial morphology to gauge the relative degree and duration of neuroinflammation. The widespread cholinergic, neurodegenerative, neuropathological, and inflammatory state observed in sleep-related regions in the BF and BS in AD3 very likely contributed to the sleep disturbances noted in the clinical profile. However, the circadian disturbances experienced by AD3 are more likely to be correlated to changes in other brain regions such as the SCN. In summary, the findings from AD1 and AD3 illustrate how different neuropathological and neuroinflammatory profiles can lead to varied sleep disturbances.

Comparing cases AD1 and AD3 is particularly valuable since both individuals passed away at the same age of 58, but their duration of living with AD differed by a decade. AD1's longer disease duration and extensive neuropathology and neuroinflammation correlate with REMBD, while AD3's shorter disease duration but significant neuropathology and evidence of neuroinflammation correlate with insomnia and circadian disturbances. This study underscores the importance of considering the multifaceted nature of neuropathology when addressing sleep disturbances in AD.

On a separate note, several important observations arise regarding case AD2. This case demonstrated mixed neuropathology, exhibiting both AD-related and α-synuclein pathology. Typically, α-synuclein pathology correlates with a loss of pigmented neurons, such as those in the LC (Haglund et al., 2016; Vila, 2019; S. Xu & Chan, 2015). However, it was unexpected to find that the LC in this case was well-preserved, with LC pigmented neuron counts comparable to those in CN cases. Notably, this case did not have any recorded sleep disturbances in the clinical information available, though this absence of documentation does not necessarily indicate that the patient did not experience any sleep issues. This observation is consistent with case AD5, which also showed mixed pathology, exhibiting both AD-related and pTDP-43 pathology. Similarly, AD5 had a well-preserved LC despite the presence of mixed neuropathology, albeit without α-synuclein pathology.

The mechanisms underlying sleep-wake cycle disturbances may also be linked to the cholinergic, neuropathological, and neuroinflammatory changes outlined in the results of the DLB group. These general inferences suggest how sleep disturbances might arise from significant pathological changes observed in DLB brains in this study. Though,

specific clinicopathological correlations can be deduced based on the available clinical information for the DLB cases. Sleep-wake disturbances were reported in the clinical profile of DLB patients DLB1, DLB3, and DLB4. Sleep disturbances are very common in DLB, with 70-80% of patients experiencing REMBD. In fact, REMBD is a core clinical criterion for DLB diagnosis (McKeith et al., 2017). Therefore, it is reasonable to consider that despite no sleep disturbances being recorded for DLB2 and DLB5, it is highly likely they did experience some type of sleep disturbance, particularly REMBD. DLB1 experienced nightmares and hallucinations. This case demonstrated reduced cholinergic, NADPH-d, and pigmented LC neuron counts compared to CN brains. Neuropathologically, DLB1 exhibited mild-to-moderate α-synuclein pathology and sparse-to-moderate tau pathology. Additionally, this case had very high microglial counts, which were morphologically activated, indicating significant neuroinflammation. The findings suggest significant changes within the BF and BS nuclei involved in sleep regulation. Nightmares, though not fully understood, are known to occur during REM sleep (Stefani & Högl, 2021). The involvement of the LC, which plays a crucial role in regulating REM sleep and the associated atonia, is noteworthy as a possible underlying contributor to REMBD, given the significant degeneration observed. The reduced number of pigmented neurons in the LC, along with changed in other REM-related regions in the BF and BS, may contribute to dysregulation of REM sleep, potentially leading to nightmares. Hallucinations in DLB are more likely associated with changes in the sensory cortices and other higher-order processing areas. The presence of mild-to-moderate α-synuclein and tau pathology in DLB1 indicates that these neurodegenerative changes could extend to regions beyond the BF and BS, affecting sensory and perceptual

pathways. Next, DLB3 experienced REMBD. This case also demonstrated overall reduced cholinergic, NADPH-d, and pigmented LC neuron counts compared to CN brains. Neuropathologically, DLB3 exhibited mild α-synuclein pathology, with no other types of pathology observed. This case had the highest microglial counts among all examined cases, with microglia showing activated morphologies. The REMBD in this case likely stemmed from a combination of neurodegeneration, α-synuclein pathology, and an intense neuroinflammatory response impeding proper functioning of the REM-related BF and BS regions. Following, DLB4 experienced REMBD, possible sleep apnea, and had a history of Systemic Lupus Erythematosus (SLE). This case demonstrated relatively mild cholinergic neuron loss, but pronounced NADPH-d and pigmented LC neuron loss. Neuropathologically, DLB4 showed mixed pathology for DLB, with Aβ and ChE-positive plaque abundances ranging from mild to frequent abundance, and tau pathology being mild to moderate throughout the examined areas. Neuroinflammation was also notable, with high levels of microglial counts and activated morphologies. These findings correlate with the REMBD experienced by this case, as the significant neurodegeneration and neuroinflammation within sleep-regulatory regions likely contributed to the disturbance. The possible sleep apnea, while not specified if central or obstructive, would more likely be related to factors and/or brain regions not examined in this study. It was important to note that this patient lived with SLE because sleep disturbances are common in SLE (Palagini et al., 2014). SLE is a chronic autoimmune disease characterized by the immune system erroneously attacking healthy tissues, leading to widespread inflammation and damage to organs such as the skin, kidneys, and brain. The hypothesized neuroimmune pathways comprise the blood-brain barrier (BBB),

the meningeal tissues, and the glymphatic system (Ota et al., 2022). Patients with SLE frequently experience sleep disturbances, including insomnia, fatigue, and sleep apnea, which can be attributed to chronic pain, the side effects of medications, and the overall systemic inflammation associated with the disease (Palagini et al., 2014). This comorbidity may have compounded the sleep disturbances experienced by DLB4.

The mechanisms underlying sleep-wake cycle disturbances in MS patients do not appear to be associated with changes in cholinergic, NADPH-d, or LC pigmented neurons, as none of these were found to be close to significance. Instead, sleep disturbances, in the context of brain changes, are likely related to neural disconnection caused by demyelination and a chronic neuroinflammatory response that negatively impacts neuronal functioning. These inferences provide a general understanding of how sleep disturbances may arise from significant pathological changes observed in MS brains in this study. However, specific clinicopathological correlations can be deduced based on the available clinical information for the MS cases.

Sleep-wake disturbances were reported in the clinical profile of the MS case MS1. MS1 experienced possible REMBD, poor transitions between wakefulness and sleep, and slow brain waves during sleep. This case demonstrated preserved cholinergic, NADPH-d, and LC pigmented neurons, as indicated by average counts across all regions. However, demyelination was observed only in the LC region, with no evidence of demyelination within the other regions of interest. Tau pathology was sparsely present in the Ch4a and LC regions. Despite the preservation of cholinergic neurons and sparse NFT pathology, robust neuroinflammation was evident, characterized by high microglial counts and activated glial morphologies. The severe sleep disturbances observed in MS1 are likely

not solely attributable to the elevated neuroinflammation, the very sparse NFT pathology, or the partial demyelination of the LC region. It is more plausible that demyelination in other regions of the brain, which were not the focus of this study, underlies the sleep disturbances experienced by this patient. The presence of demyelination in regions important for sleep regulation, such as the thalamus or cortex, could disrupt normal sleep-wake transitions and REM sleep processes due to axonal disconnection from a loss of myelin, leading to the observed symptoms.

On a related note, some of the other MS cases did have multiple demyelinated lesions within the regions of interest, notably MS2 and MS4. Examination of MS2 revealed areas of demyelination including Ch2 and Ch4p regions. Ch2 projects to the hippocampal region, which is hypothesized to be involved in the generation of theta oscillations. Again, although the Ch4p region was included as an internal control to compare sleep-related and non-sleep-related areas within the Ch4 complex, it remains part of a crucial nucleus for the sleep-wake cycle and may still influence sleep-wake regulation. Following, case MS4 presented extensive demyelination, affecting nearly the entire BS which involved all BS nuclei of interest, as well as a portion of the Ch2 region. Notably, the LC pigmented neurons appeared relatively preserved despite the widespread demyelination. Given the demyelination of projecting axons from numerous BS regions, it is reasonable to infer that a broad range of symptoms would arise, including those related to sleep disturbances, based on functional disconnections.

CN cases were included in this study as a relative control group. Although these individuals exhibited normal cognitive functioning, their brains were not devoid of neuropathological changes like those seen in neurodegenerative diseases like AD.

Furthermore, their sleep patterns were not necessarily unaffected, especially considering that two of the CN cases were centenarians, where aging-related changes are likely to be observed (Katzman et al., 1988; Ziontz et al., 2019). These cases served as a baseline for cholinergic, NADPH-d, and LC pigmented neuron counts, as well as microglia and astrocyte counts. When comparing the centenarians to the younger adult CN cases, it was interesting to observe brain changes. No notable differences were found in neuron counts of any kind. However, inflammation varied greatly; one centenarian case (CN4) exhibited intense microglial degeneration but not astrocyte degeneration, while the other centenarian (CN3) showed elevated microglial counts compared to the younger CN cases, with no significant changes in astrocytes. Additionally, the centenarian cases had notable levels of AD-related neuropathology, likely related to aging-associated aggregation of Aβ (Jansen et al., 2015; Katzman et al., 1988) and tau (Nelson et al., 2012; Ziontz et al., 2019) pathology can occasionally be observed in cases of natural aging. It appears that there are mechanism(s) that help to compensate for pathological changes that help to maintain normal cognitive functioning (Stern, 2002). Such mechanism(s) have yet to be discovered. Though, neuroprotective factors encompass several modifiable lifestyle factors (Santiago & Potashkin, 2023). Adherence to a Mediterranean diet, characterized by high consumption of fruits, vegetables, whole grains, and healthy fats, has been associated with a reduced risk of cognitive decline. Regular physical activity confers numerous beneficial effects across multiple domains, including the cardiovascular, immune, digestive, and the CNS. Furthermore, maintaining good sleep hygiene is crucial, as sufficient sleep facilitates the clearance of Aβ and other neurotoxic waste from the brain via the glymphatic system (Xie et al., 2013), aids in consolidating memories, and

preserving cognitive functions, thereby contributing to neuroprotection (Stickgold & Walker, 2009). Other neuroprotective factors associated with a reduced risk for developing a NDD include higher education and social interaction (Livingston et al., 2020).

Examining potential contributors to specific sleep disturbances noted in the available clinical information of CN cases, CN2 and CN3 were found to experience sleep disturbances. CN4, the second centenarian, lacked available medical information for correlation. CN2 had difficulties with sleep initiation due to pain, which was not specified but likely unrelated to any changes in the examined brain regions, as no pathological findings were present. In contrast, CN3 experienced "sundowning" and other unspecified sleep disturbances that were not diagnosed. Interestingly, "sundowning" is typically seen in AD patients, despite CN3 not exhibiting AD cognitive symptoms. The sleep disturbances in CN3 are likely related to the abundant AD-related neuropathology and inflammation observed in their brain.

4.3. Limitations of the Thesis Research

The first major limitation is the small sample size, which resulted in large variances between cases within groups. This limited the ability to perform age and sex comparisons, reduced statistical power, and restricted the range of statistical tests available for analysis. Another limitation is the clinical applicability of the findings. The use of post-mortem brains and reliance on available documented clinical information posed challenges in accurately correlating the observed neuropathological changes with the sleep disturbances experienced by the cases. Many cases lacked detailed notes on sleep disturbances in their clinical information, making it difficult to determine whether

the absence of reported sleep disturbances was due to a lack of symptoms or a lack of documentation. Furthermore, not all regions of interest were available in every case. For instance, the Ch1 region and some medial brainstem nuclei (i.e., DR and Ch6) were not available due to the fragility of the tissue and issues with sectioning, respectively. This limitation potentially reduced the comprehensiveness of the findings.

Additionally, while the BF and BS are central in regulating the sleep-wake cycle, this study did not examine other key brain regions involved in sleep regulation, such as the SCN, hypothalamus, thalamus, and pineal gland. The study also did not examine other neurotransmitter systems, hormones, or other neuropeptides important in the sleep-wake cycle. Therefore, the findings provided only a partial picture of the neural mechanisms underlying sleep disturbances.

The methodology also presented limitations. More comprehensive quantification methods, such as stereology, were not feasible for this project. Instead, quantification relied on a single section per stain per region, providing only relative information rather than an absolute count of the elements of interest. Lastly, the control group used in this study was not purely a control group but rather served as a reference point for relative comparisons. While these CN cases were, in theory, expected to represent the absence of neuropathological changes, some individuals within this group did exhibit pathological alterations. This highlights the complexity of defining truly ‘normal’ aging. These CN cases also varied considerably in age, adding another layer of complexity to the interpretations.

4.4. Future Directions

To build on the findings of this study, several future research directions should be considered. Future studies should aim to include a larger sample size to increase statistical power and reduce variances between cases. This will allow for more robust statistical analyses, including age and sex comparisons, and provide a clearer understanding of the observed trends.

Additionally, future research should include a broader range of brain regions involved in sleep regulation, such as the SCN, hypothalamus, thalamus, and pineal gland. Investigating these regions will offer a more comprehensive understanding of the neural mechanisms underlying sleep disturbances. Future studies should examine other neurotransmitter systems involved in sleep regulation, such as the serotonergic, dopaminergic, and GABAergic systems. Understanding the interplay between these systems and the cholinergic system could reveal new insights into sleep-wake cycle disruptions.

Utilizing multimodal approaches that combine neuropathological assessments with pre-mortem neuroimaging, electrophysiological recordings, and behavioral analyses could also provide a more integrated view of how brain changes correlate with sleep disturbances. Additionally, future studies should aim to include detailed sleep studies, polysomnography, and actigraphy in patients to directly correlate brain changes with sleep patterns. Establishing stronger functional correlations between neuropathological findings and clinical symptoms of sleep disturbances is crucial.

Employing more comprehensive quantification techniques, such as stereology, can provide more accurate and reliable counts of neurons and glial cells. This will enhance the precision of the data and allow for better comparisons across studies.

Based on the findings of neuropathological and neuroinflammatory changes, future research should explore targeted interventions aimed at mitigating these changes. Investigating the efficacy of pharmacological and non-pharmacological treatments to improve sleep quality in patients with NDDs can have significant clinical implications.

4.5. Conclusions

In conclusion, this thesis provided insights into the cholinergic, neuropathological, and neuroinflammatory changes in BF and BS nuclei implicated in sleep-wake cycle regulation across AD, DLB, MS, and CN brains. The findings highlight significant neuronal losses, varying degrees of neuropathology, and neuroinflammation, contributing to our understanding of the mechanisms underlying sleep disturbances in NDDs. These results underscore the importance of region-specific pathology and the need for further research with larger sample sizes, comprehensive methodologies, and expanded brain region analyses. Investigating the intricate mechanisms and contributors of sleep dysfunction in NDDs could help facilitate better understanding of these conditions and provide new avenues for development of novel curative and diagnostic approaches.

References

Abadir, A., Dalton, R., Zheng, W., Pincavitch, J., & Tripathi, R. (2022). Neuroleptic Sensitivity in Dementia with Lewy Body and Use of Pimavanserin in an Inpatient Setting: A Case Report. *American Journal of Case Reports*, *23*. https://doi.org/10.12659/AJCR.937397

Abdallah, A. E. (2024). Review on anti-alzheimer drug development: Approaches, challenges and perspectives. *RSC Advances*, *14*(16), 11057–11088. https://doi.org/10.1039/D3RA08333K

Albert, M. S., DeKosky, S. T., Dickson, D., Dubois, B., Feldman, H. H., Fox, N. C., Gamst, A., Holtzman, D. M., Jagust, W. J., Petersen, R. C., Snyder, P. J., Carrillo, M. C., Thies, B., & Phelps, C. H. (2011). The diagnosis of mild cognitive impairment due to Alzheimer's disease: Recommendations from the National Institute on Aging-Alzheimer's Association workgroups on diagnostic guidelines for Alzheimer's disease. *Alzheimer's & Dementia*, *7*(3), 270–279. https://doi.org/10.1016/j.jalz.2011.03.008

Allan, L. M. (2019). Diagnosis and Management of Autonomic Dysfunction in Dementia Syndromes. *Current Treatment Options in Neurology*, *21*(8), 38. https://doi.org/10.1007/s11940-019-0581-2

Alzheimer, A. (2006). Concerning a unique disease of the cerebral cortex. In M. Jucker, K. Beyreuther, C. Haass, R. M. Nitsch, & Y. Christen (Eds.), *Alzheimer: 100 Years and Beyond* (pp. 3–11). Springer Berlin Heidelberg. https://doi.org/10.1007/978-3-540-37652-1_1

Alzheimer Society of Canada. (2023a, June 9). *Lewy body dementia*. https://alzheimer.ca/en/about-dementia/other-types-dementia/lewy-body-dementia?gad_source=1&gclid=Cj0KCQjw_qexBhCoARIsAFgBleumHavaX4OAuayiUeYG4HXlkzEk-VjjJJX9a4sOnbUyL_1MQabikAcaAvWUEALw_wcB

Alzheimer Society of Canada. (2023b, July 21). *Parkinson's disease*. https://alzheimer.ca/en/about-dementia/other-types-dementia/rare-types-dementia/parkinsons-disease

Alzheimer Society of Canada. (2024a). *Alternative treatments for dementia*. https://alzheimer.ca/en/about-dementia/how-can-i-treat-dementia/alternative-treatments-dementia?gad_source=1&gclid=CjwKCAjwrcKxBhBMEiwAIVF8rFIrMWAmDmo4SAsjEjVYmm7SDjOmgZU2ZExHDrxft40jPBysgcnr-hoCPrgQAvD_BwE

Alzheimer Society of Canada. (2024b, February 1). *Dementia numbers in Canada*. https://alzheimer.ca/en/about-dementia/what-dementia/dementia-numbers-canada

Alzheimer's Association. (2024a). *2024 Alzheimer's disease facts and figures*. https://doi.org/10.1002/alz.13809

Alzheimer's Association. (2024b). *Alzheimer's & Brain Research Milestones*. https://www.alz.org/alzheimers-dementia/research_progress/milestones

American Psychiatric Association. (2013). *Diagnostic and statistical manual of mental disorders DSM-5*.

Andersson, M. L., Møller, A. M., & Wildgaard, K. (2019). Butyrylcholinesterase deficiency and its clinical importance in anaesthesia: A systematic review. *Anaesthesia*, *74*(4), 518–528. https://doi.org/10.1111/anae.14545

Arendt, J., & Aulinas, A. (2000). Physiology of the Pineal Gland and Melatonin. In K. R. Feingold, B. Anawalt, M. R. Blackman, A. Boyce, G. Chrousos, E. Corpas, W. W. de Herder, K. Dhatariya, K. Dungan, J. Hofland, S. Kalra, G. Kaltsas, N. Kapoor, C. Koch, P. Kopp, M. Korbonits, C. S. Kovacs, W. Kuohung, B. Laferrère, … D. P. Wilson (Eds.), *Endotext*. MDText.com, Inc. http://www.ncbi.nlm.nih.gov/books/NBK550972/

Babaesfahani, A., Khanna, N. R., Patel, P., & Kuns, B. (2024). Natalizumab. In *StatPearls*. StatPearls Publishing. http://www.ncbi.nlm.nih.gov/books/NBK534201/

Babaesfahani, A., Patel, P., & Bajaj, T. (2024). Glatiramer. In *StatPearls*. StatPearls Publishing. http://www.ncbi.nlm.nih.gov/books/NBK541007/

Baghdoyan, H., Spotts, J., & Snyder, S. (1993). Simultaneous pontine and basal forebrain microinjections of carbachol suppress REM sleep. *The Journal of Neuroscience*, *13*(1), 229–242. https://doi.org/10.1523/JNEUROSCI.13-01-00229.1993

Ballard, C., Greig, N., Guillozet-Bongaarts, A., Enz, A., & Darvesh, S. (2005). Cholinesterases: Roles in the Brain During Health and Disease. *Current Alzheimer Research*, *2*(3), 307–318. https://doi.org/10.2174/1567205054367838

Bartus, R. T. (2000). On Neurodegenerative Diseases, Models, and Treatment Strategies: Lessons Learned and Lessons Forgotten a Generation Following the Cholinergic Hypothesis. *Experimental Neurology*, *163*(2), 495–529. https://doi.org/10.1006/exnr.2000.7397

Benarroch, E. E. (2018). Locus coeruleus. *Cell and Tissue Research*, *373*(1), 221–232. https://doi.org/10.1007/s00441-017-2649-1

Benca, R., Herring, W. J., Khandker, R., & Qureshi, Z. P. (2022). Burden of Insomnia and Sleep Disturbances and the Impact of Sleep Treatments in Patients with Probable or Possible Alzheimer's Disease: A Structured Literature Review. *Journal of Alzheimer's Disease*, *86*(1), 83–109. https://doi.org/10.3233/JAD-215324

Benzing, W. C., & Mufson, E. J. (1995). Increased number of NADPH-d-positive neurons within the substantia innominata in Alzheimer's disease. *Brain Research*, *670*(2), 351–355. https://doi.org/10.1016/0006-8993(94)01362-L

Bernatoniene, J., Sciupokas, A., Kopustinskiene, D. M., & Petrikonis, K. (2023). Novel Drug Targets and Emerging Pharmacotherapies in Neuropathic Pain. *Pharmaceutics*, *15*(7), 1799. https://doi.org/10.3390/pharmaceutics15071799

Birks, J. S. (2006). Cholinesterase inhibitors for Alzheimer's disease. *Cochrane Database of Systematic Reviews*, *2016*(3). https://doi.org/10.1002/14651858.CD005593

Blennow, K., Hampel, H., Weiner, M., & Zetterberg, H. (2010). Cerebrospinal fluid and plasma biomarkers in Alzheimer disease. *Nature Reviews Neurology*, *6*(3), 131–144. https://doi.org/10.1038/nrneurol.2010.4

Blennow, K., & Zetterberg, H. (2018). Biomarkers for Alzheimer's disease: Current status and prospects for the future. *Journal of Internal Medicine*, *284*(6), 643–663. https://doi.org/10.1111/joim.12816

Bø, L. (2009). The histopathology of grey matter demyelination in multiple sclerosis. *Acta Neurologica Scandinavica*, *120*, 51–57. https://doi.org/10.1111/j.1600-0404.2009.01216.x

Bø, L., Mörk, S., Kong, P. A., Nyland, H., Pardo, C. A., & Trapp, B. D. (1994). Detection of MHC class II-antigens on macrophages and microglia, but not on astrocytes and endothelia in active multiple sclerosis lesions. *Journal of Neuroimmunology*, *51*(2), 135–146. https://doi.org/10.1016/0165-5728(94)90075-2

Bø, L., Vedeler, C. A., Nyland, H., Trapp, B. D., & Mørk, S. J. (2003). Intracortical multiple sclerosis lesions are not associated with increased lymphocyte infiltration. *Multiple Sclerosis Journal*, *9*(4), 323–331. https://doi.org/10.1191/1352458503ms917oa

Boeve, B. F. (2019). REM Sleep Behavior Disorder Associated with Dementia with Lewy Bodies. In C. H. Schenck, B. Högl, & A. Videnovic (Eds.), *Rapid-Eye-Movement Sleep Behavior Disorder* (pp. 67–76). Springer International Publishing. https://doi.org/10.1007/978-3-319-90152-7_6

Boeve, B. F., Silber, M. H., & Ferman, T. J. (2004). REM Sleep Behavior Disorder in Parkinson's Disease and Dementia with Lewy Bodies. *Journal of Geriatric Psychiatry and Neurology*, *17*(3), 146–157. https://doi.org/10.1177/0891988704267465

Boeve, B. F., Silber, M. H., Saper, C. B., Ferman, T. J., Dickson, D. W., Parisi, J. E., Benarroch, E. E., Ahlskog, J. E., Smith, G. E., Caselli, R. C., Tippman-Peikert, M., Olson, E. J., Lin, S.-C., Young, T., Wszolek, Z., Schenck, C. H., Mahowald, M. W., Castillo, P. R., Del Tredici, K., & Braak, H. (2007). Pathophysiology of REM sleep behaviour disorder and relevance to neurodegenerative disease. *Brain*, *130*(11), 2770–2788. https://doi.org/10.1093/brain/awm056

Bonanni, E., Maestri, M., Tognoni, G., Fabbrini, M., Nucciarone, B., Manca, M. L., Gori, S., Iudice, A., & Murri, L. (2005). Daytime sleepiness in mild and moderate Alzheimer's disease and its relationship with cognitive impairment. *Journal of Sleep Research*, *14*(3), 311–317. https://doi.org/10.1111/j.1365-2869.2005.00462.x

Bonanni, L., Thomas, A., Tiraboschi, P., Perfetti, B., Varanese, S., & Onofrj, M. (2008). EEG comparisons in early Alzheimer's disease, dementia with Lewy bodies and Parkinson's disease with dementia patients with a 2-year follow-up. *Brain*, *131*(3), 690–705. https://doi.org/10.1093/brain/awm322

Born, J. (2010). Slow-wave sleep and the consolidation of long-term memory. *The World Journal of Biological Psychiatry*, *11*(sup1), 16–21. https://doi.org/10.3109/15622971003637637

Boucetta, S., Cissé, Y., Mainville, L., Morales, M., & Jones, B. E. (2014). Discharge Profiles across the Sleep–Waking Cycle of Identified Cholinergic, GABAergic, and Glutamatergic Neurons in the Pontomesencephalic Tegmentum of the Rat. *The Journal of Neuroscience*, *34*(13), 4708–4727. https://doi.org/10.1523/JNEUROSCI.2617-13.2014

Bousiges, O., & Blanc, F. (2022). Biomarkers of Dementia with Lewy Bodies: Differential Diagnostic with Alzheimer's Disease. *International Journal of Molecular Sciences*, *23*(12), 6371. https://doi.org/10.3390/ijms23126371

Boyce, R., Glasgow, S. D., Williams, S., & Adamantidis, A. (2016). Causal evidence for the role of REM sleep theta rhythm in contextual memory consolidation. *Science*, *352*(6287), 812–816. https://doi.org/10.1126/science.aad5252

Braak, H., Alafuzoff, I., Arzberger, T., Kretzschmar, H., & Del Tredici, K. (2006). Staging of Alzheimer disease-associated neurofibrillary pathology using paraffin sections and immunocytochemistry. *Acta Neuropathologica*, *112*(4), 389–404. https://doi.org/10.1007/s00401-006-0127-z

Broca, P., Pozzi, S., & Broca, P. (1888). *Mémoires sur le cerveau de l'homme et des primates*. C. Reinwald. https://doi.org/10.5962/bhl.title.86389

Burré, J., Sharma, M., & Südhof, T. C. (2018). Cell Biology and Pathophysiology of α-Synuclein. *Cold Spring Harbor Perspectives in Medicine*, *8*(3), a024091. https://doi.org/10.1101/cshperspect.a024091

Cairns, N. J., Neumann, M., Bigio, E. H., Holm, I. E., Troost, D., Hatanpaa, K. J., Foong, C., White, C. L., Schneider, J. A., Kretzschmar, H. A., Carter, D., Taylor-Reinwald, L., Paulsmeyer, K., Strider, J., Gitcho, M., Goate, A. M., Morris, J. C., Mishra, M., Kwong, L. K., … Mackenzie, I. R. A. (2007). TDP-43 in Familial and Sporadic Frontotemporal Lobar Degeneration with Ubiquitin Inclusions. *The American Journal of Pathology*, *171*(1), 227–240. https://doi.org/10.2353/ajpath.2007.070182

Calabresi, P., Mechelli, A., Natale, G., Volpicelli-Daley, L., Di Lazzaro, G., & Ghiglieri, V. (2023). Alpha-synuclein in Parkinson's disease and other synucleinopathies: From overt neurodegeneration back to early synaptic dysfunction. *Cell Death & Disease*, *14*(3), 176. https://doi.org/10.1038/s41419-023-05672-9

Cash, M. K., Rockwood, K., Fisk, J. D., & Darvesh, S. (2021). Clinicopathological correlations and cholinesterase expression in early-onset familial Alzheimer's disease with the presenilin 1 mutation, Leu235Pro. *Neurobiology of Aging*, *103*, 31–41. https://doi.org/10.1016/j.neurobiolaging.2021.02.025

Chokhawala, K., & Stevens, L. (2024). Antipsychotic Medications. In *StatPearls*. StatPearls Publishing. http://www.ncbi.nlm.nih.gov/books/NBK519503/

Chouliaras, L., & O'Brien, J. T. (2023). The use of neuroimaging techniques in the early and differential diagnosis of dementia. *Molecular Psychiatry*, *28*(10), 4084–4097. https://doi.org/10.1038/s41380-023-02215-8

Colloby, S. J., Elder, G. J., Rabee, R., O'Brien, J. T., & Taylor, J. (2017). Structural grey matter changes in the substantia innominata in Alzheimer's disease and dementia with Lewy bodies: A DARTEL-VBM study. *International Journal of Geriatric Psychiatry*, *32*(6), 615–623. https://doi.org/10.1002/gps.4500

Confavreux, C., Vukusic, S., Moreau, T., & Adeleine, P. (2000). Relapses and Progression of Disability in Multiple Sclerosis. *New England Journal of Medicine*, *343*(20), 1430–1438. https://doi.org/10.1056/NEJM200011163432001

Conti Filho, C. E., Loss, L. B., Marcolongo-Pereira, C., Rossoni Junior, J. V., Barcelos, R. M., Chiarelli-Neto, O., Silva, B. S. D., Passamani Ambrosio, R., Castro, F. C. D. A. Q., Teixeira, S. F., & Mezzomo, N. J. (2023). Advances in Alzheimer's disease's pharmacological treatment. *Frontiers in Pharmacology*, *14*, 1101452. https://doi.org/10.3389/fphar.2023.1101452

Cummings, J. (2023). Anti-Amyloid Monoclonal Antibodies are Transformative Treatments that Redefine Alzheimer's Disease Therapeutics. *Drugs*, *83*(7), 569–576. https://doi.org/10.1007/s40265-023-01858-9

Dani, J. A., & Bertrand, D. (2007). Nicotinic Acetylcholine Receptors and Nicotinic Cholinergic Mechanisms of the Central Nervous System. *Annual Review of Pharmacology and Toxicology*, *47*(1), 699–729. https://doi.org/10.1146/annurev.pharmtox.47.120505.105214

Darvesh, S. (2016). Butyrylcholinesterase as a Diagnostic and Therapeutic Target for Alzheimer's Disease. *Current Alzheimer Research*, *13*(10), 1173–1177. https://doi.org/10.2174/1567205013666160404120542

Darvesh, S., & Hopkins, D. A. (2003). Differential distribution of butyrylcholinesterase and acetylcholinesterase in the human thalamus. *Journal of Comparative Neurology*, *463*(1), 25–43. https://doi.org/10.1002/cne.10751

Darvesh, S., Hopkins, D. A., & Geula, C. (2003). Neurobiology of butyrylcholinesterase. *Nature Reviews Neuroscience*, *4*(2), 131–138. https://doi.org/10.1038/nrn1035

Darvesh, S., Leach, L., Black, S. E., Kaplan, E., & Freedman, M. (2005). The Behavioural Neurology Assessment. *Canadian Journal of Neurological Sciences / Journal Canadien Des Sciences Neurologiques*, *32*(2), 167–177. https://doi.org/10.1017/S0317167100003930

Darvesh, S., LeBlanc, A. M., Macdonald, I., Reid, G. A., Bhan, V., Macaulay, R. J., & Fisk, J. D. (2010). Butyrylcholinesterase activity in multiple sclerosis neuropathology. *Chemico-Biological Interactions*, *187*(1–3), 425–431. https://doi.org/10.1016/j.cbi.2010.01.037

Darvesh, S., Reid, G. A., & Martin, E. (2010). Biochemical and Histochemical Comparison of Cholinesterases in Normal and Alzheimer Brain Tissues. *Current Alzheimer Research*, *7*(5), 386–400. https://doi.org/10.2174/156720510791383868

Davies, P., & Maloney, A. J. (1976). Selective loss of central cholinergic neurons in Alzheimer's disease. *The Lancet*, *308*(8000), 1403. https://doi.org/10.1016/S0140-6736(76)91936-X

Davis, B., & Sadik, K. (2006). Circadian Cholinergic Rhythms: Implications for Cholinesterase Inhibitor Therapy. *Dementia and Geriatric Cognitive Disorders*, *21*(2), 120–129. https://doi.org/10.1159/000090630

Dawson, T. M., Bredt, D. S., Fotuhi, M., Hwang, P. M., & Snyder, S. H. (1991). Nitric oxide synthase and neuronal NADPH diaphorase are identical in brain and peripheral tissues. *Proceedings of the National Academy of Sciences*, *88*(17), 7797–7801. https://doi.org/10.1073/pnas.88.17.7797

De La Escalera, S., Bockamp, E. O., Moya, F., Piovant, M., & Jiménez, F. (1990). Characterization and gene cloning of neurotactin, a Drosophila transmembrane protein related to cholinesterases. *The EMBO Journal*, *9*(11), 3593–3601. https://doi.org/10.1002/j.1460-2075.1990.tb07570.x

DeBay, D. R., Reid, G. A., Pottie, I. R., Martin, E., Bowen, C. V., & Darvesh, S. (2017). Targeting butyrylcholinesterase for preclinical single photon emission computed tomography (SPECT) imaging of Alzheimer's disease. *Alzheimer's & Dementia: Translational Research & Clinical Interventions*, *3*(2), 166–176. https://doi.org/10.1016/j.trci.2017.01.005

Deurveilher, S., & Semba, K. (2011). Basal forebrain regulation of cortical activity and sleep-wake states: Roles of cholinergic and non-cholinergic neurons: Basal forebrain and sleep/wake states. *Sleep and Biological Rhythms*, *9*, 65–70. https://doi.org/10.1111/j.1479-8425.2010.00465.x

Dos Santos, R. R., Da Silva, T. M., Silva, L. E. V., Eckeli, A. L., Salgado, H. C., & Fazan, R. (2022). Correlation between heart rate variability and polysomnography-derived scores of obstructive sleep apnea. *Frontiers in Network Physiology*, *2*, 958550. https://doi.org/10.3389/fnetp.2022.958550

Duara, R., & Barker, W. (2022). Heterogeneity in Alzheimer's Disease Diagnosis and Progression Rates: Implications for Therapeutic Trials. *Neurotherapeutics*, *19*(1), 8–25. https://doi.org/10.1007/s13311-022-01185-z

Dubois, B., Villain, N., Frisoni, G. B., Rabinovici, G. D., Sabbagh, M., Cappa, S., Bejanin, A., Bombois, S., Epelbaum, S., Teichmann, M., Habert, M.-O., Nordberg, A., Blennow, K., Galasko, D., Stern, Y., Rowe, C. C., Salloway, S., Schneider, L. S., Cummings, J. L., & Feldman, H. H. (2021). Clinical diagnosis of Alzheimer's disease: Recommendations of the International Working Group. *The Lancet Neurology*, *20*(6), 484–496. https://doi.org/10.1016/S1474-4422(21)00066-1

Dutar, P., Bassant, M. H., Senut, M. C., & Lamour, Y. (1995). The septohippocampal pathway: Structure and function of a central cholinergic system. *Physiological Reviews*, *75*(2), 393–427. https://doi.org/10.1152/physrev.1995.75.2.393

Duysen, E. G., Stribley, J. A., Fry, D. L., Hinrichs, S. H., & Lockridge, O. (2002). Rescue of the acetylcholinesterase knockout mouse by feeding a liquid diet; phenotype of the adult acetylcholinesterase deficient mouse. *Developmental Brain Research*, *137*(1), 43–54. https://doi.org/10.1016/S0165-3806(02)00367-X

Ebell, M. H., Barry, H. C., Baduni, K., & Grasso, G. (2024). Clinically Important Benefits and Harms of Monoclonal Antibodies Targeting Amyloid for the Treatment of Alzheimer Disease: A Systematic Review and Meta-Analysis. *The Annals of Family Medicine*, *22*(1), 50–62. https://doi.org/10.1370/afm.3050

Ehrminger, M., Latimier, A., Pyatigorskaya, N., Garcia-Lorenzo, D., Leu-Semenescu, S., Vidailhet, M., Lehericy, S., & Arnulf, I. (2016). The coeruleus/subcoeruleus complex in idiopathic rapid eye movement sleep behaviour disorder. *Brain*, *139*(4), 1180–1188. https://doi.org/10.1093/brain/aww006

Eisenhofer, G., & Reichmann, H. (2012). Dopaminergic Neurotransmission. In *Primer on the Autonomic Nervous System* (pp. 63–65). Elsevier. https://doi.org/10.1016/B978-0-12-386525-0.00012-3

English, B. A., & Jones, C. K. (2012). Cholinergic Neurotransmission. In *Primer on the Autonomic Nervous System* (pp. 71–74). Elsevier. https://doi.org/10.1016/B978-0-12-386525-0.00014-7

Eskander, M. F., Nagykery, N. G., Leung, E. Y., Khelghati, B., & Geula, C. (2005). Rivastigmine is a potent inhibitor of acetyl- and butyrylcholinesterase in Alzheimer's plaques and tangles. *Brain Research*, *1060*(1–2), 144–152. https://doi.org/10.1016/j.brainres.2005.08.039

Ferrari, C., & Sorbi, S. (2021). The complexity of Alzheimer's disease: An evolving puzzle. *Physiological Reviews*, *101*(3), 1047–1081. https://doi.org/10.1152/physrev.00015.2020

Folstein, M. F., Folstein, S. E., & McHugh, P. R. (1975). "Mini-mental state." *Journal of Psychiatric Research*, *12*(3), 189–198. https://doi.org/10.1016/0022-3956(75)90026-6

Franco-Bocanegra, McAuley, Nicoll, & Boche. (2019). Molecular Mechanisms of Microglial Motility: Changes in Ageing and Alzheimer's Disease. *Cells*, *8*(6), 639. https://doi.org/10.3390/cells8060639

Freeman, S. A., & Zéphir, H. (2024). Anti-CD20 monoclonal antibodies in multiple sclerosis: Rethinking the current treatment strategy. *Revue Neurologique*, S0035378724004740. https://doi.org/10.1016/j.neurol.2023.12.013

Friede, R. L. (1967). A comparative histochemical mapping of the distribution of butyryl cholinesterase in the brains of four species of mammals, including man. *Cells Tissues Organs*, *66*(2), 161–177. https://doi.org/10.1159/000142920

Frisoni, G. B., & Visser, P. J. (2015). Biomarkers for Alzheimer's disease: A controversial topic. *The Lancet Neurology*, *14*(8), 781–783. https://doi.org/10.1016/S1474-4422(15)00150-7

Fryer, A. D., Christopoulos, A., & Nathanson, N. M. (2012). *Muscarinic receptors*. Springer.

Gale, S. A., Acar, D., & Daffner, K. R. (2018). Dementia. *The American Journal of Medicine*, *131*(10), 1161–1169. https://doi.org/10.1016/j.amjmed.2018.01.022

García-García, Ó. D., Carriel, V., & Chato-Astrain, J. (2024). Myelin histology: A key tool in nervous system research. *Neural Regeneration Research*, *19*(2), 277–281. https://doi.org/10.4103/1673-5374.375318

Gerstenslager, B., & Slowik, J. M. (2024). Sleep Study. In *StatPearls*. StatPearls Publishing. http://www.ncbi.nlm.nih.gov/books/NBK563147/

Geula, C., Dunlop, S. R., Ayala, I., Kawles, A. S., Flanagan, M. E., Gefen, T., & Mesulam, M. (2021). Basal forebrain cholinergic system in the dementias: Vulnerability, resilience, and resistance. *Journal of Neurochemistry*, *158*(6), 1394–1411. https://doi.org/10.1111/jnc.15471

Geula, C., & Mesulam, M. (1989). Special properties of cholinesterases in the cerebral cortex of Alzheimer's disease. *Brain Research*, *498*(1), 185–189. https://doi.org/10.1016/0006-8993(89)90419-8

Geula, C., & Mesulam, M. (1995). Cholinesterases and the Pathology of Alzheimer Disease. *Alzheimer Disease & Associated Disorders*, *9*, 23–28. https://doi.org/10.1097/00002093-199501002-00005

Geula, C., Schatz, C. R., & Mesulam, M. (1993). Differential localization of nadph-diaphorase and calbindin-D28k within the cholinergic neurons of the basal forebrain, striatum and brainstem in the rat, monkey, baboon and human. *Neuroscience*, *54*(2), 461–476. https://doi.org/10.1016/0306-4522(93)90266-I

Giacobini, E., Cuello, A. C., & Fisher, A. (2022). Reimagining cholinergic therapy for Alzheimer's disease. *Brain*, *145*(7), 2250–2275. https://doi.org/10.1093/brain/awac096

Goedert, M. (2008). Oskar Fischer and the study of dementia. *Brain*, *132*(4), 1102–1111. https://doi.org/10.1093/brain/awn256

Government of Canada. (2014). *Introduction: Mapping Connections: An understanding of neurological conditions in Canada*. https://www.canada.ca/en/public-health/services/reports-publications/mapping-connections-understanding-neurological-conditions/mapping-connections-understanding-neurological-conditions-canada-9.html

Grigoli, M. M., Pelegrini, L. N. C., Whelan, R., & Cominetti, M. R. (2024). Present and Future of Blood-Based Biomarkers of Alzheimer's Disease: Beyond the Classics. *Brain Research*, *1830*, 148812. https://doi.org/10.1016/j.brainres.2024.148812

Guillozet, A. L., Weintraub, S., Mash, D. C., & Mesulam, M. (2003). Neurofibrillary Tangles, Amyloid, and Memory in Aging and Mild Cognitive Impairment. *Archives of Neurology*, *60*(5), 729. https://doi.org/10.1001/archneur.60.5.729

Gunes, S., Aizawa, Y., Sugashi, T., Sugimoto, M., & Rodrigues, P. P. (2022). Biomarkers for Alzheimer's Disease in the Current State: A Narrative Review. *International Journal of Molecular Sciences*, *23*(9), 4962. https://doi.org/10.3390/ijms23094962

Haglund, M., Friberg, N., Danielsson, E. J. D., Norrman, J., & Englund, E. (2016). A methodological study of locus coeruleus degeneration in dementing disorders. *Clinical Neuropathology*, *35*(09), 287–294. https://doi.org/10.5414/NP300930

Haider, L., Simeonidou, C., Steinberger, G., Hametner, S., Grigoriadis, N., Deretzi, G., Kovacs, G. G., Kutzelnigg, A., Lassmann, H., & Frischer, J. M. (2014). Multiple sclerosis deep grey matter: The relation between demyelination, neurodegeneration, inflammation and iron. *Journal of Neurology, Neurosurgery & Psychiatry*, *85*(12), 1386–1395. https://doi.org/10.1136/jnnp-2014-307712

Haki, M., AL-Biati, H. A., Al-Tameemi, Z. S., Ali, I. S., & Al-hussaniy, H. A. (2024). Review of multiple sclerosis: Epidemiology, etiology, pathophysiology, and treatment. *Medicine*, *103*(8), e37297. https://doi.org/10.1097/MD.0000000000037297

Hamilton, R. L. (2000). Lewy Bodies in Alzheimer's Disease: A Neuropathological Review of 145 Cases Using α-Synuclein Immunohistochemistry. *Brain Pathology*, *10*(3), 378–384. https://doi.org/10.1111/j.1750-3639.2000.tb00269.x

Hamodat, H., Fisk, J. D., & Darvesh, S. (2019). Cholinergic Neurons in Nucleus Subputaminalis in Primary Progressive Aphasia. *Canadian Journal of Neurological Sciences / Journal Canadien Des Sciences Neurologiques*, *46*(2), 174–183. https://doi.org/10.1017/cjn.2019.6

Hampel, H., Mesulam, M., Cuello, A. C., Khachaturian, A. S., Vergallo, A., Farlow, M. R., Snyder, P. J., Giacobini, E., & Khachaturian, Z. S. (2018). Revisiting the Cholinergic Hypothesis in Alzheimer's Disease: Emerging Evidence from Translational and Clinical Research. *The Journal Of Prevention of Alzheimer's Disease*, 1–14. https://doi.org/10.14283/jpad.2018.43

Han, Y., Shi, Y., Xi, W., Zhou, R., Tan, Z., Wang, H., Li, X., Chen, Z., Feng, G., Luo, M., Huang, Z., Duan, S., & Yu, Y. (2014). Selective Activation of Cholinergic Basal Forebrain Neurons Induces Immediate Sleep-wake Transitions. *Current Biology*, *24*(6), 693–698. https://doi.org/10.1016/j.cub.2014.02.011

Hippius, H., & Neundörfer, G. (2003). The discovery of Alzheimer's disease. *Dialogues in Clinical Neuroscience*, *5*(1), 101–108. https://doi.org/10.31887/DCNS.2003.5.1/hhippius

Hobson, J. A., McCarley, R. W., & Wyzinski, P. W. (1975). Sleep Cycle Oscillation: Reciprocal Discharge by Two Brainstem Neuronal Groups. *Science*, *189*(4196), 55–58. https://doi.org/10.1126/science.1094539

Hogg, R. C., Raggenbass, M., & Bertrand, D. (2003). Nicotinic acetylcholine receptors: From structure to brain function. In *Reviews of Physiology, Biochemistry and Pharmacology* (Vol. 147, pp. 1–46). Springer Berlin Heidelberg. https://doi.org/10.1007/s10254-003-0005-1

Hok-A-Hin, Y. S., Del Campo, M., Boiten, W. A., Stoops, E., Vanhooren, M., Lemstra, A. W., Van Der Flier, W. M., & Teunissen, C. E. (2023). Neuroinflammatory CSF biomarkers MIF, sTREM1, and sTREM2 show dynamic expression profiles in Alzheimer's disease. *Journal of Neuroinflammation*, *20*(1), 107. https://doi.org/10.1186/s12974-023-02796-9

Holdorff, B. (2002). Friedrich Heinrich Lewy (1885-1950) and His Work. *Journal of the History of the Neurosciences*, *11*(1), 19–28. https://doi.org/10.1076/jhin.11.1.19.9106

Hone, A. J., & McIntosh, J. M. (2018). Nicotinic acetylcholine receptors in neuropathic and inflammatory pain. *FEBS Letters*, *592*(7), 1045–1062. https://doi.org/10.1002/1873-3468.12884

Hong, J., Lozano, D. E., Beier, K. T., Chung, S., & Weber, F. (2023). Prefrontal cortical regulation of REM sleep. *Nature Neuroscience*, *26*(10), 1820–1832. https://doi.org/10.1038/s41593-023-01398-1

Hope, B. T., Michael, G. J., Knigge, K. M., & Vincent, S. R. (1991). Neuronal NADPH diaphorase is a nitric oxide synthase. *Proceedings of the National Academy of Sciences*, *88*(7), 2811–2814. https://doi.org/10.1073/pnas.88.7.2811

Horváth, S., & Palkovits, M. (1987). Morphology of the human septal area: A topographic atlas. *Acta Morphologica Hungarica*, *35*(3–4), 157–174.

Howell, M., Avidan, A. Y., Foldvary-Schaefer, N., Malkani, R. G., During, E. H., Roland, J. P., McCarter, S. J., Zak, R. S., Carandang, G., Kazmi, U., & Ramar, K. (2023). Management of REM sleep behavior disorder: An American Academy of Sleep Medicine clinical practice guideline. *Journal of Clinical Sleep Medicine*, *19*(4), 759–768. https://doi.org/10.5664/jcsm.10424

Hsu, J.-C., Lee, Y.-S., Chang, C.-N., Chuang, H.-L., Ling, E.-A., & Lan, C.-T. (2003). Sleep Deprivation Inhibits Expression of NADPH-d and NOS while Activating Microglia and Astroglia in the Rat Hippocampus. *Cells Tissues Organs*, *173*(4), 242–254. https://doi.org/10.1159/000070380

Huerta-Ocampo, I., Hacioglu-Bay, H., Dautan, D., & Mena-Segovia, J. (2020). Distribution of Midbrain Cholinergic Axons in the Thalamus. *Eneuro*, *7*(1), ENEURO.0454-19.2019. https://doi.org/10.1523/ENEURO.0454-19.2019

Ishii, K., Hosokawa, C., Hyodo, T., Sakaguchi, K., Usami, K., Shimamoto, K., Hosono, M., Yamazoe, Y., & Murakami, T. (2015). Regional glucose metabolic reduction in dementia with Lewy bodies is independent of amyloid deposition. *Annals of Nuclear Medicine*, *29*(1), 78–83. https://doi.org/10.1007/s12149-014-0911-0

Ishii, M., & Kurachi, Y. (2006). Muscarinic Acetylcholine Receptors. *Current Pharmaceutical Design*, *12*(28), 3573–3581. https://doi.org/10.2174/138161206778522056

Jack, C. R., Bennett, D. A., Blennow, K., Carrillo, M. C., Dunn, B., Haeberlein, S. B., Holtzman, D. M., Jagust, W., Jessen, F., Karlawish, J., Liu, E., Molinuevo, J. L., Montine, T., Phelps, C., Rankin, K. P., Rowe, C. C., Scheltens, P., Siemers, E., Snyder, H. M., … Silverberg, N. (2018). NIA-AA Research Framework: Toward a biological definition of Alzheimer's disease. *Alzheimer's & Dementia*, *14*(4), 535–562. https://doi.org/10.1016/j.jalz.2018.02.018

Jakobson Mo, S., Axelsson, J., Jonasson, L., Larsson, A., Ögren, M. J., Ögren, M., Varrone, A., Eriksson, L., Bäckström, D., Af Bjerkén, S., Linder, J., & Riklund, K. (2018). Dopamine transporter imaging with [18F]FE-PE2I PET and [123I]FP-CIT SPECT-a clinical comparison. *EJNMMI Research*, *8*(1), 100. https://doi.org/10.1186/s13550-018-0450-0

Jansen, W. J., Ossenkoppele, R., Knol, D. L., Tijms, B. M., Scheltens, P., Verhey, F. R. J., Visser, P. J., Aalten, P., Aarsland, D., Alcolea, D., Alexander, M., Almdahl, I. S., Arnold, S. E., Baldeiras, I., Barthel, H., Van Berckel, B. N. M., Bibeau, K., Blennow, K., Brooks, D. J., … Zetterberg, H. (2015). Prevalence of Cerebral Amyloid Pathology in Persons Without Dementia: A Meta-analysis. *JAMA*, *313*(19), 1924. https://doi.org/10.1001/jama.2015.4668

Jasiecki, J., Targońska, M., & Wasąg, B. (2021). The Role of Butyrylcholinesterase and Iron in the Regulation of Cholinergic Network and Cognitive Dysfunction in Alzheimer's Disease Pathogenesis. *International Journal of Molecular Sciences*, *22*(4), 2033. https://doi.org/10.3390/ijms22042033

Johns Hopkins Medicine. (2024a). *Magnetic Resonance Imaging (MRI)*. https://www.hopkinsmedicine.org/health/treatment-tests-and-therapies/magnetic-resonance-imaging-mri#:~:text=Magnetic%20resonance%20imaging%2C%20or%20MRI,large%20magnet%20and%20radio%20waves.

Johns Hopkins Medicine. (2024b). *Multiple Sclerosis (MS)*. https://www.hopkinsmedicine.org/health/conditions-and-diseases/multiple-sclerosis-ms

Johnson, K. A., Fox, N. C., Sperling, R. A., & Klunk, W. E. (2012). Brain Imaging in Alzheimer Disease. *Cold Spring Harbor Perspectives in Medicine*, *2*(4), a006213–a006213. https://doi.org/10.1101/cshperspect.a006213

Jouanne, M., Rault, S., & Voisin-Chiret, A.-S. (2017). Tau protein aggregation in Alzheimer's disease: An attractive target for the development of novel therapeutic agents. *European Journal of Medicinal Chemistry*, *139*, 153–167. https://doi.org/10.1016/j.ejmech.2017.07.070

Kang, J.-E., Lim, M. M., Bateman, R. J., Lee, J. J., Smyth, L. P., Cirrito, J. R., Fujiki, N., Nishino, S., & Holtzman, D. M. (2009). Amyloid-β Dynamics Are Regulated by Orexin and the Sleep-Wake Cycle. *Science*, *326*(5955), 1005–1007. https://doi.org/10.1126/science.1180962

Karczmar, A. G. (Ed.). (2007). *Exploring the Vertebrate Central Cholinergic Nervous System*. Springer US. https://doi.org/10.1007/978-0-387-46526-5

Karnovsky, M. J., & Roots, L. (1964). A "Direct-Coloring" Thiocholine Method for Cholinesterases. *Journal of Histochemistry & Cytochemistry*, *12*(3), 219–221. https://doi.org/10.1177/12.3.219

Katzman, R., Terry, R., DeTeresa, R., Brown, T., Davies, P., Fuld, P., Renbing, X., & Peck, A. (1988). Clinical, pathological, and neurochemical changes in dementia: A subgroup with preserved mental status and numerous neocortical plaques. *Annals of Neurology*, *23*(2), 138–144. https://doi.org/10.1002/ana.410230206

Kelly, S. C., He, B., Perez, S. E., Ginsberg, S. D., Mufson, E. J., & Counts, S. E. (2017). Locus coeruleus cellular and molecular pathology during the progression of Alzheimer's disease. *Acta Neuropathologica Communications*, *5*(1), 8. https://doi.org/10.1186/s40478-017-0411-2

Kettenmann, H., & Ransom, B. R. (2013). *Neuroglia* (Third). Oxford University Press.

Khanna, N. R., & Gerriets, V. (2024). Interferon. In *StatPearls*. StatPearls Publishing. http://www.ncbi.nlm.nih.gov/books/NBK555932/

Kim, W., Zandoná, M. E., Kim, S.-H., & Kim, H. J. (2015). Oral Disease-Modifying Therapies for Multiple Sclerosis. *Journal of Clinical Neurology*, *11*(1), 9. https://doi.org/10.3988/jcn.2015.11.1.9

Király, B., Domonkos, A., Jelitai, M., Lopes-dos-Santos, V., Martínez-Bellver, S., Kocsis, B., Schlingloff, D., Joshi, A., Salib, M., Fiáth, R., Barthó, P., Ulbert, I., Freund, T. F., Viney, T. J., Dupret, D., Varga, V., & Hangya, B. (2023). The medial septum controls hippocampal supra-theta oscillations. *Nature Communications*, *14*(1), 6159. https://doi.org/10.1038/s41467-023-41746-0

Koutcherov, Y., Huang, X.-F., Halliday, G., & Paxinos, G. (2004). Organization of Human Brain Stem Nuclei. In *The Human Nervous System* (pp. 267–320). Elsevier. https://doi.org/10.1016/B978-012547626-3/50011-9

Kroeger, D., Ferrari, L. L., Petit, G., Mahoney, C. E., Fuller, P. M., Arrigoni, E., & Scammell, T. E. (2017). Cholinergic, Glutamatergic, and GABAergic Neurons of the Pedunculopontine Tegmental Nucleus Have Distinct Effects on Sleep/Wake Behavior in Mice. *The Journal of Neuroscience*, *37*(5), 1352–1366. https://doi.org/10.1523/JNEUROSCI.1405-16.2016

Kuns, B., Rosani, A., Patel, P., & Varghese, D. (2024). Memantine. In *StatPearls*. StatPearls Publishing. http://www.ncbi.nlm.nih.gov/books/NBK500025/

Lee, M. G., Hassani, O. K., Alonso, A., & Jones, B. E. (2005). Cholinergic Basal Forebrain Neurons Burst with Theta during Waking and Paradoxical Sleep. *The Journal of Neuroscience*, *25*(17), 4365–4369. https://doi.org/10.1523/JNEUROSCI.0178-05.2005

Leng, F., & Edison, P. (2021). Neuroinflammation and microglial activation in Alzheimer disease: Where do we go from here? *Nature Reviews Neurology*, *17*(3), 157–172. https://doi.org/10.1038/s41582-020-00435-y

Lew, C. H., Petersen, C., Neylan, T. C., & Grinberg, L. T. (2021). Tau-driven degeneration of sleep- and wake-regulating neurons in Alzheimer's disease. *Sleep Medicine Reviews*, *60*, 101541. https://doi.org/10.1016/j.smrv.2021.101541

Li, C., Zhao, R., Gao, K., Wei, Z., Yaoyao Yin, M., Ting Lau, L., Chui, D., & Cheung Hoi Yu, A. (2011). Astrocytes: Implications for Neuroinflammatory Pathogenesis of Alzheimers Disease. *Current Alzheimer Research*, *8*(1), 67–80. https://doi.org/10.2174/156720511794604543

Lia, A., Di Spiezio, A., Speggiorin, M., & Zonta, M. (2023). Two decades of astrocytes in neurovascular coupling. *Frontiers in Network Physiology*, *3*, 1162757. https://doi.org/10.3389/fnetp.2023.1162757

Liu, A. K. L., Chang, R. C.-C., Pearce, R. K. B., & Gentleman, S. M. (2015). Nucleus basalis of Meynert revisited: Anatomy, history and differential involvement in Alzheimer's and Parkinson's disease. *Acta Neuropathologica*, *129*(4), 527–540. https://doi.org/10.1007/s00401-015-1392-5

Liu, A. K. L., & Gentleman, S. M. (2021). The diagonal band of Broca in health and disease. In *Handbook of Clinical Neurology* (Vol. 179, pp. 175–187). Elsevier. https://doi.org/10.1016/B978-0-12-819975-6.00009-1

Livingston, G., Huntley, J., Sommerlad, A., Ames, D., Ballard, C., Banerjee, S., Brayne, C., Burns, A., Cohen-Mansfield, J., Cooper, C., Costafreda, S. G., Dias, A., Fox, N., Gitlin, L. N., Howard, R., Kales, H. C., Kivimäki, M., Larson, E. B., Ogunniyi, A., … Mukadam, N. (2020). Dementia prevention, intervention, and care: 2020 report of the Lancet Commission. *The Lancet*, *396*(10248), 413–446. https://doi.org/10.1016/S0140-6736(20)30367-6

Loveland, P. M., Yu, J. J., Churilov, L., Yassi, N., & Watson, R. (2023). Investigation of Inflammation in Lewy Body Dementia: A Systematic Scoping Review. *International Journal of Molecular Sciences*, *24*(15), 12116. https://doi.org/10.3390/ijms241512116

Luppi, P.-H., Clément, O., Sapin, E., Gervasoni, D., Peyron, C., Léger, L., Salvert, D., & Fort, P. (2011). The neuronal network responsible for paradoxical sleep and its dysfunctions causing narcolepsy and rapid eye movement (REM) behavior disorder. *Sleep Medicine Reviews*, *15*(3), 153–163. https://doi.org/10.1016/j.smrv.2010.08.002

Lyman, M., Lloyd, D. G., Ji, X., Vizcaychipi, M. P., & Ma, D. (2014). Neuroinflammation: The role and consequences. *Neuroscience Research*, *79*, 1–12. https://doi.org/10.1016/j.neures.2013.10.004

Macdonald, I., Maxwell, S., Reid, G., Cash, M., DeBay, D., & Darvesh, S. (2017). Quantification of Butyrylcholinesterase Activity as a Sensitive and Specific Biomarker of Alzheimer's Disease. *Journal of Alzheimer's Disease*, *58*(2), 491–505. https://doi.org/10.3233/JAD-170164

Macdonald, I., Pottie, I., Joy, E. E., Matte, G., Burrell, S., Mawko, G., Martin, E., & Darvesh, S. (2010). IC-P-051: Synthesis and Evaluation of Butyrylcholinesterase Ligands for Neuroimaging Alzheimer's Disease. *Alzheimer's & Dementia*, *6*(4S_Part_1). https://doi.org/10.1016/j.jalz.2010.05.066

Mankhong, S., Kim, S., Lee, S., Kwak, H.-B., Park, D.-H., Joa, K.-L., & Kang, J.-H. (2022). Development of Alzheimer's Disease Biomarkers: From CSF- to Blood-Based Biomarkers. *Biomedicines*, *10*(4), 850. https://doi.org/10.3390/biomedicines10040850

Manu, D. R., Slevin, M., Barcutean, L., Forro, T., Boghitoiu, T., & Balasa, R. (2023). Astrocyte Involvement in Blood–Brain Barrier Function: A Critical Update Highlighting Novel, Complex, Neurovascular Interactions. *International Journal of Molecular Sciences*, *24*(24), 17146. https://doi.org/10.3390/ijms242417146

Maschio, C., & Ni, R. (2022). Amyloid and Tau Positron Emission Tomography Imaging in Alzheimer's Disease and Other Tauopathies. *Frontiers in Aging Neuroscience*, *14*, 838034. https://doi.org/10.3389/fnagi.2022.838034

Maxwell, S. P., Cash, M. K., & Darvesh, S. (2022). Neuropathology and cholinesterase expression in the brains of octogenarians and older. *Chemico-Biological Interactions*, *364*, 110065. https://doi.org/10.1016/j.cbi.2022.110065

Mayo Clinic. (2023, February 17). *Polysomnography (sleep study)*. https://www.mayoclinic.org/tests-procedures/polysomnography/about/pac-20394877#:~:text=Polysomnography%20records%20your%20brain%20waves,or%20at%20a%20sleep%20center.

McDonald, W. I., Compston, A., Edan, G., Goodkin, D., Hartung, H., Lublin, F. D., McFarland, H. F., Paty, D. W., Polman, C. H., Reingold, S. C., Sandberg-Wollheim, M., Sibley, W., Thompson, A., Van Den Noort, S., Weinshenker, B. Y., & Wolinsky, J. S. (2001). Recommended diagnostic criteria for multiple sclerosis: Guidelines from the international panel on the diagnosis of multiple sclerosis. *Annals of Neurology*, *50*(1), 121–127. https://doi.org/10.1002/ana.1032

McKeith, I. G., Boeve, B. F., Dickson, D. W., Halliday, G., Taylor, J.-P., Weintraub, D., Aarsland, D., Galvin, J., Attems, J., Ballard, C. G., Bayston, A., Beach, T. G., Blanc, F., Bohnen, N., Bonanni, L., Bras, J., Brundin, P., Burn, D., Chen-Plotkin, A., … Kosaka, K. (2017). Diagnosis and management of dementia with Lewy bodies: Fourth consensus report of the DLB Consortium. *Neurology*, *89*(1), 88–100. https://doi.org/10.1212/WNL.0000000000004058

McKeith, I. G., & Burn, D. (2000). Spectrum of Parkinson's Disease, Parkinson's Dementia, and Lewy Body Dementia. *Neurologic Clinics*, *18*(4), 865–883. https://doi.org/10.1016/S0733-8619(05)70230-9

McKeith, I. G., Dickson, D. W., Lowe, J., Emre, M., O'Brien, J. T., Feldman, H., Cummings, J., Duda, J. E., Lippa, C., Perry, E. K., Aarsland, D., Arai, H., Ballard, C. G., Boeve, B., Burn, D. J., Costa, D., Del Ser, T., Dubois, B., Galasko, D., … Yamada, M. (2005). Diagnosis and management of dementia with Lewy bodies: Third report of the DLB consortium. *Neurology*, *65*(12), 1863–1872. https://doi.org/10.1212/01.wnl.0000187889.17253.b1

McKhann, G. M., Knopman, D. S., Chertkow, H., Hyman, B. T., Jack, C. R., Kawas, C. H., Klunk, W. E., Koroshetz, W. J., Manly, J. J., Mayeux, R., Mohs, R. C., Morris, J. C., Rossor, M. N., Scheltens, P., Carrillo, M. C., Thies, B., Weintraub, S., & Phelps, C. H. (2011). The diagnosis of dementia due to Alzheimer's disease: Recommendations from the National Institute on Aging-Alzheimer's Association workgroups on diagnostic guidelines for Alzheimer's disease. *Alzheimer's & Dementia*, *7*(3), 263–269. https://doi.org/10.1016/j.jalz.2011.03.005

McNeill, J., Rudyk, C., Hildebrand, M. E., & Salmaso, N. (2021). Ion Channels and Electrophysiological Properties of Astrocytes: Implications for Emergent Stimulation Technologies. *Frontiers in Cellular Neuroscience*, *15*, 644126. https://doi.org/10.3389/fncel.2021.644126

Mendel, B., & Rudney, H. (1943). Studies on cholinesterase. *Biochemical Journal*, *37*(1), 59–63. https://doi.org/10.1042/bj0370059

Meneses, A., Koga, S., O'Leary, J., Dickson, D. W., Bu, G., & Zhao, N. (2021). TDP-43 Pathology in Alzheimer's Disease. *Molecular Neurodegeneration*, *16*(1), 84. https://doi.org/10.1186/s13024-021-00503-x

Mergenthaler, P., Lindauer, U., Dienel, G. A., & Meisel, A. (2013). Sugar for the brain: The role of glucose in physiological and pathological brain function. *Trends in Neurosciences*, *36*(10), 587–597. https://doi.org/10.1016/j.tins.2013.07.001

Mesulam, M. (2004). The cholinergic innervation of the human cerebral cortex. In *Progress in Brain Research* (Vol. 145, pp. 67–78). Elsevier. https://doi.org/10.1016/S0079-6123(03)45004-8

Mesulam, M., & Geula, C. (1988). Nucleus basalis (Ch4) and cortical cholinergic innervation in the human brain: Observations based on the distribution of acetylcholinesterase and choline acetyltransferase. *Journal of Comparative Neurology*, *275*(2), 216–240. https://doi.org/10.1002/cne.902750205

Mesulam, M., & Geula, C. (1991). Acetylcholinesterase-rich neurons of the human cerebral cortex: Cytoarchitectonic and ontogenetic patterns of distribution. *Journal of Comparative Neurology*, *306*(2), 193–220. https://doi.org/10.1002/cne.903060202

Mesulam, M., & Geula, C. (1994). Butyrylcholinesterase reactivity differentiates the amyloid plaques of aging from those of dementia. *Annals of Neurology*, *36*(5), 722–727. https://doi.org/10.1002/ana.410360506

Mesulam, M., Geula, C., Bothwell, M. A., & Hersh, L. B. (1989). Human reticular formation: Cholinergic neurons of the pedunculopontine and laterodorsal tegmental nuclei and some cytochemical comparisons to forebrain cholinergic neurons. *The Journal of Comparative Neurology*, *283*(4), 611–633. https://doi.org/10.1002/cne.902830414

Mesulam, M., Guillozet, A., Shaw, P., Levey, A., Duysen, E. G., & Lockridge, O. (2002). Acetylcholinesterase knockouts establish central cholinergic pathways and can use butyrylcholinesterase to hydrolyze acetylcholine. *Neuroscience*, *110*(4), 627–639. https://doi.org/10.1016/S0306-4522(01)00613-3

Mesulam, M., Mufson, E. J., Levey, A. I., & Wainer, B. H. (1983). Cholinergic innervation of cortex by the basal forebrain: Cytochemistry and cortical connections of the septal area, diagonal band nuclei, nucleus basalis (Substantia innominata), and hypothalamus in the rhesus monkey. *Journal of Comparative Neurology*, *214*(2), 170–197. https://doi.org/10.1002/cne.902140206

Mesulam, M., Mufson, E. J., & Wainer, B. H. (1986). Three-dimensional representation and cortical projection topography of the nucleus basalis (Ch4) in the macaque: Concurrent demonstration of choline acetyltransferase and retrograde transport with a stabilized tetramethylbenzidine method for horseradish peroxidase. *Brain Research*, *367*(1–2), 301–308. https://doi.org/10.1016/0006-8993(86)91607-0

Mirra, S. S., Heyman, A., McKeel, D., Sumi, S. M., Crain, B. J., Brownlee, L. M., Vogel, F. S., Hughes, J. P., Belle, G. V., Berg, L., & participating CERAD neuropathologists. (1991). The Consortium to Establish a Registry for Alzheimer's Disease (CERAD): Part II. Standardization of the neuropathologic assessment of Alzheimer's disease. *Neurology*, *41*(4), 479–479. https://doi.org/10.1212/WNL.41.4.479

Monti, J. M. (2010). The structure of the dorsal raphe nucleus and its relevance to the regulation of sleep and wakefulness. *Sleep Medicine Reviews*, *14*(5), 307–317. https://doi.org/10.1016/j.smrv.2009.11.004

Montine, T. J., Phelps, C. H., Beach, T. G., Bigio, E. H., Cairns, N. J., Dickson, D. W., Duyckaerts, C., Frosch, M. P., Masliah, E., Mirra, S. S., Nelson, P. T., Schneider, J. A., Thal, D. R., Trojanowski, J. Q., Vinters, H. V., & Hyman, B. T. (2012a). National Institute on Aging–Alzheimer's Association guidelines for the neuropathologic assessment of Alzheimer's disease: A practical approach. *Acta Neuropathologica*, *123*(1), 1–11. https://doi.org/10.1007/s00401-011-0910-3

Montine, T. J., Phelps, C. H., Beach, T. G., Bigio, E. H., Cairns, N. J., Dickson, D. W., Duyckaerts, C., Frosch, M. P., Masliah, E., Mirra, S. S., Nelson, P. T., Schneider, J. A., Thal, D. R., Trojanowski, J. Q., Vinters, H. V., & Hyman, B. T. (2012b). National Institute on Aging–Alzheimer's Association guidelines for the neuropathologic assessment of Alzheimer's disease: A practical approach. *Acta Neuropathologica*, *123*(1), 1–11. https://doi.org/10.1007/s00401-011-0910-3

Morgan, C. J. (2017). Use of proper statistical techniques for research studies with small samples. *American Journal of Physiology-Lung Cellular and Molecular Physiology*, *313*(5), L873–L877. https://doi.org/10.1152/ajplung.00238.2017

Morris, G., Stubbs, B., Köhler, C. A., Walder, K., Slyepchenko, A., Berk, M., & Carvalho, A. F. (2018). The putative role of oxidative stress and inflammation in the pathophysiology of sleep dysfunction across neuropsychiatric disorders: Focus on chronic fatigue syndrome, bipolar disorder and multiple sclerosis. *Sleep Medicine Reviews*, *41*, 255–265. https://doi.org/10.1016/j.smrv.2018.03.007

Morris, J. C., Heyman, A., Mohs, R. C., Hughes, J. P., Van Belle, G., Fillenbaum, G., Mellits, E. D., & Clark, C. (1989). The Consortium to Establish a Registry for Alzheimer's Disease (CERAD). Part I. Clinical and neuropsychological assesment of Alzheimer's disease. *Neurology*, *39*(9), 1159–1159. https://doi.org/10.1212/WNL.39.9.1159

MS Canada. (2023a). *About MS*. https://mscanada.ca/about-ms#:~:text=Canada%20has%20one%20of%20the,are%20diagnosed%20with%20MS%20everyday.

MS Canada. (2023b). *Symptoms of MS*. https://mscanada.ca/intro-to-ms/ms-symptoms

MS Canada. (2023c). *Treatments for Multiple Sclerosis*. https://mscanada.ca/managing-ms/treatments-for-multiple-sclerosis

MS Canada. (2024, May 21). *INSIGHT: Highlighting the Latest Advances in MS*. https://mscanada.ca/ms-research/latest-research/latest-advances-ms

Mufson, E. J., & Cunningham, M. G. (1988). Observations on choline acetyltransferase containing structures in the CD-1 mouse brain. *Neuroscience Letters*, *84*(1), 7–12. https://doi.org/10.1016/0304-3940(88)90328-X

Nasreddine, Z. S., Phillips, N. A., Bédirian, V., Charbonneau, S., Whitehead, V., Collin, I., Cummings, J. L., & Chertkow, H. (2005). The Montreal Cognitive Assessment, MoCA: A Brief Screening Tool For Mild Cognitive Impairment. *Journal of the American Geriatrics Society*, *53*(4), 695–699. https://doi.org/10.1111/j.1532-5415.2005.53221.x

National Institute of Biomedical Imaging and Bioengineering. (2022). *Magnetic Resonance Imaging (MRI)*. https://www.nibib.nih.gov/science-education/science-topics/magnetic-resonance-imaging-mri

National Institute of Neurological Disorders and Stroke. (2023, November 28). *Multiple Sclerosis*. https://www.ninds.nih.gov/health-information/disorders/multiple-sclerosis

National Institute of Neurological Disorders and Stroke. (2024, January 19). *Lewy body dementia*. https://www.ninds.nih.gov/health-information/disorders/lewy-body-dementia

National Institute on Aging. (2022, March 14). *Inside the brain: The role of neuropathology in Alzheimer's disease research*. https://www.nia.nih.gov/news/inside-brain-role-neuropathology-alzheimers-disease-research#:~:text=Neuropathology%20is%20the%20study%20of,disease%20and%20other%20neurodegenerative%20diseases.

National Institute on Aging. (2023, September 12). *How Is Alzheimer's Disease Treated?* https://www.nia.nih.gov/health/alzheimers-treatment/how-alzheimers-disease-treated

National Institute on Aging. (2024, January 19). *What Happens to the Brain in Alzheimer's Disease?* https://www.nia.nih.gov/health/alzheimers-causes-and-risk-factors/what-happens-brain-alzheimers-disease

Nelson, P. T., Alafuzoff, I., Bigio, E. H., Bouras, C., Braak, H., Cairns, N. J., Castellani, R. J., Crain, B. J., Davies, P., Tredici, K. D., Duyckaerts, C., Frosch, M. P., Haroutunian, V., Hof, P. R., Hulette, C. M., Hyman, B. T., Iwatsubo, T., Jellinger, K. A., Jicha, G. A., … Beach, T. G. (2012). Correlation of Alzheimer Disease Neuropathologic Changes With Cognitive Status: A Review of the Literature. *Journal of Neuropathology & Experimental Neurology*, *71*(5), 362–381. https://doi.org/10.1097/NEN.0b013e31825018f7

Nelson, P. T., Dickson, D. W., Trojanowski, J. Q., Jack, C. R., Boyle, P. A., Arfanakis, K., Rademakers, R., Alafuzoff, I., Attems, J., Brayne, C., Coyle-Gilchrist, I. T. S., Chui, H. C., Fardo, D. W., Flanagan, M. E., Halliday, G., Hokkanen, S. R. K., Hunter, S., Jicha, G. A., Katsumata, Y., … Schneider, J. A. (2019). Limbic-predominant age-related TDP-43 encephalopathy (LATE): Consensus working group report. *Brain*, *142*(6), 1503–1527. https://doi.org/10.1093/brain/awz099

Neumann, M., Sampathu, D. M., Kwong, L. K., Truax, A. C., Micsenyi, M. C., Chou, T. T., Bruce, J., Schuck, T., Grossman, M., Clark, C. M., McCluskey, L. F., Miller, B. L., Masliah, E., Mackenzie, I. R., Feldman, H., Feiden, W., Kretzschmar, H. A., Trojanowski, J. Q., & Lee, V. M.-Y. (2006). Ubiquitinated TDP-43 in Frontotemporal Lobar Degeneration and Amyotrophic Lateral Sclerosis. *Science*, *314*(5796), 130–133. https://doi.org/10.1126/science.1134108

Nicolet, Y., Lockridge, O., Masson, P., Fontecilla-Camps, J. C., & Nachon, F. (2003). Crystal Structure of Human Butyrylcholinesterase and of Its Complexes with Substrate and Products. *Journal of Biological Chemistry*, *278*(42), 41141–41147. https://doi.org/10.1074/jbc.M210241200

Nuñez, A., & Buño, W. (2021). The Theta Rhythm of the Hippocampus: From Neuronal and Circuit Mechanisms to Behavior. *Frontiers in Cellular Neuroscience*, *15*, 649262. https://doi.org/10.3389/fncel.2021.649262

Ota, Y., Srinivasan, A., Capizzano, A. A., Bapuraj, J. R., Kim, J., Kurokawa, R., Baba, A., & Moritani, T. (2022). Central Nervous System Systemic Lupus Erythematosus: Pathophysiologic, Clinical, and Imaging Features. *RadioGraphics*, *42*(1), 212–232. https://doi.org/10.1148/rg.210045

Pace-Schott, E. F. (2010). Sleep Architecture. In *The Neuroscience of Sleep* (pp. 11–17).

Pace-Schott, E. F., & Hobson, J. A. (2013). The Neurobiology of Sleep and Dreaming. In *Fundamental Neuroscience* (pp. 847–869). Elsevier. https://doi.org/10.1016/B978-0-12-385870-2.00040-8

Palagini, L., Tani, C., Mauri, M., Carli, L., Vagnani, S., Bombardieri, S., Gemignani, A., & Mosca, M. (2014). Sleep disorders and systemic lupus erythematosus. *Lupus*, *23*(2), 115–123. https://doi.org/10.1177/0961203313518623

Pao, W. C., Boeve, B. F., Ferman, T. J., Lin, S.-C., Smith, G. E., Knopman, D. S., Graff-Radford, N. R., Petersen, R. C., Parisi, J. E., Dickson, D. W., & Silber, M. H. (2013). Polysomnographic Findings in Dementia With Lewy Bodies. *The Neurologist*, *19*(1), 1–6. https://doi.org/10.1097/NRL.0b013e31827c6bdd

Partch, C. L., Green, C. B., & Takahashi, J. S. (2014). Molecular architecture of the mammalian circadian clock. *Trends in Cell Biology*, *24*(2), 90–99. https://doi.org/10.1016/j.tcb.2013.07.002

Patel, K. J., Yang, D., Best, J. R., Chambers, C., Lee, P. E., Henri-Bhargava, A., Funnell, C. R., Foti, D. J., Pettersen, J. A., Feldman, H. H., Nygaard, H. B., Hsiung, G. R., & DeMarco, M. L. (2024). Clinical value of Alzheimer's disease biomarker testing. *Alzheimer's & Dementia: Translational Research & Clinical Interventions*, *10*(2), e12464. https://doi.org/10.1002/trc2.12464

Patterson, L., Firbank, M. J., Colloby, S. J., Attems, J., Thomas, A. J., & Morris, C. M. (2019). Neuropathological Changes in Dementia With Lewy Bodies and the Cingulate Island Sign. *Journal of Neuropathology & Experimental Neurology*, *78*(8), 717–724. https://doi.org/10.1093/jnen/nlz047

Perry, E. K., Perry, R. H., Blessed, G., & Tomlinson, B. E. (1978). Changes in brain cholinesterases in senile dementia of Alzheimer type. *Neuropathology and Applied Neurobiology*, *4*(4), 273–277. https://doi.org/10.1111/j.1365-2990.1978.tb00545.x

Petersen, R. C. (Ed.). (2003). *Mild Cognitive Impairment: Aging to Alzheimer's Disease*. Oxford University PressNew York, NY. https://doi.org/10.1093/oso/9780195123425.001.0001

Peterson, J. W., Bö, L., Mörk, S., Chang, A., & Trapp, B. D. (2001). Transected neurites, apoptotic neurons, and reduced inflammation in cortical multiple sclerosis lesions. *Annals of Neurology*, *50*(3), 389–400. https://doi.org/10.1002/ana.1123

Polman, C. H., Reingold, S. C., Banwell, B., Clanet, M., Cohen, J. A., Filippi, M., Fujihara, K., Havrdova, E., Hutchinson, M., Kappos, L., Lublin, F. D., Montalban, X., O'Connor, P., Sandberg-Wollheim, M., Thompson, A. J., Waubant, E., Weinshenker, B., & Wolinsky, J. S. (2011). Diagnostic criteria for multiple sclerosis: 2010 revisions to the McDonald criteria. *Annals of Neurology*, *69*(2), 292–302. https://doi.org/10.1002/ana.22366

Poon, N., Ooi, C., How, C., & Yoon, P. (2018). Dementia management: A brief overview for primary care clinicians. *Singapore Medical Journal*, *59*(6), 295–299. https://doi.org/10.11622/smedj.2018070

Preman, P., Alfonso-Triguero, M., Alberdi, E., Verkhratsky, A., & Arranz, A. M. (2021). Astrocytes in Alzheimer's Disease: Pathological Significance and Molecular Pathways. *Cells*, *10*(3), 540. https://doi.org/10.3390/cells10030540

Rabinovici, G. D. (2021). Controversy and Progress in Alzheimer's Disease—FDA Approval of Aducanumab. *New England Journal of Medicine*, *385*(9), 771–774. https://doi.org/10.1056/NEJMp2111320

Reale, M., & Costantini, E. (2021). Cholinergic Modulation of the Immune System in Neuroinflammatory Diseases. *Diseases*, *9*(2), 29. https://doi.org/10.3390/diseases9020029

Reid, G. A., Chilukuri, N., & Darvesh, S. (2013). Butyrylcholinesterase and the cholinergic system. *Neuroscience*, *234*, 53–68. https://doi.org/10.1016/j.neuroscience.2012.12.054

Roessmann, U., & Friede, R. L. (1966). Changes in butyryl cholinesterase activity in reactive glia. *Neurology*, *16*(2_part_1), 123–123. https://doi.org/10.1212/WNL.16.2_Part_1.123

Ross, J. S., Berg, K. M., & Ramachandran, R. (2023). Ensuring Public Trust in an Empowered FDA. *New England Journal of Medicine*, *388*(14), 1249–1251. https://doi.org/10.1056/NEJMp2300438

Rothman, S. M., & Mattson, M. P. (2012). Sleep Disturbances in Alzheimer's and Parkinson's Diseases. *NeuroMolecular Medicine*, *14*(3), 194–204. https://doi.org/10.1007/s12017-012-8181-2

Sakkas, G. K., Giannaki, C. D., Karatzaferi, C., & Manconi, M. (2019). Sleep Abnormalities in Multiple Sclerosis. *Current Treatment Options in Neurology*, *21*(1), 4. https://doi.org/10.1007/s11940-019-0544-7

Santiago, J. A., & Potashkin, J. A. (2023). Physical activity and lifestyle modifications in the treatment of neurodegenerative diseases. *Frontiers in Aging Neuroscience*, *15*, 1185671. https://doi.org/10.3389/fnagi.2023.1185671

Sastre, P. J.-P., & Jouvet, M. (1979). Le comportement onirique du chat. *Physiology & Behavior*, *22*(5), 979–989. https://doi.org/10.1016/0031-9384(79)90344-5

Saxena, A., Redman, A. M. G., Jiang, X., Lockridge, O., & Doctor, B. P. (1999). Differences in active-site gorge dimensions of cholinesterases revealed by binding of inhibitors to human butyrylcholinesterase. *Chemico-Biological Interactions*, *119–120*, 61–69. https://doi.org/10.1016/S0009-2797(99)00014-9

Scales, K., Zimmerman, S., & Miller, S. J. (2018). Evidence-Based Nonpharmacological Practices to Address Behavioral and Psychological Symptoms of Dementia. *The Gerontologist*, *58*(suppl_1), S88–S102. https://doi.org/10.1093/geront/gnx167

Scammell, T. E., Arrigoni, E., & Lipton, J. O. (2017). Neural Circuitry of Wakefulness and Sleep. *Neuron*, *93*(4), 747–765. https://doi.org/10.1016/j.neuron.2017.01.014

Scheltens, P., De Strooper, B., Kivipelto, M., Holstege, H., Chételat, G., Teunissen, C. E., Cummings, J., & Van Der Flier, W. M. (2021). Alzheimer's disease. *The Lancet*, *397*(10284), 1577–1590. https://doi.org/10.1016/S0140-6736(20)32205-4

Schumacher, J., Gunter, J. L., Przybelski, S. A., Jones, D. T., Graff-Radford, J., Savica, R., Schwarz, C. G., Senjem, M. L., Jack, C. R., Lowe, V. J., Knopman, D. S., Fields, J. A., Kremers, W. K., Petersen, R. C., Graff-Radford, N. R., Ferman, T. J., Boeve, B. F., Thomas, A. J., Taylor, J.-P., & Kantarci, K. (2021). Dementia with Lewy bodies: Association of Alzheimer pathology with functional connectivity networks. *Brain*, *144*(10), 3212–3225. https://doi.org/10.1093/brain/awab218

Silver, A. (1974). *The biology of cholinesterases*. North-Holland Publ. Co. [u.a.].

Soreq, H., & Seidman, S. (2001). Acetylcholinesterase—New roles for an old actor. *Nature Reviews Neuroscience*, *2*(4), 294–302. https://doi.org/10.1038/35067589

Stebbins, G. T. (2007). Neuropsychological Testing. In *Textbook of Clinical Neurology* (pp. 539–557). Elsevier. https://doi.org/10.1016/B978-141603618-0.10027-X

Stedman, E., Stedman, E., & Easson, L. H. (1932). Choline-esterase. An enzyme present in the blood-serum of the horse. *Biochemical Journal*, *26*(6), 2056–2066. https://doi.org/10.1042/bj0262056

Stefani, A., & Högl, B. (2021). Nightmare Disorder and Isolated Sleep Paralysis. *Neurotherapeutics*, *18*(1), 100–106. https://doi.org/10.1007/s13311-020-00966-8

Stelzmann, R. A., Norman Schnitzlein, H., & Reed Murtagh, F. (1995). An english translation of alzheimer's 1907 paper, "über eine eigenartige erkankung der hirnrinde." *Clinical Anatomy*, *8*(6), 429–431. https://doi.org/10.1002/ca.980080612

Steriade, M., Datta, S., Pare, D., Oakson, G., & Curro Dossi, R. (1990). Neuronal activities in brain-stem cholinergic nuclei related to tonic activation processes in thalamocortical systems. *The Journal of Neuroscience*, *10*(8), 2541–2559. https://doi.org/10.1523/JNEUROSCI.10-08-02541.1990

Stern, Y. (2002). What is cognitive reserve? Theory and research application of the reserve concept. *Journal of the International Neuropsychological Society: JINS*, *8*(3), 448–460.

Sterniczuk, R., & Rusak, B. (2016). Sleep in relation to aging, frailty, and cognition. In *Brocklehurst's Textbook of Geriatric Medicine and Gerontology* (8th ed., pp. 908–912a). Elsevier.

Stickgold, R., & Walker, M. (2009). *The Neuroscience of Sleep*. Elsevier.

Streit, W. J., Xue, Q.-S., Tischer, J., & Bechmann, I. (2014). Microglial pathology. *Acta Neuropathologica Communications*, *2*(1), 142. https://doi.org/10.1186/s40478-014-0142-6

Sussman, J. L., Harel, M., Frolow, F., Oefner, C., Goldman, A., Toker, L., & Silman, I. (1991). Atomic Structure of Acetylcholinesterase from *Torpedo californica*: A Prototypic Acetylcholine-Binding Protein. *Science*, *253*(5022), 872–879. https://doi.org/10.1126/science.1678899

Takeuchi, Y., Nagy, A. J., Barcsai, L., Li, Q., Ohsawa, M., Mizuseki, K., & Berényi, A. (2021). The Medial Septum as a Potential Target for Treating Brain Disorders Associated With Oscillopathies. *Frontiers in Neural Circuits*, *15*, 701080. https://doi.org/10.3389/fncir.2021.701080

Tao, Z., Van Gool, D., Lammens, M., & Dom, R. (1999). NADPH-Diaphorase-Containing Neurons in Cortex, Subcortical White Matter and Neostriatum Are Selectively Spared in Alzheimer's Disease. *Dementia and Geriatric Cognitive Disorders*, *10*(6), 460–468. https://doi.org/10.1159/000017190

Tatineny, P., Shafi, F., Gohar, A., & Bhat, A. (2020). Sleep in the Elderly. *Missouri Medicine*, *117*(5), 490–495.

Thal, D. R., Rüb, U., Orantes, M., & Braak, H. (2002). Phases of Aβ-deposition in the human brain and its relevance for the development of AD. *Neurology*, *58*(12), 1791–1800. https://doi.org/10.1212/WNL.58.12.1791

The Multiple Sclerosis International Federation. (2021, April). *Atlas of MS - 3rd Edition, part 2: Clinical management of multiple sclerosis around the world*.

Thompson, A. J., Banwell, B. L., Barkhof, F., Carroll, W. M., Coetzee, T., Comi, G., Correale, J., Fazekas, F., Filippi, M., Freedman, M. S., Fujihara, K., Galetta, S. L., Hartung, H. P., Kappos, L., Lublin, F. D., Marrie, R. A., Miller, A. E., Miller, D. H., Montalban, X., … Cohen, J. A. (2018). Diagnosis of multiple sclerosis: 2017 revisions of the McDonald criteria. *The Lancet Neurology*, *17*(2), 162–173. https://doi.org/10.1016/S1474-4422(17)30470-2

Thorne, M. W. D., Cash, M. K., Reid, G. A., Burley, D. E., Luke, D., Pottie, I. R., & Darvesh, S. (2021). Imaging Butyrylcholinesterase in Multiple Sclerosis. *Molecular Imaging and Biology*, *23*(1), 127–138. https://doi.org/10.1007/s11307-020-01540-6

Tiraboschi, P., Hansen, L. A., Alford, M., Merdes, A., Masliah, E., Thal, L. J., & Corey-Bloom, J. (2002). Early and Widespread Cholinergic Losses Differentiate Dementia With Lewy Bodies From Alzheimer Disease. *Archives of General Psychiatry*, *59*(10), 946. https://doi.org/10.1001/archpsyc.59.10.946

Townsend, L. T. J., Anderson, K. N., Boeve, B. F., McKeith, I., & Taylor, J. (2023). Sleep disorders in Lewy body dementia: Mechanisms, clinical relevance, and unanswered questions. *Alzheimer's & Dementia*, *19*(11), 5264–5283. https://doi.org/10.1002/alz.13350

Tsoi, K. K. F., Chan, J. Y. C., Hirai, H. W., Wong, S. Y. S., & Kwok, T. C. Y. (2015). Cognitive Tests to Detect Dementia: A Systematic Review and Meta-analysis. *JAMA Internal Medicine*, *175*(9), 1450. https://doi.org/10.1001/jamainternmed.2015.2152

Valiukas, Z., Ephraim, R., Tangalakis, K., Davidson, M., Apostolopoulos, V., & Feehan, J. (2022). Immunotherapies for Alzheimer's Disease—A Review. *Vaccines*, *10*(9), 1527. https://doi.org/10.3390/vaccines10091527

Valotassiou, V., Malamitsi, J., Papatriantafyllou, J., Dardiotis, E., Tsougos, I., Psimadas, D., Alexiou, S., Hadjigeorgiou, G., & Georgoulias, P. (2018). SPECT and PET imaging in Alzheimer's disease. *Annals of Nuclear Medicine*, *32*(9), 583–593. https://doi.org/10.1007/s12149-018-1292-6

Van Dort, C. J., Zachs, D. P., Kenny, J. D., Zheng, S., Goldblum, R. R., Gelwan, N. A., Ramos, D. M., Nolan, M. A., Wang, K., Weng, F.-J., Lin, Y., Wilson, M. A., & Brown, E. N. (2015). Optogenetic activation of cholinergic neurons in the PPT or LDT induces REM sleep. *Proceedings of the National Academy of Sciences*, *112*(2), 584–589. https://doi.org/10.1073/pnas.1423136112

Van Dyck, C. H., Swanson, C. J., Aisen, P., Bateman, R. J., Chen, C., Gee, M., Kanekiyo, M., Li, D., Reyderman, L., Cohen, S., Froelich, L., Katayama, S., Sabbagh, M., Vellas, B., Watson, D., Dhadda, S., Irizarry, M., Kramer, L. D., & Iwatsubo, T. (2023). Lecanemab in Early Alzheimer's Disease. *New England Journal of Medicine*, *388*(1), 9–21. https://doi.org/10.1056/NEJMoa2212948

Van Egroo, M., Koshmanova, E., Vandewalle, G., & Jacobs, H. I. L. (2022). Importance of the locus coeruleus-norepinephrine system in sleep-wake regulation: Implications for aging and Alzheimer's disease. *Sleep Medicine Reviews*, *62*, 101592. https://doi.org/10.1016/j.smrv.2022.101592

Vila, M. (2019). Neuromelanin, aging, and neuronal vulnerability in Parkinson's disease. *Movement Disorders: Official Journal of the Movement Disorder Society*, *34*(10), 1440–1451. https://doi.org/10.1002/mds.27776

Waiskopf, N., & Soreq, H. (2015). Cholinesterase Inhibitors. In *Handbook of Toxicology of Chemical Warfare Agents* (pp. 761–778). Elsevier. https://doi.org/10.1016/B978-0-12-800159-2.00052-X

Walker, Z., Possin, K. L., Boeve, B. F., & Aarsland, D. (2015). Lewy body dementias. *The Lancet*, *386*(10004), 1683–1697. https://doi.org/10.1016/S0140-6736(15)00462-6

Wang, H., Yu, M., Ochani, M., Amella, C. A., Tanovic, M., Susarla, S., Li, J. H., Wang, H., Yang, H., Ulloa, L., Al-Abed, Y., Czura, C. J., & Tracey, K. J. (2003). Nicotinic acetylcholine receptor α7 subunit is an essential regulator of inflammation. *Nature*, *421*(6921), 384–388. https://doi.org/10.1038/nature01339

Wang, J., Jin, C., Zhou, J., Zhou, R., Tian, M., Lee, H. J., & Zhang, H. (2023). PET molecular imaging for pathophysiological visualization in Alzheimer's disease. *European Journal of Nuclear Medicine and Molecular Imaging*, *50*(3), 765–783. https://doi.org/10.1007/s00259-022-05999-z

Wang, Y.-T. T., Rosa-Neto, P., & Gauthier, S. (2023). Advanced brain imaging for the diagnosis of Alzheimer disease. *Current Opinion in Neurology*, *36*(5), 481–490. https://doi.org/10.1097/WCO.0000000000001198

Whitehouse, P. J., Price, D. L., Clark, A. W., Coyle, J. T., & DeLong, M. R. (1981). Alzheimer disease: Evidence for selective loss of cholinergic neurons in the nucleus basalis. *Annals of Neurology*, *10*(2), 122–126. https://doi.org/10.1002/ana.410100203

Wong, R., & Lovier, M. A. (2023). Sleep Disturbances and Dementia Risk in Older Adults: Findings From 10 Years of National U.S. Prospective Data. *American Journal of Preventive Medicine*, *64*(6), 781–787. https://doi.org/10.1016/j.amepre.2023.01.008

World Health Organization. (2023, March 15). *Dementia*. https://www.who.int/news-room/fact-sheets/detail/dementia

Wu, W., Ji, Y., Wang, Z., Wu, X., Li, J., Gu, F., Chen, Z., & Wang, Z. (2023). The FDA-approved anti-amyloid-β monoclonal antibodies for the treatment of Alzheimer's disease: A systematic review and meta-analysis of randomized controlled trials. *European Journal of Medical Research*, *28*(1), 544. https://doi.org/10.1186/s40001-023-01512-w

Xie, L., Kang, H., Xu, Q., Chen, M. J., Liao, Y., Thiyagarajan, M., O'Donnell, J., Christensen, D. J., Nicholson, C., Iliff, J. J., Takano, T., Deane, R., & Nedergaard, M. (2013). Sleep Drives Metabolite Clearance from the Adult Brain. *Science*, *342*(6156), 373–377. https://doi.org/10.1126/science.1241224

Xing, S., Li, Q., Xiong, B., Chen, Y., Feng, F., Liu, W., & Sun, H. (2021). Structure and therapeutic uses of butyrylcholinesterase: Application in detoxification, Alzheimer's disease, and fat metabolism. *Medicinal Research Reviews*, *41*(2), 858–901. https://doi.org/10.1002/med.21745

Xu, M., Chung, S., Zhang, S., Zhong, P., Ma, C., Chang, W.-C., Weissbourd, B., Sakai, N., Luo, L., Nishino, S., & Dan, Y. (2015). Basal forebrain circuit for sleep-wake control. *Nature Neuroscience*, *18*(11), 1641–1647. https://doi.org/10.1038/nn.4143

Xu, S., & Chan, P. (2015). Interaction between Neuromelanin and Alpha-Synuclein in Parkinson's Disease. *Biomolecules*, *5*(2), 1122–1142. https://doi.org/10.3390/biom5021122

Yamout, B., Al-Jumah, M., Sahraian, M. A., Almalik, Y., Khaburi, J. A., Shalaby, N., Aljarallah, S., Bohlega, S., Dahdaleh, M., Almahdawi, A., Khoury, S. J., Koussa, S., Slassi, E., Daoudi, S., Aref, H., Mrabet, S., Zeineddine, M., Zakaria, M., Inshasi, J., … Alroughani, R. (2024). Consensus recommendations for diagnosis and treatment of Multiple Sclerosis: 2023 revision of the MENACTRIMS guidelines. *Multiple Sclerosis and Related Disorders*, *83*, 105435. https://doi.org/10.1016/j.msard.2024.105435

Yoshikawa, T., Nakamura, T., & Yanai, K. (2021). Histaminergic neurons in the tuberomammillary nucleus as a control centre for wakefulness. *British Journal of Pharmacology*, *178*(4), 750–769. https://doi.org/10.1111/bph.15220

Ziontz, J., Bilgel, M., Shafer, A. T., Moghekar, A., Elkins, W., Helphey, J., Gomez, G., June, D., McDonald, M. A., Dannals, R. F., Azad, B. B., Ferrucci, L., Wong, D. F., & Resnick, S. M. (2019). *Tau pathology in cognitively normal older adults*. https://doi.org/10.1101/611186